Abstracts 7545-7845

SOLID STATE ABSTRACTS

an abstract journal devoted to the theory, production and use of solid state materials and devices

VOLUME 1 NUMBER 6

PHYSICS
METALLURGY
ELECTRONICS

METALS
SEMICONDUCTORS
SUPERCONDUCTORS
PHOSPHORS
MAGNETICS
DIELECTRICS

SOLID STATE ABSTRACTS

VOLUME 1, NUMBER 6

March 1961

Abstracts 7545–7845

TABLE OF CONTENTS

Abstracts of the Solid State Literature

Metallurgy and Chemistry of Solids

Alloys . . . 273
Crystal Structure (including Imperfections and Impurities) . . . 273
Crystal Growth . . . 277
Crystal Surfaces . . . 278
Effects of Radiation . . . 278

Solid State Physics

General . . . 279
Crystal Physics (including Energy Band Structure) . . . 279
Dielectric Properties (including Ferroelectrics) . . . 280
Carrier Properties . . . 281
Conductivity . . . 283
Superconductivity . . . 284
Other Electrical Properties . . . 285
Ferro- and Ferrimagnetism . . . 286
Paramagnetism . . . 289
Diamagnetism . . . 291
Optical Properties . . . 291
Thermal Properties . . . 293
Mechanical Properties . . . 294

Solid State Devices

General . . . 295
Diodes . . . 295
Transistors . . . 296
Photodevices . . . 297
Thermal Devices . . . 298
Magnetic Devices . . . 298
Other Solid State Devices . . . 299

Solid State Device Measurements

Transistors . . . 300

Basic Solid State Device Circuits

General . . . 300
Amplifiers . . . 301
Oscillators . . . 304
Switching Circuits . . . 304
Other Solid State Device Circuits . . . 306

Applications of Solid State Devices

General . . . 306
Radio . . . 306
Television . . . 307
Telephony and Telegraphy . . . 308
Radar . . . 308
Recording and Reproduction . . . 308
Computers . . . 309
Power . . . 311
Control . . . 312
Instrumentation . . . 313

New Products . . . 314

Subject Index . . . 316

Author Index . . . 322

Conference Programs Abstracted in Solid State Abstracts, Vol. 1, No. 6; see page 315

Editor: GEOFFREY KNIGHT, JR., Ph.D.

Assistant Editor: MYRON A. COHEN

PUBLISHED MONTHLY BY

Cambridge Communications Corporation, 238 Main Street, Cambridge 42, Massachusetts, Tel. Klrkland 7-1997

Subscription Rate: $25.00 per year. Single Copies and Back Issues: $2.50. Advertising Rates on Request.

Cambridge Communications Corp. is not prepared to furnish copies of the articles abstracted. However, there are many libraries throughout the country which maintain photocopying services.

SYMBOLS USED IN THE ABSTRACTS

L: Letter to the Editor. A: Only an abstract is given in the reference. R: Only a review is given in the reference. E: Erratum.

The reference numbers in the indices are the abstract numbers, not the page numbers.

ABSTRACTS OF THE SOLID STATE LITERATURE

METALLURGY AND CHEMISTRY OF SOLIDS

ALLOYS

7545 SOLUBILITY OF FLAWS IN HEAVILY-DOPED SEMICONDUCTORS by W. Shockley (Shockley) and J. L. Moll (Stanford U.); Phys. Rev., Vol. 119, pp. 1480-1482, Sept. 1, 1960

The dependence of the solubility of a charged impurity in a semiconductor upon the Fermi level is discussed. This dependence may be understood in terms of a conceptual model in which an impurity is allowed to diffuse in a specimen containing a p-n junction, so that the Fermi level varies in respect to the band edges. If the impurity can exist in many states of charge (i.e., is a "flaw"), then the concentration of flaws with charge r times the electronic charge varies as the rth power of the hole density. Summing the concentrations for the different states of charge gives the solubility and its dependence upon hole concentration, and, hence, Fermi level.

7546 EFFECTS OF SOLID SOLUTION OF In_2Te_3 WITH $A^{II}B^{VI}$ TELLURIDES by J. C. Woolley and B. Ray (U. Nottingham); J. Phys. Chem. Solids, Vol. 15, pp. 27-32, Aug. 1960

The preparation of alloys for the three systems In_2Te_3—CdTe, In_2Te_3—ZnTe and In_2Te_3—HgTe and their annealing to obtain equilibrium conditions are discussed. The ranges of solid solution, the variation of lattice parameter with composition, and the ranges and types of ordering that occur have been investigated for each system. For the systems In_2Te_3—CdTe and In_2Te_3—ZnTe, the variation of optical energy gap, E_g, with composition have been determined by infrared transmission measurements, and the effects on E_g of solid solution and ordering have been observed.

Solid Solutions in the Bi_2Te_3—Bi_2Se_3 System - See 7551

Solid Solutions of Te and Se - See 7552

Solid Solutions of (Zn, Hg) S - See 7677

Alkali Halide Solid Solutions - See 7554

Solubility of Ag, Fe, Cd, Te, and Ta Radioisotopes in Ge - See 7569

7547 THE DISTRIBUTION COEFFICIENT OF TIN IN SELENIUM by D. M. Chizhikov and V. M. Edel'shtein (Baikov Inst. Metall.); Soviet Phys.-Solid State, Vol. 2, pp. 790-792, Nov. 1960

The distribution of tin in selenium is evaluated. The radioactive isotope Sn^{113} was introduced into molten selenium, and the mixture was stirred at a temperature of from 450 to 500°C for one hour. Zone recrystallization was then carried out for a period of 90 to 100 hours, and followed by a radioactivity counter. The experiment was repeated three times at different zone temperatures. The distribution coefficient of tin in selenium ranges between 0.85 and 0.95, and the effective diffusion coefficient of tin in selenium is 1.9×10^{-3} cm.

7548 AN INVESTIGATION OF THE CUBIC-HEXAGONAL TRANSITION IN BARIUM TITANATE by R. M. Glaister and H. F. Kay (U. Bristol); Proc. Phys. Soc., Vol. 76, pp. 763-771, Nov. 1960

The conversion of normal Perovskite-type barium titanate to the hexagonal polymorph by firing in a hydrogen atmosphere at 1330°C, 130° lower than that previously reported for firing in air, is described. With suitable additives such as $MnCO_3$ the conversion begins at temperatures as low as 1100°C. Conversion is inhibited by a number of impurities, especially Si, Fe and Sr, such as are present in barium titanate of commercial quality. The effect of atmospheres of hydrogen and oxygen on the rate of reconversion to the cubic polymorph has also been studied. In hydrogen this reaches a peak rate at about 1200°C, while in oxygen it rises continuously. All the phenomena associated with the transition appear to be compatible with a proposed hypothesis about the dependence of free energy on vacancy concentration. The hexagonal polymorph has a permittivity of about 440 and a temperature coefficient of $+0.0028\ (\text{deg C})^{-1}$.

CRYSTAL STRUCTURE (including Imperfections and Impurities)

7549 ON THE POLYMORPHISM OF THE THALLIUM HALIDES by I. H. Khan (Imperial Coll., London); Proc. Phys. Soc., Vol. 76, pp. 507-512, Oct. 1960

Experiments on the polymorphism of thallium halides formed as thin oriented layers by deposition in vacuo onto a variety of bases, in particular on the cleavage faces of crystals, are described. The effect of varying the temperature of the base has

been studied in some detail. Measurements of the lattice constant of the abnormal rocksalt type form, using both the reflection and the transmission techniques, are reported. In the latter, which gives more accurate results, thallium halides were deposited onto a thin polycrystalline layer of alkali halide previously formed on an amorphous base.

Polymorphism of $BaTiO_3$ - See 7548

7550 MORPHOLOGY OF SYNTHETIC SUBMICROSCOPIC CRYSTALS OF α AND γ FeOOH AND OF γFe_2O_3 PREPARED FROM FeOOH by G. W. van Oosterhout (N. V. Philips); Acta Cryst., Vol. 13, pp. 932-935, Nov. 1960

The orientation of the needle axis of synthetic acicular crystals of α and γFeOOH with respect to the unit cell has been determined by selected area electron diffraction. The needle axis is [001] for αFeOOH (c = 3.03 A) and γFeOOH (c = 3.06 A) and [110] for γFe_2O_3 prepared either by dehydration of γFeOOH or by reduction of αFeOOH or γFeOOH followed by oxidation. The results are compared with previous work on this subject and the possible causes of the discrepancies between these results and those of Osmond and of Campbell are discussed.

7551 LATTICE CONSTANTS OF Bi_2Te_3—Bi_2Se_3 SOLID SOLUTION ALLOYS by J. R. Wiese and L. Muldawer (Franklin Inst. Labs.); J. Phys. Chem. Solids, Vol. 15, pp. 13-16, Aug. 1960

The Bi_2Te_3—Bi_2Se_3 quasi-binary system is rhombohedral for all compositions. Lattice constants a_0 and c_0 (based on a hexagonal lattice) for the entire range determined using powder pattern film techniques are reported. The constant a_0 follows Vegard's rule over the entire range of compositions, while the constant c_0 exhibits a positive deviation over the range from 40 mol % Bi_2Te_3 to Bi_2Se_3. Bi_2Te_3 has a layered structure with planes of atoms of a single type parallel to the basal plane. The lattice constant data can be explained in terms of Se-atom substitution in preferred planes for the range Bi_2Te_3—Bi_2Te_2Se. Interlayer spacings for Bi_2Te_3 and Bi_2Te_2S are given and discussed.

7552 X-RAY INVESTIGATION OF THE TELLURIUM-SELENIUM SYSTEM by T. P. Smorodina (Tech. Inst., Leningrad); Soviet Phys.-Solid State, Vol. 2, pp. 807-809, Nov. 1960

The lattice constants and density of members of a continuous series of solid solutions of Te-Se are evaluated. The compositions studied represented the complete range of substitution, although emphasis was placed on the high tellurium region of the system. The solid solutions crystallize in the hexagonal system, as indicated by powder x-ray analysis. Lattice constants and density are plotted as a continuous function of the composition.

7553 APPLICATION OF THERMOLUMINESCENCE AND REFLECTANCE METHODS TO STUDY OF LATTICE DEFECTS IN ALUMINA CERAMICS by L. M. Atlas and R. F. Firestone (Ill. Inst. Tech.); J. Am. Ceram. Soc., Vol. 43, pp. 476-484, Sept. 1960

Alumina ceramics irradiated with gamma rays emit light of varying intensity as they are warmed. The resulting glow curve may be resolved into discrete peaks, each of which corresponds to a separate electron trapping level. The energy depth of each trap may be estimated from the glow-peak temperature and the temperature at which the light intensity reaches half its maximum value. Resolved glow curves are presented for a series of alumina ceramics including specimens having less than 100 PPM of impurities as well as others contaminated with low concentrations of Si, Ti, Fe, Mg, and Ca oxides. Curves are also given for high-purity aluminas which were heated in oxygen and in hydrogen after firing. Where possible, glow peaks are identified with the causative impurity ion or annealing treatment, and estimated trap depths are tabulated. Because of its inverse relation to optical absorption, reflectance is also sensitive to changes in the number and type of lattice defects. Annealing in oxygen and introduction of Ca^{2+} ions produce a significant lowering of the reflectance of irradiated alumina ceramics, whereas exposure to hydrogen has the opposite effect.

7554 THE EFFECT OF ANNEALING ON THE PHYSICAL PROPERTIES OF ALKALI HALIDE SOLID SOLUTIONS by E. K. Zavadovskaya, J. S. Ivankina, and I. Ya. Melik-Gaikazyan (Tomsk Polytechnic Inst.); Soviet Phys.-Solid State, Vol. 2, pp. 617-620, Oct. 1960

Annealing of equimolar KCl-KBr and NaCl-NaBr as a means for decreasing structural defects is discussed. Annealing was employed for 5, 10, 20, 25, 50, and 75 hours, at 600°C; no marked decrease in structural defects was noted. However, annealing permitted escape of excess vacancies at internal defects in the crystal and at the surface, resulting in a slight increase in density.

7555 DEPENDENCE OF THE OPTICAL BLEACHING RATE OF X-IRRADIATED KCl CRYSTALS ON LIGHT INTENSITY by W. E. Bron and W. R. Heller (IBM); Phys. Rev., Vol. 119, pp. 1864-1868, Sept. 15, 1960

Measurements of the changes in the bleaching rate of the F band as the result of varying the intensity of F light are reported. Bleaching was done on KCl crystals which had been irradiated at room temperature with hard x rays into either the first or second stage of coloration. In the first stage irradiated crystals the total bleaching of the F centers during the first ten seconds of illumination varied approximately linearly with light intensity at low intensities, but became saturated at intensities greater than 5×10^{14} photons/sec cm^2. The bleaching process is thought to occur primarily through the capture of photoelectrons at preexisting electron traps. Based on this model it is possible to set up the kinetic equations for the bleaching process. Using reasonable values for photoelectron capture coefficients forces one to conclude that the number of photoelectrons is always very small throughout the bleaching process. The resulting simplification in the analysis of the kinetic equations leads to a prediction of the experimentally observed variation of the initial bleaching rate with light intensity. The analysis shows that the ratio of the capture coefficient for photoelectrons of the electron trapping centers to that of negative-ion vacancies is about unity, which strongly suggests that the trapping centers are either traps with net positive charge or are neutral traps located close to the original F centers. The rate of bleaching during the second stage of bleaching saturated at the lowest intensity used which was about 1×10^{14} photons/sec cm^2. This result is discussed in terms of the analysis given for the first stage of bleaching.

Measurement of Color Center Concentration by Microwave Faraday Rotation - See 7666

7556 ON THE FORMATION OF INTERSTITIALS IN ALKALI HALIDES by R. E. Howard, R. Smoluchowski and D. A.

Wiegand (Carnegie Inst. Tech.); Acta Cryst., Vol. 13, pp. 1064-1065 (A), Dec. 1960

Evidence for the formation of interstitial halogens in LiF at low temperatures by x-ray photons which have too low an energy to produce displaced atoms directly is presented. Changes in configuration of the interstitials account for density changes observed during annealing. It appears further that the mechanism and kinetics of defect formation depends strongly on temperature and on the nature of the metallic and halogen ions. In particular, the time constant associated with the rate of generation of defects in KCl at room temperature appears to be proportional to the square of intensity, while it is linear in LiF at room temperature and at low temperature. The influence of previous plastic deformation and of heat treatment also differs for the different alkali halides. Possible models and theoretical correlations were suggested.

7557 ROOM-TEMPERATURE DISLOCATION DECORATION INSIDE LARGE CRYSTALS by C. B. Childs (NASA) and L. Slifkin (U. North Carolina); Phys. Rev. Lett., Vol. 5, pp. 502-503 (L), Dec. 1, 1960

A technique which displays dislocation configurations in the interior of large single crystals of silver chloride is described. It was discovered that after production of only moderate print-out silver densities using the Haynes-Shockley method, a room temperature aging of the crystal resulted in extensive migration of silver from random submicroscopic specks into dislocations. After several days the dislocations became so sharply decorated that they were observable using ordinary bright field microscopy and a simple 20x objective. Random dislocations, pure tilt boundaries, square and hexagonal nets, and helices have been observed. Photographs illustrating the resolution and contrast obtainable are shown. Further investigations and suggested uses of the technique are discussed.

7558 ON THE MECHANISM OF FORMATION OF HELICAL DISLOCATIONS IN SILICON by W. C. Dash (GE Res. Lab.); Acta Cryst., Vol. 13, p. 1129 (A), Dec. 1960

Screw dislocations climb to form helices when gold is diffused into silicon crystals at about 1200°C. The following experiments have been performed to elucidate the mechanism of formation of the helices. From localized surface damage, a small number of dislocation loops are moved into an otherwise dislocation-free crystal by an applied stress at 900°C. The geometry of deformation is such that the screw portions of the loops are left-handed. Upon diffusion of gold only right-handed helices are formed. This leads to the conclusion that in effect a vacancy deficiency produces the climb. Investigation has shown that only those screw dislocations which are substantially free from impurities climb to form helices. In other cases either distorted helices form, or there may be no climb of the screw dislocations. In such specimens randomly distributed prismatic loops are frequently found.

7559 DISLOCATIONS AND BRITTLE FRACTURE IN ELEMENTAL AND COMPOUND SEMICONDUCTORS by M. S. Abrahams and L. Ekstrom (RCA Labs.); Acta Met., Vol. 8, pp. 654-662, Sept. 1960

The predominant {110} cleavage plane of the IIIb-Vb compounds is explained by means of a dislocation model. This model postulates the formation and coalescence of Lomer dislocations to form (nucleate) a microcrack; cleavage results from the propagation of the microcrack. Unlike previous models, this one is able to account for the unique three-fold symmetry of the crack pattern which results from indenting a (111) surface with a pointed, conical diamond. The fact that Ge only exhibits {110} cleavage under special conditions is attributed to a difference in structure of the Lomer dislocation between the IVb elements and IIIb-Vb compounds. The occurrence of octahedral cleavage in the IVb elements is thought to be due to the growth of a microcrack resulting from the piling-up and coalescence of glissile dislocations on {111} planes. A combination of this mechanism with the one yielding dodecahedral cleavage accounts for cleavage on planes other than those of the {110} type in the IIIb-Vb compounds.

7560 POSSIBILITY OF THE EXISTENCE OF ATTRACTIVE FORCES BETWEEN DISLOCATIONS OF LIKE SIGN by J. Weertman (Northwestern U.); Phys. Rev., Vol. 119, pp. 1871-1872, Sept. 15, 1960

It is concluded that two moving dislocations of the same sign and on the same slip plane can sometimes attract rather than repel one another (and two of unlike sign repel rather than attract each other). This reversal over the usual behavior will occur at velocities where the kinetic energy in the displacement field of an isolated moving dislocation is larger than the strain energy in the same field.

Effect of Screw Dislocations on the Yield Strength of Crystals - See 7694

7561 IMPERFECTIONS IN CRYSTALS OF ZINC SULFIDE by W. L. Roth (GE Res. Lab.); Acta Cryst., Vol. 13, p. 1064 (A), Dec. 1960

The use of x-ray diffraction and electron microscope studies to elucidate the nature and origin of the imperfections in single crystals of zinc sulfide crystallized from the vapor phase was described. Although most crystals are imperfect and contain large concentrations of stacking faults and dislocations, a few crystals have been found to be essentially perfect in both respects. There is considerable difference in the physical properties of the perfect and imperfect crystals: their strength, resistance to phase transformation upon heat treatment, photoconductivity, and sublimation characteristics. Most of these properties can be explained by the dislocation and fault structures in the crystals. A quantitative study of the stacking faults in quenched and annealed crystals has been accomplished by measuring the diffuse x-ray scattering in the reciprocal lattice. From these data a probability distribution function is constructed which describes the variation in stacking sequence of planes perpendicular to the C axis. The measured function is compared with functions computed for various models. It was concluded that the faults originate from shear processes which occur when the crystal is cooled through the phase transitio region.

Solubility of Flaws in Heavily-Doped Semiconductors - See 7545

7562 APPLICATION OF RADIOCHEMISTRY TO THE PREPARATION OF HIGH-PURITY SILICON by T. Ichimiya, H. Baba, and T. Nozaki (Nippon Tel. and Tel.); J. Appl. Rad. Isotopes, Vol. 9, pp. 164-165 (A), Dec. 1960

The use of radiochemical techniques to study the behavior of trace impurities during the purification of silicon by the iodide process and the determination of these impurities, especially

halogens, in the resultant high-purity silicon, etc., in order to improve the method and establish an industrial procedure was described.

7563 FLUORIMETRIC DETERMINATION OF BORON: APPLICATION TO SILICON, SEA WATER AND STEEL by C. A. Parker and W. J. Barnes (Admiralty Metals Lab.); Analyst, Vol. 85, pp. 828-838, Nov. 1960

The fluorimetric determination of very small amounts of boron by the reaction of borate ion with benzoin is discussed. Factors affecting the reaction are considered and a high-vacuum distillation method for separating boron from large amounts of interfering materials is described. In favorable instances a simpler method of separation with an ion-exchange resin is suitable. Procedures for determining boron in high purity silicon (limit of detection about 0.03ppm), in sea water (with a precision of better than ±2 per cent) and in steel (limit of detection about 1 ppm) are described.

7564 PURIFICATION FACTOR CHARACTERIZATION OF ZONE REFINING by L. Gold (Princeton U.) and V. Johnson (Lincoln Lab.); J. Franklin Inst., Vol. 270, pp. 367-381, Nov. 1960

The quantity π_T, termed the purification factor, defines the potential state of purity realizable in a specimen that has undergone zone-refinement treatment. An exact analysis appears intractable, but neglect of the terminal zone perturbation (which becomes vanishingly small for the infinite ingot) allows a lower bound to be established on the remanent solute impurity. Such numerical values of π_T are evaluated for some sensible distribution coefficients and zone dimensions involving a maximum of ten passes. An original expression for the solute impurity distribution is deduced and numerically appraised for a range of operational conditions not presently tabulated; the relation has been applied to the indicated π_T determinations.

7565 PURIFICATION OF TELLURIUM BY THE ZONE MELTING METHOD by N. F. Shvartsenau (Semicon. Inst., Leningrad); Soviet Phys.-Solid State, Vol. 2, pp. 797-799, Nov. 1960

Purification of tellurium by zone melting and a technique for evaluation of results are described. The resulting degree of purity is determined from the ratio of the resistance of various parts of the ingot at liquid nitrogen temperature (-196°C) to that of the same parts at room temperature (20°C). Results obtained from up to nine passages of the molten zone are reported. The degree of purity was greater than 99.9999%. This measuring technique overcomes difficulties inherent in purity measurement by chemical or spectrochemical means.

Apparatus for the Floating-Zone Refining of GaAs - See 7576

7566 THE DIFFUSION OF IONIZED IMPURITIES IN SEMICONDUCTORS by J. W. Allen (SERL); J. Phys. Chem. Solids, Vol. 15, pp. 134-139, Aug. 1960

A simple one-dimensional model is used to illustrate the fact that the diffusion coefficient of an impurity in a semiconductor depends on the state of ionization of the impurity, i.e., on whether the Fermi level lies above or below the impurity energy level. The results are applied to the diffusion of zinc in gallium arsenide.

7567 ANISOTROPY OF THE DIFFUSION OF ZINC IN POLYCRYSTALLINE CUPROUS OXIDE by A. V. Sandulova and C. Yueh-ch'ing (L'vov Polytech. Inst.); Soviet Phys.-Solid State, Vol. 2, pp. 800-802, Nov. 1960

The diffusion of zinc in polycrystalline cuprous oxide both parallel to, and perpendicular to the crystal-growth axis is discussed. Measurements were made in 50-degree intervals between 600 and 1050°C, inclusive, using Zn^{65}, a radioactive tracer. Diffusion in the perpendicular direction is greater than in the parallel direction for the entire temperature range, although the difference between the rates decreases with increasing temperature. Each diffusion rate shows one discontinuity, indicating that the mechanism of diffusion differs at high and low temperatures. The reasons are discussed.

7568 DETERMINATION OF THE DIFFUSION COEFFICIENT OF ARSENIC IN GERMANIUM BY THE MEASUREMENT OF THE THERMOELECTRIC VOLTAGE [in French] by E. Batifol and G. Duraffourg (Centre Natl. d'Etudes des Télécommun.); J. Phys. Radium, Vol. 21, Suppl. to No. 11, pp. 207A-216A, Nov. 1960

A value of the diffusion coefficient of As in Ge deduced from the measurement of thermoelectric power along a bevelled sample of As-diffused germanium is reported. The As surface concentration has been obtained both by the measurement of thermoelectric power and by the measurement of sheet resistance. The average value of the As diffusion coefficient at 800°C is $D = 1.3 \times 10^{-11}\ cm^2/sec$.

7569 STUDY OF THE DIFFUSION AND SOLUBILITY OF VARIOUS INGREDIENTS IN GERMANIUM by E. G. Miselyuk, V. E. Kosenko, L. A. Khomenko and V. D. Ignatkov (USSR); J. Appl. Rad. Isotopes, Vol. 9, p. 192 (A), Dec. 1960

Studies of the diffusion and solubility of the radioisotopes Ag^{11}, Fe^{59}, Cd^{115}, Te^{127}, and Ta^{182} in monocrystalline germanium in the temperature range from 700° to 930°C were described. The results were as follows: (1) The volume diffusion coefficients for Ag, Fe, Cd and Ta were found to be respectively (at 800°C) 8×10^{7}, 1.6×10^{-6}, 4.2×10^{-12} and $6.5 \times 10^{-13}\ cm^2/sec$. (2) Maximum values of solubility were fixed at $C_{Ag} = 1.1 \times 10^{15} cm^{-3}$, $C_{Fe} = 1.5 \times 10^{15} cm^{-3}$, $C_{Cd} = 4 \times 10^{18} cm^{-3}$, and $C_{Ta} = 2 \times 10^{18} cm^{-3}$. (3) The coefficient of surface diffusion for Ag proved to be higher than the volume diffusion coefficient by one order of magnitude at 850°C and six orders of magnitude at 200°C. (4) An intense evaporation of germanium, two orders of magnitude higher than in a vacuum, was observed in tellurium fumes.

7570 THE DIFFUSION OF OXYGEN IN SILICON AND GERMANIUM by C. Haas (N. V. Philips); J. Phys. Chem. Solids, Vol. 15, pp. 108-111, Aug. 1960

Using a simple model for the structure of oxygen in silicon and germanium crystals and making the assumption that internal friction and diffusion are both due to the same relaxation phenomenon, the diffusion coefficient of oxygen is calculated from experimental data on internal friction. The results are: $D = D_0 \exp - (U/kT)$; O in Si: $D_0 = 0.21\ cm^2/sec$, $U = 2.55$ ev; O in Ge: $D_0 = 0.17\ cm^2/sec$, $U = 2.02$ ev. The calculated values of D are in reasonable agreement with available experimental data.

7571 DIFFUSION RATE OF Li IN Si AT LOW TEMPERATURES by E. M. Pell (GE Res. Labs.); Phys. Rev., Vol. 119, pp. 1222-1225, Aug. 15, 1960

The method of ion drift in the electric field of an n-p junction

has been used to measure the diffusion constant of Li in Si between 25°C and 125°C, taking particular care to avoid chemical and electrical interactions which might affect the results. When these data are combined with previous high-temperature data, there is obtained $D = (2.5 \pm 0.2) \times 10^{-3} \exp [-(0.655 \pm 0.01) e/kT] cm^2/sec$, the data extending over eight decades in D. The results are compared with those from ion-pair relaxation experiments, and it is shown that the latter are consistant with the ion-drift results.

7572 DIFFUSION OF ZINC IN GALLIUM ARSENIDE by F. A. Cunnell and C. H. Gooch (SERL); J. Phys. Chem. Solids, Vol. 15, pp. 127-133, Aug. 1960

Measurements of the diffusion of zinc into gallium arsenide from the vapor phase over a range of diffusion temperatures and zinc pressures are reported. Experiments to investigate the influence of arsenic pressure on the diffusion have also been performed. The results obtained depart radically from those expected for a constant diffusion coefficient; possible reasons for this are discussed.

Diffusion Coefficient of Tin in Selenium - See 7547

Diffusion in Cuprous Halide Films - See 7580

7573 THE INTERACTION OF POINT DEFECTS WITH DISLOCATIONS IN SILICON by R. C. Newman, J. Wakefield, J. B. Willis and R. Bullough (AEI Res. Lab.); Acta Cryst., Vol. 13, pp. 1129-1130(A), Dec. 1960

The phenomenon of strain aging in silicon crystals known to contain oxygen and probably carbon was discussed. By the use of infrared spectrographic techniques it has been shown that oxygen precipitates on annealing at a temperature of 1000°C and there is indirect evidence of interaction with dislocations. A direct observation of these precipitation phenomena, in single crystals containing controlled grown-in dislocation densities from zero up to $10^5 cm^{-2}$, together with some isolated crystal boundaries, was reported. The effect of plastic deformation was also considered. The location of any precipitated oxygen after annealing has been revealed by a novel method using crystals which contain accurately predetermined concentrations of aluminum and phosphorus, the aluminum being slightly in excess so that initially the crystal is wholly p-type. It is shown thermodynamically that the aluminum will undergo an exchange reaction with the 'precipitated' silicon-oxygen complex, similar to that observed in chromium steels. In the vicinity of the oxygen precipitates the aluminum concentration is therefore reduced and the crystal becomes locally n-type. From the nature of the resulting p-n junctions, which are delineated by etching, the type of nucleating site (random, dislocations, or boundaries) can be readily ascertained. The actual precipitates can be revealed by transmission optical microscopy and correlated with the former surface features. Observations have been made over the temperature range 950 to 1350°C; the mode of precipitation is dependent both on this temperature and on the oxygen concentration. Electron diffraction observations indicate that carbon is also involved in the precipitation process.

7574 EFFECT OF Li-B ION PAIRING ON Li^+ ION DRIFT IN Si by E. M. Pell (GE Res. Lab.); J. Appl. Phys., Vol. 31, pp. 1675-1679, Sept. 1960

When Li^+ and B^- ions are present simultaneously in Si, relatively immobile Li-B ion pairs are formed. Only those Li^+ ions which have not become paired with B^- are free to diffuse through the Si, and measurement of the effective diffusion rate of the Li^+ can thus be used to determine the fraction of Li^+ paired. Such measurements made in the range 2 - 100°C using the method of ion drift in a p-n junction are reported. The results agree well with the Reiss model for ion pairing, yielding a distance of closest approach between Li^+ and B^- of 2.5 - 2.7 A. This value is larger than that given by the sum of Li^+ and B^- radii; it is roughly equal to the distance from a lattice-atom site to the next-nearest interstitial site (2.72 A). The kinetics of the ion-pairing reaction have been investigated by the same technique. The resulting value for the capture radius of the B^- ion agrees satisfactorily with theory.

7575 THE PREPARATION AND CRYSTALLOGRAPHY OF FeNiN AND THE SERIES $Fe_{4-x}Ni_xN$ by R. J. Arnott and A. Wold (Lincoln Lab.); J. Phys. Chem. Solids, Vol. 15, pp. 152-156, Aug. 1960

An investigation of the system $Fe_{4-x}Ni_xN$, $0 \leq x \leq 4$, is reported. In the range $0 \leq x \leq 3.33$, the compounds have the γ' (Fe_4N) structure; when $3.33 \leq x \leq 4$, a two phase region $Ni_3M + M_4N$ exists. Calculation of x-ray line intensities from diffraction patterns of the series $Fe_{4-x}Ni_xN$ indicate that the first nickel atom replaces the iron on the corners of the unit cell and that additional nickel replaces iron in a random manner. At ratios of Fe:Ni close to 1:1 a new phase is formed having the approximate composition FeNiN. This phase can be assigned a primitive tetragonal cell having a = 2.830 A and c = 3.713 A. The iron and nickel atoms are ordered with iron atoms located at the corners of the unit cell and nickel atoms at the body centers. The nitrogen atoms apparently lie at the c-face centers.

CRYSTAL GROWTH

7576 APPARATUS FOR THE FLOATING-ZONE REFINING OF GALLIUM ARSENIDE by F. A. Cunnell and R. Wickham (SERL); J. Sci. Instr., Vol. 37, pp. 410-414, Nov. 1960

The design and operation of equipment to purify and to grow single crystals of gallium arsenide are described. Features of the design include a demountable quartz system, adjustment of the relative position of the ends of the gallium arsenide rod during operation, excellent visibility, a traversable heater system and close control of the arsenic pressure in the tube. The latter feature has reduced the problem of ejection of molten material from the zone found in previous work.

7577 USE OF HIGH PRESSURE FURNACE IN THE PREPARATION OF INTERMETALLIC SEMICONDUCTOR COMPOUNDS [in French] by L. Giraudier (Ecole Normale Supérieure); J. Phys. Radium, Vol. 21, Suppl. to No. 11, pp. 149 A - 154 A, Nov. 1960

A high-pressure furnace for preparing compounds of magnesium with elements of group IV of the periodic table is described.

7578 PREPARATION AND PROPERTIES OF SILICON FILMS by W. J. McAleer, P. I. Pollak and H. Kallmann (New York U. and Merck); J. Electrochem. Soc., Vol. 107, p. 199C (A), Aug. 1960

A vacuum evaporation method for the preparation of silicon thin films from single crystal silicon emitters of known type and resistivity was described. These films exhibit larger than band gap photovoltages which vary markedly with the wavelength of the incident light and the temperature at which the measurements are made. Electron microscopic and x-ray diffraction examinations have been made to determine the mechanism responsible for these photovoltages.

Preparation of GaP Crystals - See 7703

Preparation of Ge-Si Alloys - See 7619

Preparation of AlP - See 7589

Preparation of (Zn, Hg) S and (Zn, Cd, Hg) S Electroluminescent Phosphors - See 7677

Preparation of FeNiN and the Series $Fe_{4-x}Ni_xN$ - See 7575

7579 GROWTH POISONING OF LITHIUM FLUORIDE FROM AQUEOUS SOLUTIONS by G. W. Sears (GE Res. Lab.); J. Chem. Phys., Vol. 33, pp. 1068-1074, Oct. 1960

The presence of a few parts per million of step poisons strongly alters both crystal growth and dissolution rates. It was known that a few PPM ferric fluoride was a poison for the dissolution of lithium fluoride. It is shown that ferric fluoride is also a growth poison for lithium fluoride from aqueous solution. Ferric fluoride has the properties characterizing a step poison for the lithium fluoride-water system.

7580 CUPROUS HALIDE FILMS ON ALKALI HALIDE CRYSTALS by L. M. Kraemer (Argonne Natl. Lab. and U. Chicago); J. Chem. Phys., Vol. 33, pp. 991-993, Oct. 1960

The formation of films of cuprous halides by evaporation and condensation in a vacuum onto substrates of alkali halide crystals at room temperature is described. The films were annealed for 15 min periods at temperatures between 60 and 150°C. Optical absorption spectra indicate that the annealing causes diffusion of CuCl and CuBr into KCl and KBr, but not into KI or NaCl, and of CuI into RbI, but not into KCl, KBr, KI, or NaCl. An interstitial mechanism for diffusion is consistent with the data but is not sufficient to account for the behavior of CuI.

Preparation of Thin Layers of the Thallium Halides - See 7549

Preparation of Single Crystals of LiH - See 7681

CRYSTAL SURFACES

7581 THE INITIAL STAGES OF OXIDATION OF GERMANI by J. R. Ligenza (Bell Labs.); J. Phys. Chem., Vol. 64, pp 1017-1022, Aug. 1960

Studies of the initial stages of oxidation on a germanium surface freed of combined and adsorbed oxygen by reduction with carbon monoxide at 600°, carried out with a vacuum microbalance sensitive to 1/300th of a GeO_2 layer, are reported. These experiments were done at an oxygen pressure of 75 mm and at temperatures from 25 to 400°. The oxidation laws were found to change with temperature and the extent of oxidation. The initial oxygen uptake is consistent with the viewpoint that the surfaces prepared by reduction in carbon monoxide behave as if they are atomically clean. The first oxygen layer, as one oxygen per surface germanium atom, forms in less than a minute on the clean surface. At temperatures below 250° a second layer of one oxygen per surface germanium atom forms according to the logarithmic rate law in agreement with the results of Green and Kafalas. Subsequent oxidation beyond the second layer is not logarithmic but obeys a Mott and Cabrera thin film-type equation. At temperatures about 250° the second layer forms in less than one minute. The subsequent oxidation rates beyond the second layer where only GeO_2 is formed, are very slow and even at 400° only 17.5 A of GeO_2 formed in three hours. Activation energies for the logarithmic law and for the Mott and Cabrera equations have been calculated.

7582 SURFACE HETEROGENEITY IN IRRADIATED SOLIDS by D. A. Young (Brookhaven Natl. Lab.); J. Phys. Chem. Solids Vol. 15, pp. 119-126, Aug. 1960

Experiments on the physical adsorption of krypton on unirradiated and neutron irradiated alumina are analyzed in terms of localized adsorption without marked lateral interaction on surfaces of varying heterogeneity. This interpretation is supported by the shape of the isotherm on unirradiated material and the dependence on coverage of the differential molar entropy of the adsorbed phase. The nature of the surface heterogeneities introduced by irradiation is discussed speculatively.

EFFECTS OF RADIATION

7583 THE ANNEALING OF ELECTRON IRRADIATION DAMAGE IN GRAPHITE by W. N. Reynolds and P. R. Goggin (Atomic Energy Res. Est.); Phil. Mag., Vol. 5, pp. 1049-1058, Oct. 1960

The irradiation of samples of pure artificial graphite with electrons at 79°K and the annealing characteristics of the changes in electrical conductivity, Hall effect and magnetoresistance are discussed. All three quantities show an anomalous annealing range below 120°K, and a simplified band theory calculation indicates that the concentrations of both electrons and positive holes increase during irradiation and also in the anomalous annealing range.

SOLID STATE PHYSICS

GENERAL

7584 CRYSTAL-CHEMICAL CHARACTERISTICS OF SEMICONDUCTING COMPOUNDS OF TRANSITION METALS by L. D. Dudkin (A. A. Baikov Inst. Metallurgy); Soviet Phys.-Solid State, Vol. 2, pp. 371-376, Sept. 1960

Two criteria for the formation of semiconducting phases in systems with transition metals are discussed. The first criterion is related to the possibility of change in the energy spectrum of d-electrons of the transition metal atoms; the second criterion is applied to those compounds wherein d^2sp^3 hybridization occurs in the metal atom. Applying the criteria, the nature of electron conductivity in a series of compounds of structural types NiAs, NaCl, $CrSi_2$, $MoSi_2$, CrSb, $CuAl_2$, and FeS_2 is discussed and predicted.

CRYSTAL PHYSICS
(including Energy Band Structure)

7585 PROTON MOTIONS IN AMMONIUM HALIDES BY SLOW NEUTRON CROSS-SECTION MEASUREMENTS by J. J. Rush, T. I. Taylor and W. W. Havens, Jr., (Columbia U.); Phys. Rev. Lett., Vol. 5, pp. 507-509 (L), Dec. 1, 1960

Measurements of the neutron scattering cross section per hydrogen atom for ammonia and the ammonium halides, as a function of neutron wavelength, are presented. The magnitude and limiting slopes of the scattering cross section curves are compared with data on the phase transition temperatures, torsional vibration frequencies, potential barrier to rotation, and types of motions in ammonium halide salts. Definite correlations between the data exist and are interpreted. It is concluded that total cross-section measurements can be used to provide evidence of the dynamics and strength of chemical binding of hydrogen in molecules and crystals.

Binding Properties of LiH - See 7681

7586 LOW TEMPERATURE TRANSPORT IN "SPLIT p-GERMANIUM" by S. H. Koenig and J. J. Hall (IBM); Phys. Rev. Lett., Vol. 5, pp. 550-553 (L), Dec. 15, 1960

The sign, ratio and approximate magnitude of the deformation potentials which describe the change, under shear, of the valence band are determined from conductivity and Hall mobility data taken on p-type Ge. The velocity dependence of the hole-acceptor recombination cross section is found to be independent of the acceptor ground-state energy over a limited range. Expressions for the splitting, under shear, of the valence band in Ge are given in terms of deformation potential constants b (strain of tetragonal symmetry) and d (strain of rhombohedral symmetry). From Hall mobility vs strain data taken at $T \leq 10°K$ the ratio of the deformation potential constants is found, $d/b = 2.1 \pm 15\%$. An estimate of valence band splitting allows a determination of $d \approx 1$ ev. Measurement of transverse conductivity at saturation strain indicated both d and $b < 0$. The activation energy, measured with a strain of 0.7×10^{-2} along the <100> direction and $T \approx 6°K$, is found to be 6.8×10^{-3} ev.

7587 INFRARED INVESTIGATION OF THE ACCEPTOR LEVELS FORMED BY COPPER IN GERMANIUM by D. L. Greenaway (U. Reading); Proc. Phys. Soc., Vol. 76, pp. 900-908, Dec. 1960

Infrared absorption measurements from 1 to 34μ made on germanium containing varying amounts of antimony and copper at temperatures down to 20°K are reported. The results indicate that the three acceptor levels introduced by copper into germanium can be identified by their effect on the low temperature absorption spectra of suitably doped samples. The appearance of the levels is in good agreement with the existing theory, and in addition to this, an excited state of the shallow acceptor level has been identified which has not been previously reported.

Strain-Induced Changes of Donor State Wave Functions - See 7614

Energy Gap of Solid Solutions of In_2Te_3 with II-VI Tellurides - See 7546

7588 SURFACE STATES IN A ONE-DIMENSIONAL PERFECT SEMI-INFINITE CRYSTAL by P. Phariseau (Lab. Krist. en Studie van Vaste Stoffen, Ghent); Physica, Vol. 26, pp. 737-743, Sept. 1960

The energy-spectrum of an electron moving in a one-dimensional lattice containing only one type of atom, represented as a Dirac δ-function, is studied by means of a Green's-function method in the one electron approximation. The formula giving the surface energy levels corresponds completely with that given by other authors. It can be proved by continuous variation of the parameters that the extra energy-levels leave the bottom of the upper energy-band and in this approximation never attain the top of the lower energy-band.

7589 PREPARATION, ELECTRICAL, AND OPTICAL CHARACTERISTICS OF AlP [in German] by H. G. Grimmeiss, W. Kischio and A. Rabenau (Philips); J. Phys. Chem. Solids, Vol. 16, pp. 302-309, Nov. 1960

Methods of preparing and doping AlP crystals are described. By measuring the reflectivity and transmission, the band gap of AlP was found to be 2.42 ev at 20°C. Undoped crystals show electroluminescence in bands at 5550 and 6150 A. The electroluminescence is shown to be due to recombination of charge carriers injected from p-n junctions. The peak of the photoluminescence is found at 6100 A. Together with conductivity measurements these results suggest a band picture for undoped AlP. Furthermore, the crystals exhibit point contact rectification and photovoltaic effects. The peak of the photoconductivity is found between 5000 and 5150 A.

7590 CLASSICAL ENERGY TRANSPORT IN DISORDERED LATTICES by R. J. Rubin (NBS); Bull. Am. Phys. Soc., Ser. II, Vol. 5, p. 422 (A), Nov. 25, 1960

For a simple cubic lattice consisting of an arbitrary distribution of two kinds of isotopes, the following initial value problem has been solved. At time $t = 0$, in a region R of the lattice, the velocities and positions of the atoms are canonically distributed at a temperature T: the rest of the lattice is at absolute zero. What is the mean square dispersion $\langle \sigma^2 \rangle$ of the velocity of

lattice particle A in R as a function of time if at t = 0 energy is allowed to move freely out of R? The solution is obtained by generalizing a method used recently by the author. The dispersion $<\sigma^2>$ at time t is equal to the energy which resides in region R at time t for the special initial state in which all lattice particles are at their equilibrium positions and all particles are at rest except A whose velocity is the rms value for the temperature T. The application of this result in a computing machine experiment was discussed.

7591 EFFECT OF SPIN-ORBIT SPLITTING ON THE FERMI SURFACES OF THE HEXAGONAL-CLOSE-PACKED METALS by M. H. Cohen and L. M. Falicov (U. Chicago); Phys. Rev. Lett., Vol. 5, pp. 544-546 (L), Dec. 15, 1960

The theory of the electronic properties of metals and alloys having the hcp structure is extended to include the effect of spin-orbit coupling. For a general point in the hexagonal face of the first Brillouin zone the degeneracy is lifted. The spin-orbit splitting is very small near the symmetry point A and increases from A along S initially as $(\Delta k)^3$ towards a maximum value at H. Calculated values of the splittings at H for magnesium are given. While the effect of spin-orbit splitting requires no major change of existing alloy theories, the Fermi surfaces of pure metals are fundamentally changed since the double zone scheme is no longer valid. It is shown that changes in the connectivity properties of the Fermi surface caused by spin-orbit coupling can explain the observed magnetoresistance in Mg.

DIELECTRIC PROPERTIES (including Ferroelectrics)

7592 A RADIO-FREQUENCY PERMITTIMETER by R. C. Powell and A. L. Rasmussen (NBS); IRE Trans., Vol. I-9, pp. 179-184 Sept. 1960

The use of a coaxial RF impedance transformer, in which the secondary is a single turn of the material to be measured, with a two-terminal impedance bridge to determine the complex permittivity or complex conductivity of low-impedance materials is described. No electrodes are needed, and many conductors, semiconductors, electrolytes and high-permittivity materials can be evaluated to about 1 per cent, since errors due to electrode impedance and interaction as well as first-order series inductance are eliminated. The design, calibration, range, and accuracy are given along with measured values of such materials as ferrites and strong electrolytic solutions, showing complex conductivities differing considerably from those previously observed by other methods.

7593 AN INVESTIGATION OF UHF SPECTRA OF SINGLE CRYSTALS OF $BaTiO_3$ by H. Diamond (Sylvania); U.S. Gov. Res. Rep., Vol. 34, p. 424 (A), Oct. 14, 1960 PB 147 439

The need for spectral information on good, single crystals of $BaTiO_3$ is discussed. The frequency range from 65 to 300 mc has been investigated using a method which continuously displays dielectric constant versus frequency; the particular range was chosen to check a previously reported resonance at 120 mc. Using spectrographic techniques, no such resonance was found. In the frequency and temperature ranges considered, the crystals showed a gradual reduction of dielectric constant at the higher frequencies.

7594 THE INFLUENCE OF IONIC CONDUCTIVITY ON THE ELECTRIC STRENGTH OF KCl AND NaCl by R. Cooper, R. M. Higgin and W. A. Smith (U. Manchester); Proc. Phys. Soc., Vol. 76, pp. 817-825, Dec. 1960

At high temperatures, the electric strengths of the alkali halides appear to decrease rapidly with rise in temperature. This behavior is qualitatively similar to that predicted by Froehlich's high temperature theory of breakdown. It can also be explained in terms of space charge and thermal effects due to the transport of ions and therefore speculation exists about the operative mechanism. The ionic conductivity of alkali halide crystals depends upon the amount of bivalent impurity they contain. This fact has been used to determine the influence of ionic conductivity upon the electric breakdown of KCl and NaCl. No evidence is provided to support Froehlich's high temperature theory, the observed negative temperature coefficient of KCl being attributed to ionic phenomena. Changes of up to sixtyfold in the ionic conductivity of NaCl did not influence the impulse electric strength of this material except at temperatures below about $-50^{\circ}C$, when the effect of increased conductivity was to increase the electric strength.

7595 POLARIZATION EFFECTS IN ELECTRICAL "CONDUCTIVITY" OF ARTIFICIAL SAPPHIRE AT HIGH TEMPERATURES by J. Cohen (Genl. Tel. Electronics); J. Phys. Chem. Solids, Vol. 16, pp. 285-290, Nov. 1960

Measurement of the apparent electrical conductivity of artificial sapphire in vacuo in the temperature range $900-1300^{\circ}C$ is described. The potential probe method was used to eliminate effects of high contact resistance. Ohm's law was not applicable, and the apparent conductivity was nonuniform. Polarization effects were prominent; e.g. large polarization voltages, anomalous potential distributions and decays in current immediately after application of a voltage. It is suggested that these effects are due to electronic and ionic space charges resulting principally from impurities.

7596 TRANSITIONAL DC CONDUCTION PROCESSES IN CERAMIC BARIUM TITANATE by V. M. Gurevich and I. S. Rez; Soviet Phys.-Solid State, Vol. 2, pp. 624-628, Oct. 1960

The d-c resistance of polycrystalline piezoelectric barium titanate is discussed. Both polarized and unpolarized specimens were investigated and shown to differ in electrical conductivity. Current through the specimen is not instantaneous, but develops over a period of minutes. During that period the so-called transitional processes of conduction take place. The application of transitional conduction processes in the investigation of piezoelectric polarization is discussed.

7597 IONIC HALL EFFECT IN SODIUM CHLORIDE by P. L. Read and E. Katz (U. Michigan); Phys. Rev. Lett., Vol. 5, pp. 466-467 (L), Nov. 15, 1960

The theory of the ionic Hall effect and a technique for measurement of the high temperature Hall mobility are described. High temperature ($610-780^{\circ}C$) ionic Hall effect measurements on pure single crystal NaCl were performed. The observed Hall voltage was proportional to the applied electric and magnetic fields and was insensitive to electrode pressure. An extrapolation to low temperature of the measured Hall mobility allowed an estimate of the activation energy and the pre-exponential coefficient A, for Na ions in NaCl. $\mu_H = AT^{-1}\exp(-E/kT)$, $A = 2.0^{+8}_{-1.5}$ $m^2 - {}^{\circ}K/v\text{-sec}$, $E = 0.87 \pm 0.1$ ev.

7598 THE REVERSAL OF THE SPONTANEOUS POLARIZATION IN GUANIDINE ALUMINUM SULFATE HEXAHYDRATE by E. Fatuzzo (RCA, Ltd.); Helv. Phys. Acta., Vol. 33, No. 5, pp. 429-436, 1960

An investigation of switching in Guanidine Aluminum Sulfate Hexahydrate (GASH) at high electric fields is reported. The samples were subjected to electrical and thermal treatment and their switching properties were studied under various conditions. Results of these studies indicate that at high fields the domain wall motion time is longer than the nucleation time and hence controls the switching process.

7599 THE NATURE OF A HIGH-TEMPERATURE PHASE TRANSITION IN SOME $BaTiO_3$-$BaSnO_3$ SOLID SOLUTIONS by S. V. Bogdanov and R. Ya. Razbash (P.N. Lebedev Phys. Inst.); Soviet Phys.-Solid State, Vol. 2, pp. 621-623, Oct. 1960

An investigation of the phase transition in the Curie region of polycrystalline solutions of 5, 7.5, 10, and 15 per cent barium stannate in barium titanate is discussed. The temperature dependence of permittivity on heating and cooling, as well as the simultaneous effect of constant fields of various intensities are the parameters studied. The results suggest that the phase transition in the Curie region is more likely a transition of the first type rather than of the second type.

7600 X-RAY STUDY OF PHASE TRANSITIONS IN FERROELECTRIC $PbNb_2O_6$ AND RELATED MATERIALS by E. C. Subbarao (Westinghouse); J. Am. Ceram. Soc., Vol. 43, pp. 439-442, Sept. 1960

The phase transitions in $PbNb_2O_6$ and in compositions of the type $Pb_{1+x}(B_xNb_{1-x})_2O_6$, where $B = Ti^{4+}$, Zr^{4+}, or Sn^{4+}, have been investigated between 25° and 650°C, using x-ray and dilatometric techniques. The modified $PbNb_2O_6$ compositions possess orthorhombic $PbNb_2O_6$-type structure, with the additional Pb^{2+} ions occupying vacant lattice sites. The lattice parameters a and c expand and b contracts during heating until, at the ferroelectric Curie temperature, a and b suddenly coincide and c expands slightly. Besides this phase change at the Curie temperature, the nonstoichiometric compounds show an additional phase transition in the range 450° to 300°C depending on composition. The intermediate phase of $Pb_{1+x}(Ti_xNb_{1-x})_2O_6$ appears to possess orthorhombic symmetry.

Cubic-Hexagonal Transition in $BaTiO_3$ - See 7548

7601 QUANTITATIVE STUDY OF LOW FREQUENCY HYSTERESIS LOOPS OF POLARIZED POLYCRYSTALLINE BARIUM TITANATE by G. S. Marks and D. A. Hanna (U.S. Navy Electronics Lab.); Acta Cryst., Vol. 13, p. 1074(A), Dec. 1960

Quantitative studies at 25°C of the 60 cps hysteresis loops of polarized barium titanate ceramics containing the following additives: 0%, 2%, 4%, $PbTiO_3$, and 12% $PbTiO_3$ plus 8% $CaTiO_3$ were described. Polarization versus time and field strength versus time curves have been analyzed by the Fourier method. The latter curves do not depart greatly from a sine wave. It is found that the energy loss represented by the area enclosed by a ferroelectric hysteresis loop varies as the square of the maximum applied field over a range from an initial value on the field axis up to saturation. Differential permittivities have been deduced from measured angles of slope at points on the hysteresis loops. Maxima are found in all curves when the applied field is opposite to the direction of polarization, and the value is constant or nearly so when the applied field is in the polarized direction. The normal permittivity has also been deduced from the hysteresis loops. By replacing the mica condenser in series with the polarized ceramic with a non-inductive resistor in the display circuit, current density versus field strength diagrams have been obtained. From such diagrams the differential complex conductivity has been determined. A small anomalous loop is observed in these diagrams at high field strengths. A partial explanation for this occurrence is given.

7602 DETERMINATION OF NONLINEAR CHARACTERISTICS OF FERROELECTRIC CERAMICS by P. N. Wolfe (Westinghouse); IRE Trans., Vol. I-9, pp. 161-167, Sept. 1960

Analysis of the behavior of devices employing low-dissipation-factor ferroelectric ceramics as nonlinear dielectrics requires a simple method of specifying numerically the relation between electric displacement and field. A technique for reducing experimental data to three parameters, descriptive of the nonlinear material behavior over a large electrical operating range, is described. Preparation of standard samples and experimental precautions to be observed are discussed.

7603 DIELECTRIC PROPERTIES OF LEAD TITANATE ZIRCONATE CERAMICS AT VERY LOW FREQUENCIES by R. Gerson (Clevite); J. Appl. Phys., Vol. 31, pp. 1615-1617, Sept. 1960

Measurements of the dielectric properties of lead titanate zirconate made between room temperature and 140°C at frequencies between 0.1 and 10 cps are reported. An observed increase in dielectric constant and dissipation factor at low frequency and high temperature is interpreted as an anomalous conduction phenomenon, rather than as an effect due to ferroelectric polarization. Over the frequency and temperature range studied the relationship between the real and the imaginary components of the dielectric constant is found to be linear. The data for unpoled ceramic and for material which had been poled to a maximum in piezoelectric activity are quite similar.

CARRIER PROPERTIES

7604 DIRECT OBSERVATION OF EXCITON MOTION IN CdS by D. G. Thomas (Bell Labs.); Phys. Rev. Lett., Vol. 5, pp. 505-507 (L), Dec. 1, 1960

A new experiment which gives a direct observation of exciton motion and a determination of the exciton mass in CdS is described. In a magnetic field the velocity, $\hbar\vec{k}/M$, of an intrinsic direct exciton created by a photon of wave vector $\vec{k}$ gives rise to a quasi-electric field which can shift the plane of symmetry of the Stark effect on excitons. This effect is observed from the separation between two pairs of lines in the Zeeman spectra of the n=2 exciton state in CdS at 1.6°K as a function of applied electric field. The measured mean displacement of the symmetry planes of 95±10 v/cm yields an exciton mass M of 1.1 electron masses. Shifts in the position of the symmetry planes by transverse Hall fields and experimental details are discussed.

7605 CONCERNING THE HOLE-CAPTURE CROSS SECTION OF DEFECTS PRODUCED BY γ-IRRADIATION by R. F. Konopleva, S. M. Ryvkin and I. D. Yaroshetskii (Physicotech. Inst.,

Leningrad); Soviet Phys.-Solid State, Vol. 2, pp. 533-535, Oct. 1960

The dependence of lifetime on gamma-ray irradiation in n-type germanium is discussed and the hole-capture cross section is determined. The Shockley-Read expression for lifetime is used, assuming that for each defect two adjacent charged states produce a single level which has the greatest significance in recombination. An average value of 3.8×10^{-15} cm^2 for hole-capture cross section is obtained, which is the same order of magnitude as that resulting from defects produced by neutron irradiation.

7606 ELECTRON EFFECTIVE MASS IN SOLIDS — A GENERALIZATION OF BARDEEN'S FORMULA by M. H. Cohen and F. S. Ham (GE); J. Phys. Chem. Solids, Vol. 16, pp. 177-183, Nov. 1960

A formula for the effective mass of an electron in a crystal which replaces the sum over excited states in the usual sum rule by an integral over the surface of the unit cell is derived. The integrand of the surface integral involves the wave function(s) at the symmetry point of band extremum k_0 and a second solution of Schroedinger's equation at the same energy satisfying inhomogeneous boundary conditions on the cell surface. The procedure is applicable whether or not there is a degeneracy at k_0, and spin-orbit coupling may be taken into account. The result thus represents a generalization of Bardeen's formula for the effective mass of an s-band at $k = 0$ in the Wigner-Seitz spherical approximation to an arbitrary band at any point k_0, using the polyhedral cell. A related variational principle for the components of the effective mass matrix is also derived.

7607 THE HOLE MOBILITY IN SELENIUM by W. E. Spear (U. Leicester); Proc. Phys. Soc., Vol. 76, pp. 826-832, Dec. 1960

A pulse method, developed for the study of effective mobility in insulating solids, is applied to evaporated specimens of vitreous Se. Charge carriers are generated near the top electrode by a 13 mμsec electron pulse and drift across the specimen in a pulsed applied field. The transit time of holes is measured with improved electronic apparatus having a bandwidth of 27 Mc/s. At 20°C the effective hole mobility μ lies between 0.13 and 0.14 cm^{2}sec^{-1}v^{-1}. The temperature dependence of μ shows that it is controlled by a level of acceptor states lying $\epsilon = 0.14$ev above the valence band. The values of μ and ϵ are in close agreement with those found for single crystals of hexagonal Se which suggests that the centers controlling μ are common to both forms of Se. It is concluded that the hole conduction is determined by the short range order within the Se chain itself or in close proximity to it. The carrier density, however, depends on the arrangement of the chains in the solid. From x-ray data the density of acceptor states is estimated as 10^{20}cm^{-3}, giving a value of about 60 cm^{2}sec^{-1}v^{-1} for the microscopic mobility.

7608 HOLE AND ELECTRON MOBILITIES IN DOPED SILICON FROM RADIOCHEMICAL AND CONDUCTIVITY MEASUREMENTS by K. B. Wolfstirn (Bell Labs.); J. Phys. Chem. Solids, Vol. 16, pp. 279-284, Nov. 1960

Room temperature (300°K) conductivity mobilities of holes and electrons in Ga, As, and Sb doped silicon are calculated from electrical and radiochemical measurements using the effective mass approximation. The concentration range investigated is from 10^{16} to 2×10^{18} cm^{-3} and from 4×10^{15} to 2.5×10^{19} cm^{-3} for p- and n-type silicon respectively. Ionization energies from Hall effect measurements and their concentration dependence are estimated for the nondegenerate specimens. Ionization is assumed to be complete in the degenerate cases. In addition, the results are compared with published drift, conductivity and Hall mobilities.

7609 THE DRIFT MOBILITY OF ELECTRONS AND HOLES IN GERMANIUM AT LOW TEMPERATURES by E. G. S. Paige (RRE); J. Phys. Chem. Solids, Vol. 16, pp. 207-219, Nov. 1960

Measurements of the drift mobility of electrons and holes in the temperature range from 20°K to 300°K in samples of germanium containing impurity concentrations from 7×10^{12} cm^{-3} to 4×10^{15} cm^{-3} are reported. Conductivity measurements were also made. Below 100°K the observed minority carrier mobility is less than the mobility calculated from the effects of scattering by phonons and ionized and neutral impurity atoms. The discrepancy, which is greater than a factor of 2 in some cases, has been attributed to electron-hole scattering. It is proposed that the unexpectedly large effect of electron-hole scattering is due to a drag exerted on the minority carriers by the majority carriers when an electric field is applied. Qualitative observations on the drift mobility of electrons were made below 20°K. There is no evidence that electrons remain localized about the same minimum in k space for the duration of a transit time (1/2 μsec). An extreme example of conductivity modulation of the injected carrier distribution has been observed when impact ionization takes place.

7610 ELECTRON MOBILITY AND SCATTERING PROCESSES IN AgBr AT LOW TEMPERATURES by D. C. Burnham, F. C. Brown and R. S. Knox (U. Illinois); Phys. Rev., Vol. 119, pp. 1560-1570, Sept. 1, 1960

Measurements of the Hall effect for electrons released by light in high-purity crystals of AgBr in the temperature range 4° to 120°K are reported. The observed mobilities exceed 20 000 cm^2/volt-sec at very low temperatures. The general features of the dependence of low-field Hall mobility on temperature can be understood by comparison with standard theory. A nearly exponential dependence of mobility on 1/T is observed from 40° to 120°K, as predicted for scattering by optical vibrations of the lattice. The slope of the (log μ) versus 1/T data agrees quite well with the Debye Θ for the longitudinal optical mode as deduced from reststrahlen data. Below 40°K the observed mobilities can be explained in terms of a combination of the effects of optical, acoustical and charged impurity scattering. The last process appears to dominate below 15°K. High-field effects are observed which can be explained by classical transport theory assuming a conduction band of standard form as well as isotropic scattering.

Mobilities in Ge-Si Alloys - See 7619

7611 A MONTE-CARLO CALCULATION FOR A SIZE EFFECT PROBLEM by B. Luethi and P. Wyder (ETH); Helv. Phys. Acta, Vol. 33, Nos. 6/7, pp. 667-674, 1960

Application of the Monte-Carlo method to the calculation of a size effect in electrical conductivity is discussed. In the case considered small angle electron-phonon scattering is present in addition to impurity and surface scattering. The calculated

mean free path shows a dependence on the diameter of the conductor, in agreement with recent experimental results by Olsen.

7612 A THEORY OF THE EFFECTS OF CARRIER-CARRIER SCATTERING ON MOBILITY IN SEMICONDUCTORS by T. P. McLean and E. G. S. Paige (RRE); J. Phys. Chem. Solids, Vol. 16, pp. 220-236, Nov. 1960

A theory which accounts for the effects of carrier-carrier scattering on the mobilities of the carriers in a semiconductor is developed. It is valid, in general, at low temperatures where carrier-carrier scattering effects are most important; and it assumes that the carriers are non-degenerate and move in bands which can be characterized by simple isotropic effective masses. Electron-electron and hole-hole scattering usually produce only small reductions in the mobility although, if ionized impurity scattering were the predominant scattering mechanism, they could reduce it by as much as ~40 per cent. Electron-hole scattering, due mainly to the opposite drift velocities of the electrons and holes and a consequent drag effect can produce large effects on the mobility, altering both its magnitude and temperature dependence. These effects are most clearly seen in the minority carrier mobility, and their inclusion yields mobilities in substantial agreement with those measured in Ge. In some cases, e.g. holes in n-type InSb, the drag effect is strong enough to give the minority carriers a negative mobility.

Phonon Scattering by Chemical Impurities in NaCl - See 7684

CONDUCTIVITY

7613 LOW-TEMPERATURE IMPURITY CONDUCTION AND MAGNETORESISTIVITY IN N-TYPE GERMANIUM by P. Csavinszky (Hughes Semicon.); Phys. Rev., Vol. 119, pp. 1605-1609, Sept. 1, 1960

The resistivities of several lightly doped (Sb) n-type germanium samples are calculated and compared with values measured at 2.5°K. An order of magnitude agreement has been obtained for a span of five orders of magnitude in the resistivities. It is assumed that the mechanism of conductivity consists of electrons jumping from occupied to empty donors. The number of charge carriers has been determined by calculating the number of "free" donor ions. The "trapped" donor ions, due to the presence of charged compensating acceptors, have been assumed not to participate in the conduction process. The effect of a constant magnetic field on impurity conduction has also been investigated and a simple theory of magnetoresistivity is presented. The calculated magnetoresistive ratio is in order of magnitude agreement with the measured value.

7614 EFFECT OF SHEAR ON IMPURITY CONDUCTION IN N-TYPE GERMANIUM by H. Fritsche (U. Chicago); Phys. Rev., Vol. 119, pp. 1899-1900, Sept. 15, 1960

Shear strains, which change the donor wave functions, greatly affect impurity conduction, which depends sensitively on the wave function overlap of neighboring impurity states. The change of impurity conduction of germanium containing 5.2 x 10^{15} antimony atoms per cc and about 3% compensation has been measured at 1.9°K as a function of shear strains produced by uniaxial tension and compression along [110]. It is shown that the anisotropy and the saturation of the conductivity changes observed at stresses larger than 4×10^8 dynes/cm^2 can be understood from the strain-induced changes of the donor state wave functions.

7615 RESISTIVITY MEASUREMENTS OF SEMICONDUCTORS AT 9000 MC by G. L. Allerton and J. R. Seifert (Western Electric); IRE Trans., Vol. I-9, pp. 175-179, Sept. 1960

A new approach to the measurement of volume resistivity of semiconductors is described. At present volume resistivity is measured by sending a direct current through a sample of the material and measuring the voltage drop across two points on the surface of the material. The new method uses a high frequency test signal and test samples to load the transmission system. The resistivity of limited areas and depths of material can be determined in this way.

7616 THE MEASUREMENT OF MICROWAVE RESISTIVITY BY EDDY CURRENT LOSS IN SMALL SPHERES by T. Kohane (Raytheon); IRE Trans., Vol. I-9, pp. 184-186, Sept. 1960

A cavity perturbation method for measuring the resistivity at microwave frequencies of small spherical polycrystalline samples is described. The sample is placed in the cavity at a region of maximum magnetic field and zero electric field. The eddy currents induced in the sample result in losses which are measured, thus permitting determination of the sample resistivity. No assumption is made regarding the depth of penetration of fields, the influence of skin effect being taken into account in an exact manner. Measurements have been carried out both above and below room temperatures.

Measurement of the Complex Conductivity of Low-Impedance Materials - See 7592

7617 CONCERNING THE EFFECT OF HEAT TREATMENT ON THE ELECTRICAL PROPERTIES OF P-TYPE SILICON by I. D. Kirvalidze and V. F. Zhukov (Physicotech. Inst.); Soviet Phys.-Solid State, Vol. 2, pp. 537-539, Oct. 1960.

The resistivity of silicon samples which have been heated to 800°C and quenched in oil to 50°C is discussed. Specific resistance rises sharply as a result of quenching, but then decreases spontaneously with time. The original resistivity value is recovered by annealing the quenched sample at 100°C for one hour. For samples subjected to a preliminary anneal at 1200°C for eight hours, a much smaller increase in resistivity after quenching is recorded.

7618 ANISOTROPIC CONDUCTION IN NONSTOICHIOMETRIC RUTILE (TiO_2) by L. E. Hollander, Jr. and R. L. Castro (Lockheed); Phys. Rev., Vol. 119, pp. 1882-1885, Sept. 15, 1960

Measurements of the anisotropic conductivity in rutile for different nonstoichiometric compositions are reported. This anisotropy, ρ_a/ρ_c, has a peak in excess of 10,000 to 1 and is a maximum at the nonstoichiometric composition corresponding to $\rho_c = 10^3$ ohm cm. Based on these data, it is proposed that for very nonstoichiometric material, impurity band conduction predominates, and as the material is made more stoichiometric, a transition to conventional conduction via the conduction band occurs. This transition occurs at very different nonstoichiometric compositions for the two crystal directions. Thus, a large anisotropy is observed in the intermediate region.

7619 ELECTRICAL CONDUCTIVITY AND HALL EFFECT OF Ge-Si ALLOYS [in German] by G. Busch and O. Vogt (ETH); Helv. Phys. Acta, Vol. 33, No. 5, pp. 437-458, 1960

The preparation of Ge-Si single crystal or coarsely polycrystalline alloys is extensively described. The composition of the samples has been determined by measurements of densities and lattice constants. Hall-constants and electrical conductivities have been measured as functions of temperature between 20 and 900°C. Mobilities for electrons and holes and intrinsic carrier concentrations are calculated as functions of the alloy composition.

7620 AN INVESTIGATION OF THE SEMICONDUCTING PROPERTIES IN THE SILICON-COBALT SYSTEM by E. N. Nikitin (Inst. Semicon., Leningrad); Soviet Phys.-Solid State, Vol. 2, pp. 588-591, Oct. 1960

The electrical conductivity and thermoelectric power of compounds in the silicon-cobalt system are discussed. On the electrical conductivity-composition curve, maxima occur at Co_3Si, Co_2Si, CoSi, and $CoSi_2$, indicating they have properties of an intermetallic compound. The steepness of the curve near the stoichiometric points made it difficult to obtain reproducible results. For CoSi, both the temperature coefficient of the electrical conductivity and the thermoelectric power, when related to minor deviations from stoichiometry, do not represent changes characteristic of semiconductors.

7621 ELECTRONIC CONDUCTION AND EXCHANGE INTERACTION IN A NEW CLASS OF CONDUCTIVE ORGANIC SOLIDS by R. G. Kepler, P. E. Bierstedt, and R. E. Merrifield (duPont); Phys. Rev. Lett., Vol. 5, pp. 503-504(L), Dec. 1, 1960

Measurements of the electrical conductivity, the activation energy, and the magnetic susceptibility and its temperature dependence of three tetracyanoquinodimethan $[TCNQ\cdot]^-$ radical-anion salts are reported. Quinolinium salt exhibits the largest electrical conductivity reported for an organic solid, virtual absence of an activation energy for conductivity, temperature-independent paramagnetism, and a density of states at the Fermi surface of 7.5 states/ev molecule. Measurements of magnetic susceptibility in triethylammonium salt yield a J value of 0.041 ev. The electrical conductivity is highly anisotropic. A thermoelectric power of -100 μv/°C is reported. No Hall voltage was detected. In $K^+ [TCNQ\cdot]^-$, low electrical conductivity and a relatively high activation energy were found. The magnetic susceptibility is negative and temperature independent from 77 - 450°K.

SUPERCONDUCTIVITY

7622 AN ANALOG SOLUTION FOR THE STATIC LONDON EQUATIONS OF SUPERCONDUCTIVITY by N. H. Meyers (IBM); Proc. IRE, Vol. 48, pp. 1603-1607, Sept. 1960

A novel analog method of obtaining solutions of the static London equations of superconductivity in complicated geometries is discussed. The method makes use of the similarity in form of the static London equations and the dynamic skin-effect equations of normal conduction under exponentially-growing steady-state conditions. Conveniently scaled copper models of superconducting geometries of interest can be constructed and excited from a growing-exponential function generator. Field distributions measured in the space around the normal conductors of the model correspond with the desired distributions in the analogous superconductor geometry. The method is particularly useful in studying thin films which are appreciably penetrated by magnetic fields. The experimental setup and the measurement technique are discussed. Illustrative results from a copper model of a long rectangular superconducting strip, 1830 penetration depths wide and 3.81 penetration depths thick are presented.

7623 SOME STUDIES OF THE SUPERCONDUCTING TRANSITION IN PURIFIED TANTALUM by J. I. Budnick (IBM); Phys. Rev., Vol. 119, pp. 1578-1586, Sept. 1, 1960

Observations of extremely sharp magnetic transitions from the superconducting to the normal state in highly purified tantalum specimens with residual resistivities approaching 1×10^{-3} μ ohm cm are discussed. Negligible flux trapping and pronounced supercooling is found to occur in these samples near the transition temperature T_c. Values of T_c as high as $4.483°K \pm .002°$ and of the critical field at 0°K, H_0, as low as 830±8 gauss were measured for these specimens. The critical field curve has a maximum deviation from a parabolic temperature dependence of about 3%. For tantalum the transition temperature decreases with increasing residual resistivity in much the same way as that observed by Serin and co-workers in dilute substitutional alloys. An investigation of the current dependence of the resistance transition in a magnetic field is reported.

7624 THE MEISSNER EFFECT IN THE QUASI-CHEMICAL EQUILIBRIUM THEORY OF SUPERCONDUCTIVITY by J. M. Blatt (U. New South Wales); Prog. Theoret. Phys., Vol. 24 pp. 851-876, Oct. 1960

An explicitly gauge-invariant proof of the Meissner-Ochsenfeld effect (magnetic field expulsion from a superconductor), based on the quasi-chemical equilibrium theory of superconductivity, is presented. The essential condition for the Meissner effect is the Bose-Einstein condensation of electron pairs. Other aspects of the problem, such as the energy gap and plasma waves, are not necessary for the Meissner effect and do not appear in the calculation. The random phase approximation is not used.

7625 PROPERTIES OF SOME MAGNETIC SUPERCONDUCTORS by R. M. Bozorth, D. D. Davis and A. J. Williams (Bell Labs.); Phys. Rev., Vol. 119, pp. 1570-1576, Sept. 1, 1960

An investigation of two solid solutions in the system $GdRu_2$—$CeRu_2$, in which both ferromagnetism and superconductivity have been observed, is reported. The solid solution $Gd_{0.082}Ce_{0.918}Ru_2$ which has a Curie point θ above the critical temperature T_s for superconductivity, is both ferromagnetic and superconducting. In $Gd_{0.04}Ce_{0.96}Ru_2$, for which the expected $\theta < T_s$, no ferromagnetic moment could be measured, although a small moment may be present and not detected. In solid solutions of increasing Gd content, when θ begins to exceed the expected T_s by a considerable margin, T_s suddenly drops toward zero; and when $T_s > \theta$, θ approaches zero. Similar conclusions apply to the system $GdOs_2$—$LaOs_2$ when θ and T_s are related in the same ways. Both major and minor hysteresis loops have forms not previously observed and enable one to detect ferromagnetism and superconductivity when they exist.

forms not previously observed and enable one to detect ferromagnetism and superconductivity when they exist. The molecular fields resulting from the interaction between Gd atoms, and the Curie points calculated therefrom by molecular field theory, increase with increasing temperature; this is in accordance with the theory of long-range exchange forces developed by Brout.

7626 CRITICAL FIELDS OF THIN SUPERCONDUCTING FILMS by W. B. Ittner, III (IBM); Phys. Rev., Vol. 119, pp. 1591-1596, Sept. 1, 1960

The critical fields of thin superconducting films calculated on the basis of the Bardeen-Cooper-Schrieffer (BCS) theory of superconductivity following a method outlined by Schrieffer are discussed. It is shown that it is convenient to use the critical field formula postulated by London where the London penetration depth is replaced by an effective penetration depth which can be specified through the use of the BCS theory. The effective penetration depth, unlike the London penetration depth which, for a given material, varies only with the temperature, is found to vary, in the BCS theory, with both the film thickness and the electronic mean free path of the normal material. It is shown that the measured critical fields of thin tin films are in general qualitative agreement with the predictions of the BCS theory.

7627 ELECTRON TUNNELING BETWEEN TWO SUPERCONDUCTORS by I. Giaever (GE); Phys. Rev. Lett., Vol. 5, pp. 464-466 (L), Nov. 15, 1960

A qualitative analysis of the tunnel effect between two superconductors separated by an insulating film is presented. Measurements of tunnel current as a function of applied voltage were made on the superconducting systems Al-Al_2O_3-In and Al-Al_2O_3-Pb. The samples were in the form of metal-oxide-metal sandwiches. The values of the superconducting energy gap, measured from the I-V characteristics, are: $2\epsilon_{Pb} = (2.68 \pm 0.06) \times 10^{-3}$ev, $T = 1.0^{\circ}K$; $2\epsilon_{In} = (1.05 \pm 0.03) \times 10^{-3}$ev, $T = 1.1^{\circ}K$; $2\epsilon_{Al} = (0.32 \pm 0.03) \times 10^{-3}$ev, $T = 1.1^{\circ}K$.

OTHER ELECTRICAL PROPERTIES

Optical Radiation from Breakdown Avalanches in Ge - See 7675 and 7676

7628 EFFECT OF OXYGEN ON THE MAGNETORESISTANCE OF COPPER by R. L. Dolecek (U.S. Naval Res. Lab.); Phys. Rev., Vol. 119, pp. 1501-1502, Sept. 1, 1960

To determine the influence of physical and/or chemical impurities on the high field magnetoresistance of copper, measurements of the effect on specimen properties of work hardening and the presence of O_2 in the atmosphere used for annealing have been made. A Kohler plot of the transverse magnetoresistance for all specimens gave a single smooth curve. The plot for the longitudinal magnetoresistance of any one specimen as the concentration of defects was increased between successive measurements, also gave a smooth curve. However, the saturation value of the longitudinal magnetoresistance was markedly affected by annealing in an atmosphere containing O_2. The zero field ratio of transverse to longitudinal magnetoresistance was found to be quite insensitive to work hardening and the presence of O_2 in the annealing atmosphere.

Low-Temperature Magnetoresistivity in N-Type Ge - See 7613

Hall Effect in Ge-Si Alloys - See 7619

7629 ON THE INFLUENCE OF DIFFUSION AND SURFACE RECOMBINATION UPON THE GR NOISE SPECTRUM OF SEMICONDUCTORS by K. S. Champlin (U. Minnesota); Physica, Vol. 26, pp. 751-760, Sept. 1960

Several theories of generation-recombination (GR) noise in nearly intrinsic semiconductors which consider the effects of diffusion and surface recombination are discussed. It is shown that the earlier eigenfunction treatments of Hyde and of van Vliet and van der Ziel do not allow for the fact that Fourier coefficients of different spatial modes are correlated. A proper treatment based on a transmission line analogy is presented and the result is examined for the cases arising when the recombination process is: 1) volume-limited; 2) surface-limited; and 3) diffusion-limited. For the diffusion-limited case, it is found that the spectrum varies as ω^{-1} at high frequencies; at low frequencies, the noise determined from the turnover frequency is 5/6 that found for the volume- and surface-limited cases.

7630 THERMAL-ELECTRON EMISSION FROM BARIUM TUNGSTATE by A. I. Mel'nikov, A. V. Morosov, R. B. Sobolevskaya and A. R. Shul'man; Soviet Phys.-Solid State, Vol. 2, pp. 650-654, Oct. 1960

Electron emission properties of a pure barium tungstate cathode operating in a vacuum diode are discussed. The high current densities are related to the activation of the cathode. After twenty minutes' activation, intense emission is obtained from almost the entire surface of the cathode. Cathode work function and current density are obtained. The low value of the Schottky temperature indicates a similarity between these cathodes and semiconductor emitters.

7631 AUGER ELECTRON EJECTION FROM GERMANIUM AND SILICON BY NOBLE GAS IONS by D. Hagstrum (Bell Labs.); Phys. Rev., Vol. 119, pp. 940-952, Aug. 1, 1960

The results of a study of electron ejection from annealed atomically cleaned (111) and (100) faces of silicon and the (111) face of germanium by singly charged noble gas ions of kinetic energies in the range 10 to 1000ev are reported. Total yield and kinetic energy distribution of the ejected electrons were measured. A new method of operation of the apparatus and of obtaining the kinetic energy distributions from the recorded retarding potential data has been employed. The state of the target surfaces has been carefully documented and photomicrographs and electron micrographs of the silicon surfaces are presented. Only a brief identification of the basic results with theoretical ideas is given.

7632 ANISOTROPY OF THE SURFACE BREAKDOWN OF GERMANIUM IN STRONG FIELDS by A. I. Morozov (Radio Eng. Electronics Inst.); Soviet Phys.-Solid State, Vol. 2, pp. 578-580, Oct. 1960

The anisotropic surface breakdown of n- and p-type germanium

in the (110) and (111) planes is discussed. Single current pulses from 10 to 1000 microseconds in duration and maximum amplitude of 30 amp were applied to germanium through a point contact. When the point was positive, a certain pulse amplitude produced a directed discharge visible as a straight band emitting reddish light along the germanium surface, and resulting in channels. Photomicrographs of channelled surfaces are presented. Easy and difficult directions of channelization were found relative to the growth axis of the crystal.

7633 EFFECT OF LANDAU LEVELS UPON TUNNEL CURRENTS IN INDIUM ANTIMONIDE by A. C. Chynoweth, R. A. Logan, and P. A. Wolff (Bell Labs.); Phys. Rev. Lett., Vol. 5, pp. 548-550 (L), Dec. 15, 1960

Oscillatory variation in tunnel current with applied magnetic field is investigated. The diodes used as samples were made by alloying a 0.1% Cd pellet into n-type InSb. One diode was an Esaki junction, the other a backward diode. I-V characteristics, taken at 4°K, showed that as the magnetic field was varied from 0 to 85 kgauss the tunnel current underwent an oscillation. Oscillations were observed with H parallel to the junction field but not with H perpendicular to the junction field. The amplitude and field spacing of the observed oscillations increased with H. Level density fluctuation of the Fermi surface, due to the intersection of the bottom Landau sub-band and the Fermi-level, are shown to be responsible for the observed oscillations.

Electrical Properties of GaP - See 7703

FERRO- AND FERRIMAGNETISM

7634 SOME PROPERTIES OF CONCENTRATED AND DILUTE HEISENBERG MAGNETS WITH GENERAL SPIN by R. J. Elliott (Clarendon Lab.); J. Phys. Chem. Solids, Vol. 16, pp. 165-168, Nov. 1960

Use of the constant-coupling approximation to obtain the thermodynamic properties of a Heisenberg ferromagnet of general spin above the transition temperature is presented. The spin concentration dependence of the thermodynamic properties in an alloy is also discussed. Similar results for antiferromagnets are included.

Properties of Some Ferromagnetic Superconductors - See 7625

7635 THE BEHAVIOR OF MAGNETIC SYSTEMS WITH DILUTION by J. S. Smart (Off. Naval Res.); J. Phys. Chem. Solids, Vol. 16, pp. 169-173, Nov. 1960

A generalization of the Bethe-Peierls-Weiss method to include alloys and solid solutions is presented. The method is then used to study the effects of magnetic dilution on a classical Heisenberg ferromagnet with nearest-neighbor interactions only. The results are qualitatively and quantitatively similar to those obtained by Sato, et al. using an Ising model. In particular the limiting concentration for ferromagnetism is found to be $(z-1)^{-1}$ where z is the number of nearest neighbors.

7636 CLASSICAL THEORY OF SPIN CONFIGURATIONS IN THE CUBIC SPINEL by T. A. Kaplan (Lincoln Lab.); Phys. Rev. Vol. 119, pp. 1460-1470, Sept. 1, 1960

It is shown that the Yafet-Kittel triangular spin-configurations in the cubic spinel do not minimize the classical Heisenberg exchange energy. (Only nearest-neighbor A-B and B-B interactions, J_{AB} and J_{BB}, are included; one spin-magnitude S_A for the A sites, and one, S_B, for the B sites is assumed.) A theory of the classical ground state more general than that of Yafet and Kittel is investigated. This consists of first determining the largest value, y_0, of $y \equiv J_{BB}S_B/J_{AB}S_A$ for which the Néel configuration is stable with respect to arbitrary small spin-deviations. (y_0 is roughly 10 per cent smaller than the value of y found by Yafet and Kittel for the breakdown of the Néel configuration.) A perturbation method for finding the minimum energy configuration when $y - y_0$ is small and positive is then employed. It is concluded, (1) that equilibrium configurations exist which have nonzero angles between spins on the A sites simultaneously with angles between those on the B sites in contrast with the Yafet-Kittel results; and (2) that there will be long-range-ordered, canted spin configurations in the cubic spinel, contrary to Anderson's suggestion. These conclusions are discussed in connection with experiments on $MnCr_2O_4$ and Mn_3O_4.

7637 CALCULATION OF UNIAXIAL SPIN HAMILTONIAN CONSTANTS IN YIG by J. J. Pearson (Westinghouse); Sixth Conf. Magnetism and Magnetic Materials, Nov. 14-17, 1960, New York, N.Y.

The uniaxial spin Hamiltonian constants in YIG are calculated by a method which considers the distortion of the spherical charge cloud surrounding a magnetic ion by its non-magnetic nearest neighbors, and averages the individual electron spin-orbit and spin-spin interaction over the distorted charge distribution. In YIG there are two types of Fe^{+++} sites, one surrounded by an octahedron of 0^{--} ions and the other by a tetrahedron, each trigonally distorted from the regular figures. The constants D in a spin Hamiltonian term of the form DS_z^2 have been measured experimentally by Geschwind, and found to have the values: $D_{octahedral} = -0.14\,cm^{-1}$ and $D_{tetrahedral} = -0.093\,cm^{-1}$. The present calculation yields values: $D_{octahedral} = -0.11\,cm^{-1}$ and $D_{tetrahedral} = -0.090\,cm^{-1}$. Although the excellent agreement is certainly fortuitous because of the rough estimates of overlap and transfer integrals used, the calculation shows that the effect considered does produce anisotropy of the observed order of magnitude.

7638 CONTRIBUTION OF THE FERMI CONTACT TERM TO THE MAGNETIC FIELD AT THE NUCLEUS IN FERROMAGNETS by A. J. Freeman and R. E. Watson (MIT); Phys. Rev. Lett., Vol. 5, pp. 498-500 (L), Dec. 1, 1960

Results of a Hartree-Fock spin-polarized calculation of the Fermi-contact interaction contribution H_c to the effective magnetic field H_e at the nucleus in ferromagnets are discussed. The estimates of H_c for Fe is -280 kgauss which is insufficient to account for the observed H_e. The one-electron 3d spin and charge densities for Fe in both $3d^64s^2$ and $3d^8$ configurations are plotted; they show that while the charge density of the $3d^8$ configuration is expanded relative to $3d^64s^2$, the spin density is not. This result agrees with neutron measurements and energy band calculations. Further calculations are presented which show that H_c is a sensitive function of the maximum of the 3d orbital for Fe $3d^8$ and thus small changes in the 3d functions may yield substantial lowering of H_c.

7639 MONTE CARLO COMPUTATIONS ON THE ISING MODEL: THE BODY-CENTERED CUBIC LATTICE by L. Guttman (GE Res. Lab.); Bull. Am. Phys. Soc., Ser. II, Vol. 5, pp. 420-421 (A), Nov. 25, 1960

Use of the Monte Carlo method of computation to obtain some equilibrium properties of body-centered cubic binary solid solutions whose atoms interact according to the Ising model was described. Four cases have been treated: (a) N = 128, c = 1/2, (b) N = 1024, c = 1/2, (c) N = 1024, c = 3/8, and (d) N = 1024, c = 1/4; N being the total number of atoms and c the fraction of one kind. In all cases the heat capacity has a well-defined maximum. At the equiatomic composition, the height of this maximum is greater in the larger crystal. Discontinuities in thermodynamic properties were not observed, and it seems reasonable that the order-disorder transition in an infinite crystal would be characterized by an infinite heat capacity, as calculated by Onsager and others for two-dimensional crystals. Comparison of the results with experimental properties of β-CuZn suggests a remarkable applicability of the Ising model to this system. The potentialities and limitations of the Monte Carlo method for systems with phase transitions were discussed.

7640 TORQUE MEASUREMENTS ON DOPED YTTRIUM IRON GARNET by R. F. Pearson and R. W. Cooper (Mullard Res. Labs.); Sixth Conf. Magnetism and Magnetic Materials, Nov. 14-17, 1960, New York, N.Y.

Torque measurements made at 20°K, 4.2°K, and 1.5°K on yttrium iron garnet crystals containing small rare earth dopings are reported. For these crystals the energy surface deduced from the torque curves is consistent with the resonance field behavior observed by Dillon. The torque curve of the crystal containing Tb had more pronounced discontinuities than any other samples and variation in the applied field between 7,000 and 15,000 oersteds did not alter the angle at which they occurred whereas shifts of up to 5° had been predicted using the Kittel model. So far attempts to correlate the position of the discontinuities in the (110) and (100) planes which showed fewer discontinuities have proved unsuccessful using the above model. At 20°K the torque curve can be analyzed in the standard way giving values of K_1 and K_2 of +88,000 and −460,000 ergs/cc respectively. The torque curve for Ho sample at 4.2°K was steepest at the [110] and [100] directions, in agreement with the position of the resonance peaks reported by Dillon. However, for the Dy crystal no sharp discontinuities are observed and the torque curve shows a large $\sin 8\theta$ component. On reducing the temperature from 4.2°K to 1.5°K, no change in the curve was observed. The curves for Ho and Dy were found to be quite reversible in the fields of 15,000 oersteds.

7641 MEASUREMENT OF MICROWAVE FERRITES AT HIGH SIGNAL LEVELS by J. F. Ollom and W. H. von Aulock (Bell Labs.); IRE Trans., Vol. I-9, pp. 187-193, Sept. 1960

Waveguide configurations suitable for high power microwave measurements on ferrites are discussed. The following experiments are considered: 1) determination of the critical internal RF magnet field h_c at which the loss characteristics of the ferrite become non-linear, 2) measurement of the loss characteristic as a function of the biasing d-c magnet field at a given RF signal level, 3) observation of deterioration of the transmitted pulse, and 4) measurement of high-power effects as a function of material composition, sample shape and size. Instrumentation for measurements at peak-power levels up to several hundred kilowatts is described, and experimental results are compared with H. Suhl's theoretical predictions.

7642 STUDY OF MAGNETIC AFTER-EFFECT IN MAGNESIUM MANGANESE FERRITES by S. Krupicka (Inst. Tech. Phys., Prague); Czech. J. Phys., Vol. 10B, No. 11, pp. 782-810, 1960

An investigation of the magnetic after-effect caused by the diffusion of electrons in MnMg ferrites of the series $Mg_xMn_{1.15-x}Fe_{1.85}O_{4+\gamma}$ is reported. Measurements were also carried out on a sample of $MgFe_2O_{4+\gamma}$ ($\gamma<0$). By combining two methods, i.e. (a) investigation of the disaccommodation of initial permeability at different temperatures and (b) measurement of the displacement of the maximum of the temperature dependence of tan δ with the frequency, it was possible to study the relaxation processes whose time constants were between 0.5 sec and several hours, or between 10^{-4} to 10^{-7} sec. It was found that the processes taking place at low temperatures and studied by method (a) differ from those observed at high temperatures by method (b), particularly in the lower activation energies and greater dispersion of the time constants. In addition to these two main relaxation processes a weak relaxation superposed over the main disaccommodation was found in ferrites with non-zero content of manganese. An analysis of the intensity of different relaxation effects showed the participation of Mn ions in these relaxation effects and it was found that both main relaxations are probably equivalent as regards the final steady state, to the creation of which they lead; they differ however in the mechanism of electron diffusion by which this state is realized. The main features of the different diffusion mechanisms are discussed.

7643 POLARIZATION OF THE CONDUCTION ELECTRONS IN THE FERROMAGNETIC METALS by A. J. F. Boyle, D. St. P. Bunbury and C. Edwards (U. Manchester); Phys. Rev. Lett., Vol. 5, pp. 553-556 (L), Dec. 15, 1960

The polarization of the 4S conduction electrons in Fe, Co, and Ni is examined by determination of the sign and magnitude of the magnetic field at Sn nuclei present to 1 per cent in the ferromagnetic samples. The Zeeman splitting of the 24 Kev transition in Sn^{119} was observed using the Moessbauer effect. The results of the measurements were: $H_{s\,Fe} = -81$ Koe; $H_{s\,Co} = -20.5$ Koe; $H_{s\,Ni} = +18$ Koe; where H_s is the field at the Sn nucleus and is given by $H_s = 4\pi/3\,M + H_c$, H_c = contact interaction field. Possible mechanisms to account for the observed results are discussed.

7644 ANISOTROPIC MAGNETIZATION by E. R. Callen (U. S. Naval Ord. Lab.) and H. B. Callen (U. Pennsylvania); J. Phys. Chem. Solids, Vol. 16, pp. 310-328, Nov. 1960

In the presence of magnetocrystalline anisotropy the magnetization of a ferromagnet depends upon its orientation as well as upon the temperature. The magnitude and temperature dependence of the anisotropic magnetization and the conditions under which it should be observable, are discussed. The non-spherical terms are small in iron and nickel, but are appreciable in some uniaxial materials, and large in crystals of low Curie point and large anisotropy. In these materials the magnetization will have a temperature dependence very unlike the Brillouin or spin-wave functions.

7645 ANISOTROPY OF THE INTRINSIC DOMAIN MAGNETIZATION OF A FERROMAGNET by S. H. Charap (IBM);

Phys. Rev., Vol. 119, pp. 1538-1542, Sept. 1, 1960

The effect of pseudodipolar coupling on the intrinsic domain magnetization of a cubic ferromagnet at low temperatures is investigated. Besides the anisotropy in the magnetization resulting from the dependence of the thermal excitation of spin waves on magnetization direction in the crystal, the pseudodipolar coupling is capable of making an anisotropic contribution to the magnetization, even at $T = 0^{\circ}K$, in the same approximation as its contribution to the first order anisotropy constant K_1. Both effects are calculated and found to be in opposition to one another, tending to cancel in nickel at about $7.5^{\circ}K$.

7646 DOMAIN STRUCTURE IN YTTRIUM IRON GARNET by A. W. Smith and G. W. Williams (Def. Res. Telecommun. Est., Ontario); Can. J. Phys., Vol. 38, pp. 1187-1194, Sept. 1960

Studies of the magnetic domain structure in thin slices of yttrium iron garnet crystals by transmitted polarized light are reported. The transmitted light exhibits Faraday rotation and magnetic birefringence, and both effects have been used to observe the domain structure. An example of structure in samples having a growth face on one side is presented for each of the (110) and (112) planes. The structure for the (110) face is similar to that for an ideal sample in this plane. The structure for the (112) face differs from an ideal sample due to a large strain anisotropy.

7647 FERRIMAGNETIC RESONANCE FIELD OF TERBIUM DOPED YTTRIUM IRON GARNET by L. R. Walker (Bell Labs.); Bull. Am. Phys. Soc., Ser. II, Vol. 5, p. 418(A), Nov. 25, 1960

Dillon and Nielsen found that if small amounts, of the order of 0.1% or less, of the yttrium ions in yttrium iron garnet were replaced by terbium, the field for resonance at liquid helium temperatures showed a very strong dependence upon d-c field direction. Kittel suggested that if the lowest pair of energy levels of the terbium ions approached closely for particular d-c field directions, large excursions of the resonance field would occur. The resonance field has been calculated by actually evaluating the RF susceptibility and d-c magnetization of the terbium from its energy levels and wave functions. To evaluate these a plausible spin Hamiltonian, containing three adjustable parameters, for a terbium ion on a dodecahedral site of the host lattice was used, utilizing the point charge potential of the oxygen neighbors as a guide. A quite satisfactory quantitative fit with the observed fields is obtained which appears to be insensitive to substantial changes in some of the crystal field parameters.

7648 FERRIMAGNETIC RESONANCE IN THREE-SUBLATTICE SYSTEMS by R. K. Wangsness (U.S. Naval Ord. Lab.); Phys. Rev., Vol. 119, pp. 1496-1500, Sept. 1, 1960

Two classes of three-sublattice systems are considered: antiparallel and triangular. The general solution of the undamped equations of motion is obtained and approximated to the highest order of the molecular field coefficients of interest for each case. For the antiparallel case, the components of the susceptibility tensor are obtained up to the first correction term to the usual expressions. For the triangular case, the leading terms needed for the susceptibility tensor are obtained and the effective gyromagnetic ratio is evaluated; the latter is quite different from the form usually assumed. A new effect is also predicted for the triangular case when all sublattice gyromagnetic ratios are different; this effect consists of the production of an oscillating magnetization component perpendicular to the oscillating field and of the same frequency and is not a consequence of nonlinear terms in the equations of motion.

7649 THEORY OF FERROMAGNETIC RESONANCE LINE SHAPE IN INSULATORS by J. Loos (Inst. Tech. Phys., Prague); Czech. J. Phys., Vol. 10B, No. 11, pp. 775-781, 1960

The absorption of the energy of a high-frequency field by a magnetic sample is discussed from the point of view of the interaction of spin waves with phonons and spin waves among themselves. A general expression for the form of the absorption curve is derived, using the method known from the quantum theory of radiation and assuming very weak fields.

7650 ANISOTROPIC FERROMAGNETIC RESONANCE LINEWIDTH IN FERRITES by H. B. Callen and E. Pittelli (U. Pennsylvania); Phys. Rev., Vol. 119, pp. 1523-1531, Sept. 1, 1960

In disordered magnetic materials such as the ferrites, the dominant source of resonance linewidth can be attributed to processes involving only two elementary excitations: the destruction of a magnon with the creation either of another magnon or a phonon. The primary magnon-magnon scattering process is considered. It is shown that the random variation of the spin-orbit coupling parameters of the disordered ions leads to a resonance linewidth comparable to that observed in ferrites. The particular symmetry of the crystalline fields around the octahedrally coordinated sites causes an anisotropy in the linewidth with a minimum in the [100] directions and a maximum in the [111] directions. This anisotropy of linewidth is in general agreement with experimental observations on typical ferrites, as for example, the measurements of Schnitzler, Folen, and Rado on disordered lithium ferrite.

7651 ON SOME CALCIUM-IRON-OXYGEN COMPOUNDS by P. G. Braun and W. Kwestroo (N. V. Philips); Philips Res. Rep., Vol. 15, pp. 394-397, Aug. 1960

Three new calcium oxide-iron compounds stabilized by the addition of small amounts of a third component are described: (1) $Ca_4Fe_{14}O_{25}$, hexagonal ($R\bar{3}c$) with $a = 6.0$ A and $c = 95.0$ A. Stabilized by, e.g., Y^{3+}. Ferrimagnetic, preferential plane of magnetization. (2) $Ca_4Fe_{14}O_{25}$, hexagonal ($P3c$) with $a = 6.0$ A and $c = 31.6$ A. Stabilized by, e.g., Mg^{2+}. (3) $Ca_4Fe^{2+}{}_2Fe^{3+}{}_{18}O_{33}$, hexagonal ($R\bar{3}c$) with $a = 6.0$ A and $c = 62.3$ A, also stabilized by, e.g., Mg^{2+} ions. Ferrimagnetic, preferential plane of magnetization. Magnetic properties and x-ray data are given.

7652 UNUSUAL LOW-TEMPERATURE MAGNETIC BEHAVIOR OF SOME CUBIC CRYSTALS by M. B. Palma-Vittorelli, M. U. Palma (U. Palermo), G. W. J. Drewes and W. Koerts (Kamerlingh Onnes Lab.); Physica, Vol. 26, pp. 922-930, Nov. 1960

Electron spin resonance results on hexammine nickel halides which exhibit a low-temperature transition similar to that observed in some antiferromagnetics are reported. Static susceptibility data, also reported, do not evidence such a low-temperature transition. These results are rather striking and they cannot easily be interpreted in terms of the current knowledge on antiferromagnetism. Some remarks and suggestions are given concerning their interpretation.

7653 MAGNETIC PHASE TRANSITIONS OF COBALTCHLORIDE by W. van der Lugt and N. J. Poulis (Kamerlingh Onnes Lab.); Physica, Vol. 26, pp. 917-921, Nov. 1960

Measurements of the Néel temperature in single crystals of

$CoCl_2 \cdot 6H_2O$ as a function of the external magnetic field are reported. The external magnetic field was varied from 0-10,000 Oe and was directed along the preferred axis and along a direction perpendicular to it. The threshold field was determined as a function of the temperature in the temperature range from 1.0°K up to the Néel point. The spontaneous magnetization was measured as a function of temperature in zero external field from 1°K up to 0.1°K below the Néel temperature.

PARAMAGNETISM

Susceptibility of Some Radical-Anion Salts - See 7621

7654 SPIN HAMILTONIAN OF Co^2 by F. S. Ham, G. W. Ludwig, G. D. Watkins and H. H. Woodbury (GE Res. Lab.); Phys. Rev. Lett., Vol. 5, pp. 468-470 (L), Nov. 15, 1960

The experimental significance of additional terms, derived from mixing of excited states with the ground state, in the spin Hamiltonian for an S = 3/2 ion is described. It is shown that the additional terms described give rise to anisotropic spectra. Microwave resonance spectra of Co^{2+} in ZnS, ZnSe, ZnTe, CdTe, CaF_2 were taken at 14 Kmc/sec and T = 10°K. Three transitions are permitted: $M\ 1/2 \rightarrow -1/2$ and $M \pm 3/2 \rightarrow \pm 1/2$; only the $M\ 1/2 \rightarrow -1/2$ transition was observed. The absence of the $M \pm 3/2 \rightarrow \pm 1/2$ transition is discussed. The value S = 3/2 for Co^{2+} in ZnS was verified by detection of a weak transition corresponding to $M + 3/2 \rightarrow -3/2$. Experimentally determined anisotropy of the spectra is found to fit predicted angular variation quite satisfactorily. An analysis using fourth order perturbation theory to describe the contributions of the excited states to the ground state spin Hamiltonian is presented.

7655 NEW METHOD FOR PARAMAGNETIC RELAXATION TIME MEASUREMENTS by J. A. Giordmaine (Columbia U.); Bull. Am. Phys. Soc., Ser. II, Vol. 5, pp. 418-419 (A), Nov. 25, 1960

A method of measuring relaxation times T_1 in which microwave saturating power is amplitude-modulated at an audio frequency ω was described. The phase difference ϕ between the power modulation and the resulting modulation of a reflected signal proportional to the imaginary part of the susceptibility is measured as a function of ω. For a single relaxation time $\tan\phi$ has a maximum value of $2WT_1\,(1 - 4W^2T_1^2)^{-\frac{1}{2}}$ occurring when ω is $(1/T_1)\,(1 - 4W^2T_1^2)^{\frac{1}{2}}$. W is the RF-induced transition probability. From the frequency and magnitude of the maximum phase difference, T_1 is obtained at a particular spin temperature. This method, which involves only measurements of audio frequency and phase, is convenient and appears to be capable of higher precision than other microwave methods. It is particularly sensitive to distributions of T_1. Results are reported for Cr^{+3} impurities in ruby at 78°K where both single and multiple relaxation times are observed for various transitions at X band.

7656 ON THE TEMPERATURE DEPENDENCE OF THE SHAPE OF PARAMAGNETIC RESONANCE LINES by M. McMillan and W. Opechowski (U. Brit. Columbia); Can. J. Phys., Vol. 38, pp. 1168-1186, Sept. 1960

A theory of the temperature dependence of the shape of paramagnetic resonance lines is developed for temperatures sufficiently low to make the effects of the spin-lattice interaction and thermal expansion negligible. General expressions for the first and second moments of the line shape function as functions of the temperature are obtained, and the approximations used are discussed in detail. These expressions are applied to the case of effective spin S = 1/2 and 1. As an illustration of the general theory numerical results are given for the paramagnetic resonance lines of nickel fluosilicate. In this case the moments become strongly temperature dependent below 10°K.

7657 LINE WIDTH VARIATIONS IN THE MAGNETIC SPECTRUM OF DIVALENT NICKEL IN SAPPHIRE by T. T. Kikuchi, S. A. Marshall and A. R. Reinberg (Armour Res. Found.); Bull. Am. Phys. Soc., Ser. II, Vol. 5, p. 419 (A), Nov. 25, 1960

Observations made on the paramagnetic resonance absorption of divalent nickel in sapphire show a strong line width dependence upon crystal orientation. Line widths, taken at boiling nitrogen temperature and under conditions of negligible saturation, were measured at intervals of 5 deg of arc from the parallel to the perpendicular orientations. It is found that for the $E_3 \Leftrightarrow E_2$ transition, the line width between points of inflection varies from 8.6 oe at $\theta = 5°$ to 34 oe at $\theta = 90°$ with a maximum of 52 oe at $\theta = 75°$. An analysis of the resonance Zeeman field strength vs crystal orientation for this transition indicates that the line width variation can be correlated to a distribution of randomly oriented crystallites. On the basis of the magnetic resonance line widths, the half-width of mosaic distribution is estimated at 0.14 deg of arc.

7658 ON THE THEORY OF SPIN-SPIN RELAXATION I. by W. J. Caspers (U. Leiden and Kamerlingh Onnes Lab.); Physica, Vol. 26, pp. 778-797, Oct. 1960

A method for determining the asymptotic form for large times of the so-called relaxation function of spin systems in the case of a large external magnetic field H is presented. The spin-spin relaxation phenomena are described within the framework of the spin hamiltonian. Most attention is paid to those systems in which all ions are identical and occupy equivalent lattice sites. For these systems the asymptotic form of the relaxation function is given by a function of the type: $A \exp(-t/\tau) + B$, where τ is the spin-spin relaxation time. For the quantity $1/\tau$ a series expansion is obtained: $1/\tau = \Sigma_{n=1}^{\infty}\, 1/\tau_n$, in which the different terms $1/\tau_n$ correspond to different relaxation processes. For more complicated systems the ions are divided into groups, according to the kind of ion and the occupied lattice site. When all ions have the same g-value and the interaction between the different groups is strong enough, the asymptotic form of the relaxation function will be, in a good approximation, of the type indicated above, which means that there is only one relaxation time. If this coupling is small there will be in general a number of different relaxation times, this number being equal to the number of groups. The same will be true for systems, containing different groups, corresponding with different g-values.

7659 ON THE THEORY OF SPIN-SPIN RELAXATION II. by W. J. Caspers (U. Leiden and Kamerlingh Onnes Lab.); Physica, Vol. 26, pp. 798-808, Oct. 1960

A previously described method for computing spin-spin relaxation times [see abstract 7658] is worked out in more detail for

systems containing only one magnetic specimen. Numerical calculations are performed for two types of lattices, and the results are compared with the experimental value of τ for the ammonium cupric Tutton salt. In addition the older theories on spin-spin relaxation are discussed and compared with the new theory.

7660 ON THE THEORY OF SPIN-SPIN RELAXATION III by W. J. Caspers (U. Leiden and Kamerlingh Onnes Lab.); Physica, Vol. 26, pp. 809-824, Oct. 1960

A typical relaxation mechanism, for which the change in magnetic energy accompanying a spin flip is compensated or partly compensated by the change in electric energy is discussed. The spin flips are all two or more spin processes for this mechanism. An essential part of the argument is the partition of the operators of the total magnetic moment and of the total spin moment into a diagonal and non-diagonal part, in a representation diagonalizing the zero order hamiltonian, containing only the one spin parts of the total spin hamiltonian (Zeeman parts and electric parts). Only the diagonal part of the moments contribute to the spin-spin relaxation. As for the more simple case, the number of relaxation times equals the number of groups of ions. Most attention is paid to simple systems, containing only one group.

7661 CROSS RELAXATION EFFECT OF CHROMIUM AND IRON IN $K_3(Co, Cr, Fe)(CN)_6$ by J. M. Minkowski (Johns Hopkins U.); Phys. Rev., Vol. 119, pp. 1577-1578, Sept. 1, 1960

Strong coupling between spins of Cr^{3+} and Fe^{3+} and large ratio of spin-lattice relaxation times of these two ions at 4.2°K are demonstrated by inversion of ν_{14} transition of Cr^{3+}, when ν_{13} and ν_{24} transitions are saturated. At 1.9°K the spin-lattice relaxation times are nearly equal and no inversion takes place.

7662 ON THE POWER TRANSFER BETWEEN PARAMAGNETIC SPINS AND CRYSTAL LATTICE I. by B. Boelger (Kamerlingh Onnes Lab.); Physica, Vol. 26, pp. 761-774, Oct. 1960

The determination of the heat contact η between a system of paramagnetic spins and the crystal lattice is discussed. The relation between the transient and the steady state method is shown to depend on the degree of internal spin equilibrium. The temperature and field dependences of η for concentrated salts as determined previously by the relaxation method are still unexplained. The influence of spin-spin interactions is considered, but can explain these dependences only when strong spin-spin interactions are present. The failure of the hot phonon theory for concentrated salts is explained on the base of the broadness of the spin spectrum over which energy exchange with the lattice vibrations can take place. The formulae used in the relaxation and the saturation method are for linear systems shown to become identical by a suitable transformation.

7663 ADDITIONAL SPIN RESONANCE SPECTRUM IN ANTIMONY-DOPED GERMANIUM by R. W. Keyes and P. J. Price (IBM); Phys. Rev. Lett., Vol. 5, pp. 473-474(L), Nov. 15, 1960

The observation of four anomalous spin-resonance lines in antimony-doped germanium subjected to large elastic shear strain is discussed. It is proposed that strains normally occurring in Ge are such that strain components at a point may be sufficiently severe to give rise to localized donor wave functions that are derived only from the strain-distorted potential valley. This argument is applied to antimony-doped Ge, to account for the observed additional spin resonances.

7664 SPIN RELAXATION OF F-CENTER ELECTRONS by W. E. Blumberg (U. California); Phys. Rev., Vol. 119, pp. 1842-1850, Sept. 15, 1960

Several possible mechanisms leading to spin transitions in the electron-nuclear spin system of an F-center electron and its neighboring nuclei are examined. Calculations show that the most probable transition is one in which the electron spin changes, but the nuclear spin does not change, and which results from the second-order perturbation of the spin-orbit coupling of the electron due to lattice vibrations. The spin-lattice relaxation time of the F-center electrons in NaCl at 300°K has been measured at 70, 1950, and 8300 gauss. The relaxation time is 2×10^{-6} second, independent of the magnetic field, in approximate agreement with the theory.

7665 ELECTRON PARAMAGNETIC RESONANCE OF COLOR CENTERS IN BLEACHED ADDITIVELY COLORED KCl by G. A. Noble and J. J. Markham (Armour Res. Found.); Bull. Am. Phys. Soc., Ser. II, Vol. 5, p. 419(A), Nov. 25, 1960

As potassium chloride crystals containing an excess of potassium are irradiated with light at 300°K, the peak and width of the absorption in the F region changes and the M, R_1, R_2, and N bands appear. Observations of the electron paramagnetic resonance in the equilibrium state where there is very little change upon further illumination were reported. The g factor does not change from the value 1.9964 ± 0.0005. However, the width at maximum slope decreases from 47 to 34 gauss. Both these quantities remain isotropic. The magnetic resonance relaxation time of the new center is much shorter than that of the F center. At 78°K the saturation data do not fit Portis's equation for an inhomogeneously broadened line. At 4°K one portion of the absorption does not saturate and recover independently of the rest. The shape corresponds to only one Gaussian line at all power levels. These observations indicate that all the F centers are removed by the bleaching process and that the remaining optical absorption in the F region represents entirely new centers. These centers also may be responsible for the other absorption bands. These experiments were discussed, considering the model for the M, N, and R centers based upon association of F centers.

7666 MEASUREMENT OF F-CENTER CONCENTRATION AND RELAXATION TIME BY MICROWAVE FARADAY ROTATION by D. T. Teaney, W. E. Blumberg and A. M. Portis, (U. California); Phys. Rev., Vol. 119, pp. 1851-1853, Sept. 15, 1960

The use of a bimodal cavity for the observation of electron spin resonance is described. The two samples of NaCl containing F centers used by Blumberg have been investigated by electron spin resonance. Their F-center concentrations are found to be 4.4×10^{-17} and 2.3×10^{-18} electrons/cm^3, respectively. The spin-lattice relaxation time at room temperature of the F-center electrons is found to be 1.7 microseconds.

7667 PARAMAGNETIC RESONANCE AND OPTICAL SPECTRUM OF IRON IN BERYL by M. Dvir and W. Low (Hebrew U.); Phys. Rev., Vol. 119, pp. 1587-1591, Sept. 1, 1960

Measurements of the paramagnetic resonance spectrum of Fe^{3+} in beryl at 20° and 290°K are reported. In addition to this spectrum many weak lines were observed and possible explana-

tions of these lines are discussed. The optical spectrum shows a spectrum characteristic of trivalent iron. In the infrared region there are several groups of sharp lines whose origin is not yet known.

7668 SPIN ECHO EXPERIMENTS IN CERIUM AND ERBIUM DOPED CALCIUM TUNGSTATE by W. B. Mims and K. Nassau (Bell Labs.); Bull. Am. Phys. Soc., Ser. II, Vol. 5, pp. 419-420 (A), Nov. 25, 1960

Electron spin echoes observed in samples of $Ce/CaWO_4$ and $Er/CaWO_4$ having magnetic concentrations $\sim 10^{-4}$ rare earth: calcium ratio are reported. Echo decay envelopes show phase memory times up to 50 μsec, from which it appears that T_2 (in the Bloch equations) is long and that the lines are inhomogeneous. Studies have been made of the effect of varying concentration, "g" factor, and temperature in the 1.8°K to 4.2°K range. No appreciable temperature dependence was observed for cerium, whose lattice times are long, but a strong dependence was seen in the case of erbium when the lattice time fell below 1 msec. In a mixed $Ce/Er/CaWO_4$ sample the cerium echo times were limited by erbium relaxation. Echo memory times give an indication of the rate of change of local magnetic fields within the material and point to some of the factors which control the rate of cross relaxation within a paramagnetic resonance line.

7669 STIMULATED INFRARED EMISSION FROM TRIVALENT URANIUM by P. P. Sorokin and M. J. Stevenson (IBM); Phys. Rev. Lett., Vol. 5, pp. 557-559 (L), Dec. 15, 1960

Stimulated infrared emission from U^{3+} ions in CaF_2, observed using maser techniques, is described. Oscillations at 2.5 microns occur between a metastable state and a terminal state approximately 515 cm^{-1} above the ground state. Since at low temperatures this state can be depopulated by a factor of 10^{10} relative to the ground state, the pump power required is about 500 times less than that for a ruby laser. A xenon flash lamp is used as a pump and a stimulated to spontaneous emission ratio >1000 is obtained with a beam width of 0.01 radian. Oscilloscope photographs of a lead sulfide detector response which show relaxation oscillation spikes in the maser output are presented and discussed.

DIAMAGNETISM

7670 SOLUTION OF THE SCHROEDINGER EQUATION IN A CONSTANT MAGNETIC FIELD AND DIAMAGNETISM by N. Minnaja (U. Pisa); Physica, Vol. 26, pp. 827-833, Oct. 1960

The Schroedinger equation for charged particles without spin in a cylindrical box and subject to a constant magnetic field is solved exactly. The energy eigenvalues are determined, and the results are compared with those of Landau for the diamagnetism of a gas of charged particles.

OPTICAL PROPERTIES

7671 REFLECTION SPECTROSCOPY AND SELECTIVE REFLECTION OF COPPER HALIDES AT LOW TEMPERATURES [in French] by S. Nikitine and R. Reiss (U. Strasbourg); J. Phys. Chem. Solids, Vol. 16, pp. 237-245, Nov. 1960

It is shown that investigations of reflection spectra of thin solid films at low temperature can give some information about absorption lines which cannot be observed by transmission if the crystal available is too thick. It is also shown how interference fringes of thin films can be used to obtain dispersion curves of copper halides. These curves are used to evaluate the oscillator strength of the absorption lines using Drude's anomalous dispersion theory. A selective reflection curve can also be used to obtain an order of magnitude of the oscillator strength. In the case of a strong absorption line, the reflection spectrum has a maximum (excitonic residual rays) followed by a minimum of shorter wavelength ("missing rays"). It is shown that the edge of a continuous absorption should correspond to a maximum of reflection only near the wavelength of the edge.

7672 THE INFRARED SPECTRA OF CRYSTALS by B. Szigeti (U. Liverpool); Proc. Royal Soc., Vol. 258, pp. 377-401, Oct. 25, 1960

The higher-order effects in the intrinsic infrared absorption of crystals are investigated in a systematic way. In agreement with a previous paper which dealt with the static dielectric constant, it is found that in the case of ionic crystals the third- and fourth-order potential, and second- and the third-order dipole moment, and the cross-terms between the second-order moment and the third-order potential, all contribute terms of the same order to the infrared spectrum. In the lowest approximation, the third-order moment and the fourth-order potential only affect the absorption in the immediate neighborhood of the maximum and hence have little effect on the shape of the spectrum. The broadening of the main band is due mainly to the third-order potential, while the side bands may be caused by the second-order moment as well as by the third-order potential and by cross-terms between the two. But due to an internal field effect, in strongly ionic crystals a large second-order moment automatically leads to a large third-order potential; thus a large second-order moment may increase the width of the main band as well as the intensity of the side bands. Although the intrinsic infrared absorption of valency crystals, such as diamond or germanium, is due to the second-order moment only, nevertheless, there is a strong similarity between the expressions for the infrared absorption of valency crystals and for the side-band absorption of ionic crystals. This similarity suggests that the spectra of all ionic crystals should exhibit a number of secondary maxima. The available experimental evidence does not seem sufficient to decide whether this suggestion is correct.

7673 LATTICE ABSORPTION BANDS IN INDIUM ANTIMONIDE by S. J. Fray, F. A. Johnson and R. H. Jones (RRE); Proc. Phys. Soc., Vol. 76, pp. 939-948, Dec. 1960

A series of detailed measurements of the absorption spectrum of high quality single crystals of n-type indium antimonide in the wavelength range 15 to 130 μ, and over the temperature range 4.2 to 90°K is reported. Some new absorption bands have been found, and an explanation is offered for the positions and temperature dependence of all the principal absorption peaks in terms of multiple phonon interactions involving phonons with energies corresponding to temperatures of 259, 224, 169 and 62°K.

Bleaching of Color Centers - See 7555

7674 VITREOUS SEMICONDUCTORS VIII. OPTICAL PROPERTIES OF GLASSES OF SULFUR GROUP COMPOUNDS OF THALLIUM, ARSENIC, AND ANTIMONY by B. T. Kolomiets and B. V. Pavlov (Leningrad Physicotech. Inst.); Soviet Phys.-Solid State, Vol. 2, pp. 592-597, Oct. 1960

Optical absorption measurements performed in sulfur-group compounds of thallium, arsenic, and antimony which form glasses are discussed in detail. The systems As_2Se_3-As_2Te_3, As_2Se_3-Tl_2Se, As_2Se_3-Sb_2Se_3, As_2Se_3-Tl_2S, As_2S_3-As_2Se_3, As_2S_3-Sb_2S_3, and As_2S_3-As_2Te_3 have been investigated. The general nature of optical absorption for the glasses apparently is determined by the inherent optical properties of As_2S_3 and As_2Se_3, the glass-forming compounds present.

7675 THEORY OF OPTICAL RADIATION FROM BREAKDOWN AVALANCHES IN GERMANIUM by P. A. Wolff (Bell Labs.); J. Phys. Chem. Solids, Vol. 16, pp. 184-190, Nov. 1960

A theory to explain the spectrum of light emitted from avalanching germanium junctions, in terms of known properties of the band structure and breakdown process in this material, is developed. The low frequency peak in the spectrum is ascribed to intraband transitions by holes near $k = 0$; higher frequency light arises from electron-hole recombinations. Good agreement with experiment is obtained with a carrier temperature of 0.25 ev and a pair production threshold of 1.5 ev. From the intensity ratio of the two parts of the spectrum an estimate of 10^{19} cm^{-3} is made for the carrier density in the radiating regions.

7676 PHOTON EMISSION FROM AVALANCHE BREAKDOWN IN GERMANIUM P-N JUNCTIONS by A. G. Chynoweth and H. K. Gummel (Bell Labs.); J. Phys. Chem. Solids, Vol. 16, pp. 191-197, Nov. 1960

A study of the visible and near infrared light emission that occurs at avalanche breakdown in narrow germanium p-n junctions is presented. Similar radiation has been observed previously in silicon. The spectral distribution of the light has been measured for photon energies greater than 1.0 ev and compared with that of silicon. The highest photon energies detected by the photomultiplier were about 2.0 ev, about three times the band gap (as in the case in silicon). The emitted intensity increases steadily with wavelength but shows a sharp rise as the photon energy decreases below about 1.2 ev. It is concluded that the high energy photons are produced by recombination between electrons and holes of sufficient total kinetic energy while the most likely cause of the increased emission at the low energy end of the spectrum is intravalence band transitions of energetic holes.

7677 (Zn, Hg)S AND (Zn, Cd, Hg)S ELECTROLUMINESCENT PHOSPHORS by A. Wachtel (Westinghouse); J. Electrochem. Soc., Vol. 107, pp. 682-688, Aug. 1960

Solid solutions of (Zn, Hg)S prepared by firing in sealed silica tubes are discussed. The crystals are cubic in structure. With suitable additions of Cu and a coactivator, e.g. halides, Ga, or In, photoluminescence and electroluminescence are obtained. The electroluminescence in the red consists of two emission bands which do not appear to be analogous to the blue and green emission bands of Cu, Cl in ZnS. The quantum efficiency is of the same order of magnitude as that of ZnS:Cu, Cl, but the emission bandwidth is about twice as large and the red electroluminescence consists of emission located to a large extent in the infrared. HgS tends to retain the cubic structure of ternary (Zn, Cd, Hg)S systems provided the Cd/Hg ratio does not exceed certain limits; until this is so, the introduction of Cd causes increased electroluminescence.

Thermoluminescence in Alumina Ceramics - See 7553

Electroluminescence and Photovoltaic Effects in AlP - See 7587

7678 APPEARANCE OF THE EMF IN LEAD SULFIDE FILMS ON BEING IRRADIATED BY SLOW ELECTRONS by O. M. Artamonov and L. P. Strakhov (Leningrad State U.); Soviet Phys.-Solid State, Vol. 2, p. 715 (L), Oct. 1960

Photoelectromotive forces resulting from slow electron (3-300 e bombardment of polycrystalline films of lead sulfide condensed on glass backing are discussed. The magnitude and sign of the emf depend both on the direction and the energy of incident electrons. At certain "critical" angles of incidence (of the order of 60° to the normal) the emf increases from a few hundredths of a volt to as much as one volt.

Larger-than-Bandgap Photovoltages in Si Films - See 7578

7679 VOIGHT EFFECT IN SEMICONDUCTORS by S. Teitler and E. D. Palik (U.S. Naval Res. Lab.); Phys. Rev. Lett., Vol. 5, pp. 546-548 (L), Dec. 15, 1960

Classical expressions for n and K, the index of refraction and the extinction coefficient respectively, are derived from Maxwell's equations. The phase shift, between orthogonal components of the incident radiation, is developed in terms of the sample thickness and index of refraction, and the wavelength of the incident radiation. The Voight effect in n-type InAs has been investigated with polarized 14 μ - 19 μ infrared radiation and magnetic fields to 70 kgauss. In all measurements, the phase shift reached $\pi/2$ before absorption due to cyclotron resonance occurred. The results were unchanged upon reversal of the magnetic field, thus indicating that the Voight effect is an even function of the field. A measure of the electron effective mass ratio was found by extrapolating the measured phase shifts to zero magnetic field. For $H=0$, $m^*/m=0.0313$. Preliminary measurements also indicate the presence of the Voight effect in InSb.

7680 OPTICAL ACTIVITY IN TELLURIUM by R. C. Nomura (Honeywell); Phys. Rev. Lett., Vol. 5, pp. 500-501 (L), Dec 1, 1960

Measurements of optical activity in single crystals of tellurium are discussed. The specific rotatory power is plotted as a function of wave number from 0.14×10^4 to $0.26 \times 10^4 cm^{-1}$ for both levo- and dextrorotatory crystals. Using Fresnel's expression for the specific rotatory power, the difference in refractive indices for the ordinary and extraordinary rays in the direction of the optic axis is $\pm 1.58 \times 10^{-3}$ at 5 microns. Deviations from normal dispersion occur for wavelengths greater than 5 microns. Crystal growth, sample preparation, and experimental procedure are described.

7681 PROPERTIES OF LITHIUM HYDRIDE I. SINGLE CRYSTALS by F. E. Pretzel, G. N. Rupert, C. L. Mader, E. K. Storms, G. V. Gritton and C. C. Rushing (Los Alamos Scientific Lab.); J. Phys. Chem. Solids, Vol. 16, pp. 10-20, Nov. 1960

The preparation of single crystals of optical quality LiH by slow crystallization of the melt under hydrogen gas at moderate

pressure is described. Measured and reported values of the physical, thermal, chemical, and optical properties of LiH and LiD are compared to those of LiF and NaCl. These properties bear out the predominantly ionic nature of crystalline LiH. The optical properties of LiH differ from those expected by a comparison with the properties of the alkali halides or the other alkali hydrides. The difference is related to distortion and polarization effects on the hydride ion in the LiH crystal lattice. There is a tendency toward covalency which may contribute to the binding energy of crystalline LiH, and this also may be responsible for its somewhat anomalous behavior.

THERMAL PROPERTIES

7682 FUSED QUARTZ AS A MODEL MATERIAL IN THERMAL CONDUCTIVITY MEASUREMENTS by E. D. Devyamkova, A. V. Pemrov, I. A. Smirnov, and B. Ya. Moizhes (Semicon. Inst.); Soviet Phys.-Solid State, Vol. 2, pp. 681-688, Oct. 1960

Three experimental methods to determine the coefficient of thermal conductivity of fused quartz are described. The equipment and technique are discussed in detail and possible sources of error are considered. Plots of thermal conductivity versus temperature, over the range from 80 to 1100°K are presented and compared with results of similar work in England and America. The use of fused quartz as a calibration standard in thermal conductivity measurements is encouraged.

7683 THERMAL CONDUCTIVITY OF P- AND N-TYPE GERMANIUM WITH DIFFERENT CARRIER CONCENTRATIONS IN THE TEMPERATURE RANGE 80 TO 440°K by E. D. Devyatkova and I. A. Smirnov (Semicon. Inst.); Soviet Phys.-Solid State, Vol. 2, pp. 527-532, Oct. 1960

The effect of electrically neutral dissolved gases on the thermal resistance of n-type germanium is discussed. The thermal conductivity of two pairs of n- and four pairs of p-type samples was measured and plotted. From 80 to 340°K both types exhibited a linear inverse relationship between thermal resistance and temperature; a gallium-doped sample retained the linear inverse relationship between 80 and 440°K. The values obtained agree well with those recorded in the literature.

7684 PHONON SCATTERING BY CHEMICAL IMPURITIES IN NaCl by M. V. Klein (Cornell U.); Bull. Am. Phys. Soc., Ser. II, Vol. 5, p. 422 (A), Nov. 25, 1960

Measurements of the thermal conductivity of NaCl crystals from several sources which vary by as much as two orders of magnitude on the low-temperature side of the maximum at ~10°K were reported. The conductivity of air-grown crystals (Harshaw) was particularly low. A semi-quantitative correlation has been found between the low-temperature thermal resistivity and the ultraviolet oxygen absorption band at 185 mμ. Both the resistivity and the absorption can be removed by high-temperature treatment in Cl_2 vapor. The original data can be reproduced by subsequent doping in the melt with NaOH. To reproduce Harshaw, 10^{-3} mole fraction melt-doping is necessary. In another series of experiments the effect of precipitation of Mn^{++} on phonon scattering in OH^--free NaCl has been studied by measuring the conductivity of quenched crystals containing 10^{-4} mole fraction $MnCl_2$. Kinetics of the room-temperature precipitation were measured by means of electron spin resonance. Most of the ions clustered during the first 12 hr; the rest clustered slowly over a period of several days. The accompanying changes in the thermal conductivity were surprisingly small and first appeared during the second precipitation stage.

7685 THE THERMAL CONDUCTIVITY OF IMPURE InAs AT HIGH TEMPERATURES by F. W. Sheard (Cavendish Lab.); Phil. Mag., Vol. 5, pp. 887-898, Sept. 1960

The addition of impurities affects both the lattice and electronic thermal conductivities of a semiconductor. At high temperatures the lattice resistance is increased by an amount independent of temperature. For the small concentrations normally present in semiconductors the impurity resistance can be derived very simply from the variational principle. The electronic contribution is normally obtained from the electrical conductivity via a Lorentz number. For a degenerate electron gas assuming polar scattering dominates an approximate calculation shows that at high temperatures the Lorentz number can be considerably reduced below the 'standard' value $L_0 = (\pi^2/3)(k/e)^2$. These theoretical calculations do not completely agree with the observed conductivity of impure InAs between 300 and 700°K. The disagreement is attributed to the electronic contribution. To give agreement the Lorentz number would have to be reduced further but the precise amount is uncertain owing to experimental errors.

7686 THEORY OF LATTICE THERMAL CONDUCTIVITY AT LOW TEMPERATURES by P. G. Klemens (Westinghouse Res. Lab.); Bull. Am. Phys. Soc., Ser. II, Vol. 5, p. 422 (A), Nov. 25, 1960

In the theory of the low-temperature lattice thermal conductivity one must solve an integral equation for the phonon distribution, describing the combined effect of processes conserving the phonon momentum (three-phonon N-processes) and processes tending to obliterate excess momentum. Various approximations have been proposed; these were discussed and compared, with particular reference to the approximation of Callaway.

Thermoelectric Power of Some Radical-Anion Salts - See 7621

Thermoelectric Power of Si-Co Compounds - See 7620

7687 THE ANALYSIS OF BISMUTH TELLURIDE AND RELATED THERMOELECTRIC MATERIALS by H. J. Cluley and P. M. C. Proffitt (GE Ltd.); Analyst, Vol. 85, pp. 815-822, Nov. 1960

Methods for analyzing thermoelectric materials based on bismuth telluride are presented. The materials examined included modifications of this compound in which bismuth was partly replaced by antimony and tellurium partly replaced by selenium; some materials contained a small amount of iodine. Bismuth is determined in the presence of the other constituents by direct titration with ethylenediamine-tetra-acetic acid. In the absence of antimony, tellurium is determined volumetrically in the presence of the other constituents by dichromate oxidation of $tellurium^{IV}$ to $tellurium^{VI}$. When antimony is present a preliminary separation of the tellurium, by precipitation in the elemental form, is effected before completing the determination by the volumetric dichromate method. For the determination of iodine, the iodine is separated by steam distillation effected while the sample is dissolving in nitric acid; the distilled iodine is oxidized to iodate and the determination completed by

addition of potassium iodide and titration of the liberated iodine with thiosulphate. The determinations of antimony and selenium are briefly described.

7688 MEASUREMENT OF THERMAL DIFFUSIVITY OF SEMICONDUCTORS BY ANGSTROM'S METHOD by A. Green and L. E. J. Cowles (GE Ltd.); J. Sci. Instr., Vol. 37, pp. 349-351, Sept. 1960

An apparatus for the accurate determination of the thermal diffusivity of semiconductors, which utilizes the thermoelectric properties of such materials, is described. In its present form, the apparatus can be used between room temperature and 180°C. The application of the method is illustrated by an experiment using a single-crystal specimen of bismuth telluride.

MECHANICAL PROPERTIES

7689 THE EFFECTS OF SURFACE CONDITION ON THE MECHANICAL PROPERTIES OF LITHIUM FLUORIDE CRYSTALS by A. R. C. Westwood (RIAS); Phil. Mag., Vol. 5, pp. 981-990, Oct. 1960

A comparative study of the mechanical behavior of as-cleaved, chemically polished and coated lithium fluoride crystals is described. Surface coatings were produced by vacuum deposition and by chemical reaction. Thin (⊁10 μ) reacted-coatings increased the yield stress some 50 per cent and were responsible for catastrophic stress drops observed at the critical resolved shear stress. Coatings also decreased the initial rate of work-hardening and the stress and strain to fracture. Failure occurred by the formation of Stroh-type cracks. An explanation for these and other results is offered based on considerations of the distribution and number of operable dislocation sources, and the piling up of dislocations at intersecting slip bands and beneath surface films. Metallographic evidence is presented for the latter phenomena. Experimental observations are more consistent with a barrier-mechanism of work-hardening than with a defect-mechanism.

7690 THE DEFORMATION OF GERMANIUM by R. L. Bell and W. Bonfield (Royal School of Mines); Acta Cryst., Vol. 13, p. 1113(A), Dec. 1960

Measurements of the deformation properties of germanium single crystals oriented for single slip in tension at 570°C are reported. A large yield-point drop was observed both in materials that had been doped with indium or gallium impurity, and in the purest (50 ohm.cm.) material. The restoration of the yield point by annealing did not occur unless the treatment was sufficient to reduce the dislocation density to values approaching that in the starting material. From studies of the postyield flow stress and its variation with strain rate, it is concluded that the major portion of the yield drop is associated with the velocity-stress dependence of the dislocations.

7691 ELASTIC CONSTANTS OF YIG by N. G. Einspruch and T. E. Hartman (Texas Instr.); Bull. Am. Phys. Soc., Ser. II, Vol. 5, p. 421(A), Nov. 25, 1960

Use of an ultrasonic pulse-echo technique to measure propagation velocities of 10 Mc/sec compressional and shear waves in polycrystalline yttrium iron garnet is described. Results of the measurements (in units of 10^5 cm/sec) are: $v_c = 7.01$, $v_s = 3.87$. The Young's and shear moduli for YIG (in units of 10^{11} d/cm^2) are: $E = \rho v_c^2 = 24.7$, $\mu = \rho v_s^2 = 7.53$, where ρ is the density of the material.

7692 RECOVERY PROPERTIES OF LITHIUM FLUORIDE SINGLE CRYSTALS by W. L. Philips, Jr. (duPont); AIME Trans., Vol. 218, pp. 947-951, Oct. 1960

An investigation of the recovery properties of compression-deformed lithium fluoride single crystals as a function of prior strain, annealing time, and annealing temperature is reported. The recovery process was studied by observation of etch pits and birefringence stress patterns. The recovery process involves first a redistribution of the dislocations and then a decrease in their number. Only by annealing at high temperatures after small strains (<0.02 in. per in.) was it possible to obtain complete recovery of mechanical properties.

7693 ELEVATED TEMPERATURE PROPERTIES OF LITHIUM FLUORIDE AND MAGNESIUM OXIDE SINGLE CRYSTALS by W. L. Philips, Jr. (duPont); AIME Trans., Vol. 218, pp. 939-947, Oct. 1960

An investigation of the plastic properties of lithium fluoride and magnesium oxide under compression in the temperature range 25° to 1000°C is reported. At the higher test temperatures, the critical resolved shear stress and the rate of work-hardening of both materials decreased. At the same time, the number of stress lines decreased and the individual stress lines became wider. The density of dislocations decreased for a given strain the higher the test temperature for lithium fluoride. The decrease in the critical resolved shear stress as a function of temperature could be fitted by the equation $\tau = \tau_0 e^{-kT}$.

7694 THE YIELD STRENGTHS OF CRYSTALS by J. J. Gilman (GE Res. Lab.); Acta Cryst. Vol. 13, p. 1113(A), Dec. 1960

Direct experimental measurements now provide abundant evidence that the stress required for plastic flow in crystals is primarily determined by the mobility of screw dislocations. The sharp dependence of this mobility on the applied stress is what causes plastic 'yielding' in a narrow range of stress. Since dislocations multiply in number as they move through a crystal, the yielding process is further sharpened, and becomes catastrophic under some conditions. Many factors influence dislocation mobilities and thereby change the yield stress of a crystal. Some of these are: dislocation type, glide plane, elastic modulus, temperature, impurities, radiation damage, and strain-hardening. These effects have not only been measured in ionic crystals (LiF), but also in metal crystals (iron-silicon).

Brittle Fracture in Elemental and Compound Semiconductors - See 7559

7695 ENVIRONMENTAL EFFECTS ON THE MECHANICAL PROPERTIES OF IONIC SOLIDS WITH PARTICULAR REFERENCE TO THE JOFFE EFFECT by R. J. Stokes, T. L. Johnston and C. H. Li (Minneapolis-Honeywell); AIME Trans., Vol. 218, pp. 655-662, Aug. 1960

Sodium chloride crystals are brittle in the presence of surface microcracks. Water immersion leads to an enhancement of ductility which is retained indefinitely in dry air providing the crystal is dried without leaving a surface precipitate. Storage

in a damp atmosphere results in a surface reaction and consequent re-embrittlement. Although elimination of surface flaws in ionic solids does not necessarily enhance ductility, there is always a change in the location of the fracture origin.

SOLID STATE DEVICES

GENERAL

7696 SPREADING RESISTANCE IN CYLINDRICAL SEMICONDUCTOR DEVICES by D. P. Kennedy (IBM); J. Appl. Phys., Vol. 31, pp. 1490-1497, Aug. 1960

Computation of the spreading resistance of cylindrical semiconductor components is considered as a boundary value problem of the solid circular cylinder. Solutions of this problem may be used, for example, to characterize the thermal spreading resistance within the package of a semiconductor device, the electrical spreading resistance in a mesa type parametric diode, and the extrinsic collector resistance of a mesa transistor. Equations describing the thermal (or electrical) spreading resistance are presented in graphical form for a range of geometrical parameters applicable to many practical situations. Examples for the potential distribution within each cylindrical structure considered in the analysis are given.

7697 STUDY OF METHODS OF COOLING SEMICONDUCTOR DEVICES by S. K. Morrison and J. P. Welsh (Cornell Aero. Lab.); U.S. Gov. Res. Rep., Vol. 34, p. 150 (A), Aug. 19, 1960 PB 146 874

Several methods for cooling semiconductor devices are discussed. These include methods of mounting, electrically insulating, and removing the dissipated heat by conduction through metals; methods of mounting, fin areas, configurations and orientation to enhance heat removal by natural convections; methods of mounting, geometry, fin configurations, air velocities, air flow rates, and other parameters pertinent to forced convection; and direct and indirect liquid cooling techniques.

DIODES

7698 HIGH-FREQUENCY VARACTOR DIODES by C. W. Mueller and R. D. Gold (RCA Labs.); RCA Rev., Vol. 21, pp. 547-557, Dec. 1960

Varactor junction diodes which give substantially better high-frequency performance than that of any previously available units are described. Typical electrical characteristics are. capacitance from 0.5 to 1 micromicrofarad, series resistance ~1 ohm, and cutoff frequency above 200 kilomegacycles. These diodes have operated as phase-locked oscillators at a signal frequency of 17 kilomegacycles (34 kilomegacycles pump frequency) and in various microwave strip line amplifiers. Fabrication of these diodes is described. Detailed measurements of the impurity gradient show that it can be approximated by a power law whose exponent is greater than unity. Since this impurity distribution cannot be explained exclusively by the out-diffusion process, an interaction of the alloying and out-diffusion is necessary. A new thin hermetically sealed ceramic enclosure with a very low inductance (0.6 millimicrohenry) and a low case capacitance (0.3 micromicrofarad) has been developed. The diode may be readily inserted directly into microwave strip transmission line, between the coils of a traveling-wave helix, or into a wave guide. A method of measuring the diode parameters at 2 kilomegacycles has been developed, and a computer has been used to obtain the desired parameters.

Silicon Epitaxial Microwave Varactor Diodes - See 7835

Gallium Arsenide Varactor Diodes - See 7836

Silicon Controlled Rectifier - See 7837

7699 CRYSTAL DETERIORATION STUDIES by P. P. Lombardini, R. J. Doviak and H. Kritikos (U. Pennsylvania); U.S. Gov. Res. Rep., Vol. 34, p. 427 (A), Oct. 14, 1960 PB 146 367

A study of deterioration of microwave crystal rectifiers is reported. In Phase A an experimental investigation was undertaken to determine the threshold power levels needed for partial and total burnout under conditions of different pulse-widths and exposure time. A new indicator of crystal burnout was developed. Phase B was concerned with a critical review of the available literature on crystal burnout.

7700 NOISE PERFORMANCE OF TUNNEL DIODES by E. G. Nielsen (GE); Proc. IRE, Vol. 48, pp. 1903-1904 (L), Nov. 1960

The frequency dependence of the noise performance of tunnel diodes considering both shot noise and thermal noise from the parasitic series resistance is calculated. By modifying the shot noise to be dependent not only on the d-c current, but also on other circuit elements, a noise figure is found that is a function of three ratios. The first assesses the shot noise relative to the negative conductance; the second, the parasitic series resistance relative to the negative resistance; and the third, the operation frequency relative to the diode cut-off frequency. The noise figure for germanium tunnel diodes is shown to deteriorate rapidly as the cut-off frequency is approached.

7701 THEORETICAL JUSTIFICATION FOR SHOT-NOISE SMOOTHING IN THE ESAKI DIODE by R. LaRosa and C. R. Wilhelmsen (Hazeltine); Proc. IRE, Vol. 48, p. 1903 (L), Nov. 1960

A theory of shot-noise smoothing in the negative conductance region of tunnel diodes is formulated to explain the total shot-noise reduction noticed in certain experimental observations. This theory predicts that eligible tunneling electrons do not have an infinitesimal probability of tunneling and that therefore the diode will not be as noisy as was first assumed.

Uni-Tunnel (Backward) Diodes - See 7838

Spreading Resistance in Mesa Diodes - See 7696

Emission of Light from Avalanching Ge Junctions - See 7675, 7676, 7719

Thermal Spreading Resistance in Mesa Diodes - See 7696

7702 SILICON SEMICONDUCTOR DEVICES by H. W. Henkels and D. L. Moore (Westinghouse); U.S. Pat. 2,964,830, Issued Dec. 20, 1960

The fabrication of a silicon diode with breakdown voltages in the 300 to 600 volt range and current capacities of up to 200 amperes is described. An assembly consisting of an end contact of tantalum, a wafer of N-type silicon, an aluminum doped alloy, and a base contact of tantalum is fired at temperatures between 800 and 1000°C. Upon cooling the fused device is placed upon an inert mask and etched with a stream of acid to avoid contamination. The assembly is then encapsulated by standard techniques.

7703 GALLIUM PHOSPHIDE FOR POWER RECTIFIERS by R. E. Davis (Westinghouse); Properties of Elemental and Compound Semicon. (Interscience), pp. 295-302, 1960

The preparation and electrical properties of gallium phosphide are discussed. The characteristics of rectifiers made from gallium phosphide are given as a function of ambient temperature and data for silicon carbide rectifiers are given for comparison. Gallium phosphide rectifiers which operate over a temperature range from -55 to +500°C have been made. In comparison, silicon carbide rectifiers display better characteristics at 500°C but much poorer characteristics at room temperature and below.

7704 DIRECT VIEWING OF IMPERFECTIONS IN GERMANIUM P-N JUNCTION by M. Tomono (Hitachi); J. Phys. Soc. Japan, Vol. 15, pp. 2254-2264, Dec. 1960

The results of putting a p-n junction made by alloying indium to an n-type germanium pellet into an electrolytic solution of a copper salt are reported. When a suitable reverse voltage was applied to the junction by a charged condenser, a copper shaded pattern was deposited on the opposite side of the alloyed surface in accordance with the density of the reverse current flowing through each part of the p-n junction. By this method, the breakdown at imperfections of the p-n junction due to the defects in the germanium crystal, those at the periphery of p-type recrystallized layer, and those inside the p-n junction grown in the alloying process were observed. Then, a cross section was made with reference to the pattern, and several kinds of imperfections were observed under a microscope.

7705 ASSEMBLY PROCESS FOR SEMICONDUCTOR DEVICE by J. D. Peterson (Texas Instr.); U.S. Pat. 2,964,831, Issued Dec. 20, 1960

A method of encapsulating a small diffused silicon diode without the use of holding fixtures is described. Lengths of conductor wire are formed into rectangular loops which join ends under alignment and compression. A cup-shaped diode case is threaded onto each loop and a diffused wafer is inserted between the wire ends to form an assembly. Compression from the loop holds the wafer in each assembly in place during the subsequent soldering, cleaning, and baking procedures. Positioning and potting the diode case with epoxy, curing, and cutting the wire loop gives the encapsulated diode.

Varactor Diode Package for Microwave Frequencies - See 7698

7706 SURFACE PASSIVATION AS APPLIED TO MICRO-COMPONENTS by T. C. Hall (Pacific Semicon.); 1960 WESCON Conv. Rec., Part 3, pp. 129-132

A new approach to semiconductor microcomponent packaging employing surface passivation is presented. The term "Passivation" is defined to mean the generation on the semiconductor surface of a strongly-bound chemical film layer which does not adversely affect those surface electronic properties leading to acceptable device characteristics. In addition, a condition of electrical stability of the surface is provided, together with isolation from those electrical and chemical environmental influences leading to change in device characteristics. The merits of the new approach in contrast to conventional hermetic packaging are considered. Experimental results demonstrating the superior device performance-reliability characteristics of diode structures treated in this manner are discussed. In addition to improved device performance and reliability, significant and critical advantages in microminiaturization and device fabrication are realized.

TRANSISTORS

7707 SWITCHING TRANSISTORS by R. C. Buschert and S. L. Miller (Bell Labs.); U.S. Pat. 2,964,689, Issued Dec. 13, 1960

Design criteria for the fabrication of a fast switching transistor are given. The need for low lifetime material at the collecting surface nearest to the base electrode to minimize carrier storage while maintaining alpha by preserving high lifetime in the base region between emitter and collector is discussed. Bombardment and the introduction of impurities (Cu in Ge, Au or Fe in Si) to decrease lifetime and the gettering of impurities (Pb for Cu in Ge, Ni for Au in Si) to increase lifetime are cited as techniques. Procedures involved in the fabrication of a mesa and an alloy type switching transistor are shown.

7708 BASE TURN-OFF OF P-N-P-N SWITCHES by R. H. van Ligten and D. Navon (Transitron); 1960 IRE WESCON Conv. Rec., Part 3, pp. 49-52

A three-terminal four-layer p-n-p-n switch is an integrated device made up of two transistors sharing a common collector. If the collector current is not much in excess of the holding current, the unit can be switched off by supplying a signal to the control base lead. Failure to switch off higher currents is caused by breakdown of the emitter junction caused by a transverse voltage drop in the base layer. This potential drop can be minimized if the current gain for turn-off is large and hence the base current required for turn-off is small. Turn-off of currents well in excess of the holding current may be achieved in two ways. First, an interdigited emitter structure will help reduce the transverse base drop and second, the turn-off beta can be increased by keeping the current gain of one of the transistors small compared with that of the other. Switch-off time can be substantially reduced by withdrawing charge through the base lead rather than by grounding the collector.

7709 THE BINISTOR - A NEW SEMICONDUCTOR DEVICE by

N. DeWolf (Transitron); Electronic Ind., pp. 84-87, Aug. 1960

A silicon p-n-p-n tetrode device for switching and storage circuits which has many properties of a flip-flop is described. The binistor resembles a four-layer switch with the output current taken from an intermediate layer and the upper junction used as a latch to hold the device on in the conducting state. There are two stable states, either fully cut off or fully conducting and saturated. Operation involves the gating of base current to the main transistor through the latching transistor. The gating depends primarily on the collector voltage and the injector clamping voltage. Injector switching gives power gain; base control provides the highest current and voltage gain; emitter control gives voltage gain without current gain. The operating range is -70 to 250°C. A binistor flip-flop requires only one binistor and three resistors in comparison to the conventional flip-flop which requires at least two transistors, seven resistors, two capacitors, and two diodes. The binistor has been successfully used in a ring counter, as a non-destructive coincident memory and as a small-signal negative resistance device.

7710 TRANSISTOR OPERATION BEYOND CUTOFF FREQUENCY by V. W. Vodicka (Lenkurt Electric) and R. Zuleeg (Hughes); Electronics, Vol. 33, pp. 56-59, Aug. 26, 1960

A mode of transistor operation using a converter circuit which extends the useful frequency response of high frequency transistors beyond their normal cutoff limits is described. By "current tuning" the input of an oscillating mesa transistor, conversion power gains of about 10 db at greater than 1 gigacycle with a signal-to-noise ratio of approximately 7 db was obtained. The output frequency was 350 Mc. Optimum noise performance was found at the point of maximum conversion gain for the regenerative mode. Optimizing all conditions for another experimental circuit gave performance figures of: input frequency, 450 Mc; bandwidth, 750 kc; conversion gain, 49 db; s/n ratio, 3 db; noise figure, 6 db; and output frequency, 2 Mc. A quantitative analysis of the mode operation including a mathematical model of the transistor is being undertaken.

Extrinsic Collector Resistance of Mesa Transistors - See 7696

Transistors as Generators of High-Speed Light Pulses - See 7719

7711 JIG ALLOYING OF SEMICONDUCTOR DEVICES by I. H. Kalish and S. Silverstein (RCA); U.S. Pat. 2,964,431, Issued Dec. 13, 1960

The use of solder-plated metal jigs in the fabrication of semiconductor devices is discussed. The jig is employed to hold semiconductor pellets in position during bonding and alloying steps and then is separated into individual tabs, each tab being bonded to a pellet. This technique eliminates the need for the individual loadings of tab and pellet and decreases handling operations. Reference is made to application in the fabrication of mesa and surface-alloyed transistors.

7712 HIGH-LEVEL HIGH-FREQUENCY GERMANIUM TRIODES by V. A. Struzhinskii; Soviet Phys.-Solid State, Vol. 2, pp. 391-395, Sept. 1960

A new method for constructing a high-power high-frequency germanium triode is discussed. A metal serving as an emitter is fused to a copper-coated germanium plate. Upon heating the structure to a high temperature, copper, having greater solubility in the metal, is extracted from the germanium, leaving a copper-free n-type layer. The remainder of the germanium retains its p-type characteristic. The basic parameters and triode characteristics are presented.

Resistivity Test Set for Semiconductor Slices - See 7834

Control of Lifetime in Transistors - See 7707

7713 MOISTURE GETTERING WITH POROUS VYCOR by M. J. Rand (Bell Labs.); J. Electrochem. Soc., Vol. 107, p. 269C(A), Dec. 1960

Extensive aging experiments on alloy transistors which have established that device reliability is much improved by including a porous Vycor moisture getter in the enclosure were reported and an apparatus to study the adsorptive capacity of the Vycor at relative humidities below 5 per cent was described. Results to date on the adsorption isotherms at various temperatures and the rate of attainment of equilibrium were presented. The activation of the Vycor by heating and pumping has also been investigated.

PHOTODEVICES

7714 PROPOSAL OF THE DETECTIVITY D** FOR DETECTORS LIMITED BY RADIATION NOISE by R. C. Jones (Polaroid); J. Opt. Soc. Am., Vol. 50, pp. 1058-1059, Nov. 1960

A new kind of detectivity, called D**, is proposed for cells that have a detectivity that is limited by radiation noise. The detectivity D** takes specific account of the solid angle Ω, from which external radiation can reach the responsive element. Usually, the external radiation is produced by objects at room temperature. D** is also appropriate for use with detectors that are non-Lambertian for reasons other than cooled radiation shields: for example, detectors that are immersed in a high-index medium, or detectors that are closely associated with a lens.

7715 INFORMATION CAPACITY OF RADIATION DETECTORS by R. C. Jones (Polaroid); J. Opt. Soc. Am., Vol. 50, pp. 1166-1170, Dec. 1960

The information capacity of a radiation detector is denoted by C and is measured in bits per second. The root-mean-square radiation power incident on the detector is denoted by P and is measured in watts. The ratio $C/P=I$, measured in bits per joule, is discussed. When I is referred to unit detector area, it is denoted by I* and is measured in bits per (joule/cm^2). It is shown that for most detectors, the information capacity I has a maximum value for a finite and determinable value of the power P, and that the maximum corresponds to an electrical signal-to-noise ratio in the output of the detector that is of the order of magnitude of unity. It is further shown, subject to a suitable simplifying approximation, that the information capacity I* is equal to one-half of the energy detectivity Δm^* of the detector, and that if the modulation of the radiation power is confined to one cps band centered at the frequency f, the information capacity I* is equal to the detectivity D*(f) of

the detector. Numerical results are given for a number of kinds of detectors, including the dark-adapted human eye, Royal-X photographic film, multiplier phototubes, and cooled infrared detectors.

PHOTRAN PNPN Silicon Photoswitch - See 7840

7716 STUDY OF THE VARIATION OF PHOTOELECTRIC SENSITIVITY OF A SELENIUM CELL SUBJECTED TO A MAGNETIC FIELD AS A FUNCTION OF TEMPERATURE [in French] by J. Vincent and G. Blet (CNRS, Marseille); J. Phys. Radium, Vol. 21, pp. 685-688, Oct. 1960

The decrease in the photoelectric sensitivity of a selenium photocell when a magnetic field is applied in a direction parallel to the barrier layer is discussed. This decrease is dependent on the wavelength and a maximum is observed at about $\lambda = 0.7\mu$; the lower the temperature the smaller the decrease.

7717 QUANTUM EFFICIENCY OF CdTe P-N JUNCTIONS IN THE ULTRAVIOLET PART OF THE SPECTRUM by G. B. Dubrovskii (Semicon. Inst., Leningrad); Soviet Phys.-Solid State, Vol. 2, p. 536, Oct. 1960

Electron multiplication in CdTe photocells illuminated by short wavelength light is discussed. The product of quantum efficiency, Q, and collection coefficient, α, plotted against the energy of incident photons, $h\nu$, has a minimum for $h\nu = 3.5$ ev. As the energy is increased from 3.5 to 5.0 ev, a corresponding increase in Q is indicated, and related to the electron (or hole) multiplication for photocarrier energies greater than the forbidden band width. The excess energy of primary photocarriers needed for impact ionization is about 2 ev, or about 0.5 ev greater than the energy gap of CdTe (1.45 ev).

7718 STORAGE LIGHT INTENSIFIER DISPLAY PANEL by H. O. Hook and W. F. Davidson, Jr. (RCA); U.S. Gov. Res. Rep., Vol. 34, p. 422 (A), Oct. 14, 1960 PB 149 103

Layer type storage light intensifiers with 40 elements per inch are described. Bi-stable storage for 30 minutes is reported. Less satisfactory results were obtained with more complicated structures. Some characteristics of powdered CdS photoconductors are reported and related to the operation of storage light intensifiers. Spectral match of the 4RCA electroluminors and CdS photoconductor is almost the same. Optical geometry and absorption in feedback paths are evaluated experimentally and theoretically.

7719 TRANSISTORS AS HIGH-SPEED LIGHT PULSERS by H. W. Kendall (Stanford U.); IRE Trans., Vol. NS-7, pp. 202-203, June-Sept. 1960

Experimental light pulsers for testing scintillation counter telescopes using fast coincidence circuitry are described. The devices utilize commercially available silicon p-n junctions operating in the avalanche mode. The base-emitter and base-collector junctions of n-p-n transistor types 2N706, 2N696, 2N697, 2N699, p-n-p type 2N1132, and an experimental high-frequency transistor with 30 watts dissipation were investigated. A pulser using the latter transistor will be made available commercially. The experimental transistor emitted about ten times as much light as the other types and showed no deterioration with testing. After several hours of operation at pulse amplitudes above 50 v, most of the base-emitter junctions of the other transistors became useless and the performance of the base-collector junctions was degraded. These junctions also did not emit enough light to simulate the light output from plastic scintillators in which more than about 100 kev has been absorbed. The light output can be increased by operating the junctions in series or parallel.

7720 MICROWAVE MODULATION OF LIGHT IN PARAMAGNETIC CRYSTALS by N. Bloembergen, P. S. Pershan, and L. R. Wilcox (Harvard U.); Phys. Rev., Vol. 120, pp. 2014-2023, Dec. 15, 1960

The considerations of Dehmelt and several other workers about the modulation of light by radio-frequency signals in atomic vapors are extended to paramagnetic solids. It is shown that these materials, driven near a microwave resonance at low temperatures, may be used both to create and to detect modulation of light at microwave frequencies. Experimental design criteria are discussed for two numerical examples, modulated circular dichroism in ruby and modulated Faraday rotation in a broad class of ionic rare earth compounds. Some possible applications of microwave modulated light are reviewed.

THERMAL DEVICES

7721 FLAKE THERMISTOR by T. L. Baasch (Servo Corp. Amer.); U.S. Pat. 2,966,646, Issued Dec. 27, 1960

An improved thermistor bolometer which may be used with lower impedance detection circuits and which employs conventional flake-thermistor material is described. A relatively lower resistance characteristic is achieved in this device by fixing two electrically conductive elements on one face of the flake and an electrically conductive sheet on the opposite side of the flake to provide a shunt-resistance path between the two electrodes. The device may be employed as a circuit element or it may be mounted as an air backed bolometer, or it may be bonded to a heat sink. Utilization of the device in an ambient temperature compensated bridge circuit is described.

7722 PERFORMANCE OF A THERMOELECTRIC CONVERTER UNDER CONSTANT HEAT FLUX OPERATION by P. S. Castro and W. W. Happ (Lockheed); J. Appl. Phys., Vol. 31, pp. 1314-1317, Aug. 1960

The performance characteristics of a conventional thermoelectric generator operating under constant heat flux conditions are computed. Expressions for power output, optimum efficiency, and optimum ratio of internal-to-load resistance show that optimization requires operating conditions appreciably different from those for the operation of thermoelectric generators having constant hot and cold junction temperatures. Performance curves are presented for the optimum ratio of internal-to-load resistance when either the internal resistance or the load resistance is under the control of the designer.

MAGNETIC DEVICES

7723 FERRITE PHASE SHIFTER FOR THE UHF REGION. PART

II by C. M. Johnson and G. V. Buehler (Electronic Commun.); U.S. Gov. Res. Rep., Vol. 34, p. 423(A), Oct. 14, 1960 PB 146 324

Ferrite properties which influence phase shifter performance are investigated, and improved versions of the ferrite-loaded, folded-stripline, UHF phase shifter are described. Some theoretical relations are derived from conventional ferromagnetic theory to explain the performance of this type of phase shifter, but good quantitative agreement with the experimental results has not been attained. This disagreement is attributed to demagnetizing effects. A preliminary investigation has been made to determine the nature of these effects and some of the results are included.

Ferrite Modulator - See 7841

7724 THE USE OF AN X-BAND SOLID-STATE RUBY MASER WITH A CONVENTIONAL DUPLEXING SYSTEM by J. L. Carter, M. Katzman, and I. Reingold (USASRDL); U. S. Gov. Res. Rep., Vol. 34, p. 420(A), Oct. 14, 1960 PB 148 002

A series of experiments performed with an X-band solid-state ruby maser and several conventional types of X-band duplexer tubes under conditions which simulated actual radar system application is described. Leakage levels for the onset of deterioration of maser performance and for saturation of the maser have been determined. Measurements of the recovery time of the maser after it had been fully saturated have also been made. The results indicate the degree of improvement required of the duplexer, or the degree of protection that must be provided in addition to the duplexer, if optimum use is to be made of the maser gain characteristics.

7725 STUDY OF ATOMIC AND MOLECULAR RESONANCES FOR MICROWAVE GENERATION AND AMPLIFICATION by T. Maiman, R. Hoskins and D. Dever (Hughes Aircraft); U. S. Gov. Res. Rep., Vol. 34, p. 153(A), Aug. 19, 1960 PB 147 425

X-band ruby maser operation observed up to a temperature of 195°K with dry ice used as a coolant is discussed. It has been found that ruby crystals with high chromium content function poorly (low gain-bandwidth product) at 4.2°K but behave normally at higher temperatures. An explanation based on cross relaxation is presented. A noise temperature of 100°K and a gain-bandwidth product of 14mc have been measured for a maser operating at 77.4°K (temperature of liquid nitrogen). Preliminary results on calculations of the fine structure levels of Cr^{+3} in TiO_2 (rutile) are reported. Pulsed magnetic field experiments have been conducted with ruby as the paramagnetic material. Inversion of successive spin levels by adiabatic fast passage at X-band followed by the application of a pulsed magnetic field resulted in pulsed amplification and oscillation at several frequencies from 14kmc to 28kmc. The rapid attainment of a Boltzmann distribution of spin populations when the energy levels become equidistant in a multilevel spin system was demonstrated directly.

Maser Action from U^{3+} Ions in CaF_2 - See 7669

Microwave Modulation of Light in Paramagnetic Crystals - See 7720

7726 AN INTRODUCTION TO THE PRACTICAL APPLICATION OF FERROELECTRICS by T. W. Butler, Jr. (Michigan U.); U.S. Gov. Res. Rep., Vol. 34, p. 426(A), Oct. 14, 1960 PB 147 225

The properties of ferroelectric materials and the physical principles involved in their applications are discussed. Three groups of applications which make use of (1) the high permittivity, (2) the non-linear properties and (3) electro-mechanical properties are considered.

7727 INVESTIGATION OF ELECTRICALLY VARIABLE DELAY LINES by S. R. Hoh and G. R. Leef (ITT Labs.); U.S. Gov. Res. Rep., Vol. 34, p. 425(A), Oct. 14, 1960 PB 146 597

An investigation of electrically variable delay lines based on ferroelectrics is reported. A material Q of 100 has been obtained with a barium-strontium titanate which is the highest ever reported in this frequency range. A new multisection delay line was developed incorporating ferroelectrics. This line has an attenuation comparable to standard delay cables and, in addition, miniaturization and controllability.

7728 AN APPROACH TO THE EXPERIMENTAL STUDY OF PERSISTENT-CURRENT DEVICES by C. R. Vail, M. S. P. Lucas, H. A. Owen and W. C. Stewart (Duke U.); Solid-State Electronics, Vol. 1, pp. 279-286, Sept. 1960

The results of an experimental study of the effects of composition and geometry on the property of superconductivity in thin-film strips and of the static and transient characteristics of the persistatron are reported. Certain techniques employed in these studies are discussed, including: the evaporation of vanadium and tantalum by electron bombardment, and of lead by the boat method; methods of masking, with reference to both metal and printed masks; and a method of testing persistent-current devices directly in a helium storage flask. The description of a flexible programmed-pulsing device is also given.

Tunneltron - See 7842

7729 A PIEZOELECTRIC FORCE GAGE FOR MEASURING DRAG ON TWO-DIMENSIONAL MODELS IN THE SHOCK TUBE by W. G. Luke and L. W. Slifer (U.S. Naval Ord. Lab.); U.S. Gov. Res. Rep., Vol. 34, p. 437 (A), Oct. 14, 1960 PB 161 872

The design, development, testing, and final evaluation of a piezoelectric force gage for measuring drag forces in a shock tube are described. The gage is a one-inch cylinder of square cross section which, when mounted, extends across the entire width of the shock tube. It has a central test section which is free to respond to applied forces while the end sections are rigidly mounted to the shock tube walls. In this way, registry of end and wall effects is minimized so that the gage configuration may be considered two-dimensional. The sensing element of the gage is a one-half-inch-diameter, four-pile, plastic-bonded, tourmaline crystal stack which is readily adaptable to other gage configurations. The plastic-bonded element is superior in ruggedness to conventional, solder-bonded elements and has a comparable sensitivity of 24 micro-microcoulombs per pound. It is capable of withstanding forces

up to 30 pounds. This is adequate for shock pressures up to 10 psi but breakage of the crystals is expected to occur frequently when larger forces are applied. Inaccuracies of the gage are estimated to be less than 15 per cent under any of the test conditions for which it is intended. The errors result primarily from the sensitivity of the gage to temperature and from record-reading inaccuracies due to noise level.

7730 PIEZOELECTRIC EXCITATION OF THICKNESS VARIABLE QUARTZ OSCILLATORS BY MEANS OF A PARALLEL FIELD [in German] by R. Bechman (USASRDL); Arch. Elekt. Übertragung, Vol. 14, pp. 361-365, Aug. 1960

AT- and BT-quartz oscillators are usually excited by two electrodes parallel to the major surfaces of the plate. This is excitation by a perpendicular field. AT- and BT-quartz oscillators can also be excited by two pairs of electrodes arranged so that each covers part of both major surfaces leaving a gap parallel to the major surface where an electric field is produced. This is excitation by a parallel field. To excite an AT- or BT-cut, the gap must be parallel to the X-axis, the field parallel to the Z'-axis. Not only the usual thickness-shear mode having a zero temperature coefficient of frequency can be excited by use of the parallel field excitation, but also the other two thickness modes, the second shear mode and the extensional mode. For excitation of these two modes the gap of the electrodes must be parallel to the Z'-axis. The parallel field excitation of AT-cuts is very advantageous for application to high precision quartz oscillators. Not only considerably higher values for the inductance are obtained but also higher values for Q. Two examples of quartz oscillators for 750 kc/s and 1 Mc/s excited by a parallel field are considered and the data of the equivalent electric circuit are given.

SOLID STATE DEVICE MEASUREMENTS

TRANSISTORS

7731 MEASUREMENT OF TRANSISTOR ADMITTANCE PARAMETERS by K. Redmond (Amperex); Electronics, Vol. 33, pp. 84-87, Dec. 16, 1960

An improved method of measuring admittance parameters of high frequency transistors is described. Instead of attenuating the signal oscillator level by a potentiometer in the oscillator plate circuit, the RF input is fed through a 20 db attenuation pad to permit operation of the oscillator unaffected by attenuation. A communications receiver tuned to the difference frequency and operated in its AGC mode is used as an external detector. An external oscillator alters the detector frequency to any desired value. Equations to obtain all admittance parameters are given and a detailed example is presented. Calculation of power gain by use of admittance parameters is illustrated.

7732 TRANSISTORIZED EQUIPMENT FOR MEASURING TRANSISTOR FREQUENCY RESPONSE by B. Reich and W. Orloff (USASRDL); Semicon. Prod., Vol. 3, pp. 38-41, Aug 1960; U.S. Gov. Res. Rep., Vol. 33, p. 496(A), May 13, 1960 PB 145 138

The theory and operation of a transistorized equipment capable of measuring the frequency response of transistors is described. The characteristic chosen for representing this parameter is the f_t frequency or the frequency at which the current gain is unity. The equipment employs a transistor oscillator and small-signal r-f amplifier as the basic elements of the system. Although the equipment is capable of indicating frequency responses in excess of 1000 Mc, the actual frequency used by the test unit does not have to exceed 100 Mc.

Transistor Frequency Response Tester - See 7843

BASIC SOLID STATE DEVICE CIRCUITS

GENERAL

7733 THE NEGATIVE RESISTANCE CONCEPT IN MODERN ELECTRONICS by G. D. Sims and I. M. Stephenson (U. Coll London); J. Electronics Control, Vol. 9, pp. 349-383, Nov. 1960

The importance of negative resistance as an equivalent circuit element for the description of power producing devices is discussed with particular reference to some of the more modern high frequency tubes. Negative resistance devices can be divided into two main classes according to whether they are current controlled or voltage controlled and the properties of each class are enumerated and contrasted. The general stability criterion for ac circuits containing negative resistance is examined and the use of negative resistance for amplifiers and oscillators, both in the transient and steady states, is discussed. Negative resistance can be produced in many circuits by the addition of positive feedback, although there are many other basic types of device in which the negative resistance property is intrinsic. These latter are classified and numerous illustrations are given. In conclusion the description of microwave travelling-wave tubes is discussed in terms of the negative resistance picture.

7734 SYNTHESIS OF DRIVING-POINT IMPEDANCES WITH ACTIVE RC NETWORKS by I. W. Sandberg (Bell Labs.); Bell Sys. Tech. J., pp. 947-962, July 1960

A general method for synthesizing driving-point impedances using RC networks and active elements is presented. The procedure realizes any real rational driving-point function and leads to rather simple structures. Only one active device, a negative-impedance converter, is required. The synthesis of biquadratic impedance functions is considered in detail.

7735 A PARAMETRIC DEVICE AS A NONRECIPROCAL ELEMENT by A. K. Kamal (Bell Labs.); Proc. IRE, Vol. 48, pp. 1424-1430, Aug. 1960

A parametric device which is equivalent to a passive nonreciprocal phase shifter has been proposed. A first-order analysis of this device is made assuming the series resistance effect in the variable capacitance diode to be negligible and a dispersion theory for matching and bandwidth of the nonreciprocal element is developed. The nonreciprocal phase behavior of the device has been exhibited experimentally over a narrow frequency band.

Instrument for Microcircuit Assembly - See 7844

7736 LAMINAR JUNCTION LAYERS — NEW CONCEPT IN MICROCIRCUITS by J. E. Allegretti and D. J. Shombert (Merck, Sharp, Dohme); Electronics, Vol. 33, pp. 55-57, Dec. 2, 1960

Formation of complex solid-state configurations by continuous deposition of single-crystal silicon layers on a single-crystal silicon substrate by vapor-phase reduction of a volatile silicon derivative with hydrogen is described. The laminar layers can be controlled to form a number of semiconductor device configurations during growth of the single crystal. Areas of several square inches can be formed. Layers with controlled resistivity gradients can be deposited. Electrical isolation can be achieved between layers and highly doped layers can be put in the interior of a structure during the growth process. A number of layers can be consecutively deposited to produce individual devices at predetermined locations within the crystal. Functional elements that have been deposited include capacitors, resistors, rectifiers, zener diodes, p-n-p-n transistors, and solar cells.

7737 PARALLELING POWER TRANSISTORS by R. J. Zelinka and D. C. Mogen (Minn.-Honeywell); Electronic Equipm. Engrg., Vol. 8, pp. 62-66, Sept. 1960; p. 56, Oct. 1960

The factors necessary for parallel operation of transistors with different current gain and transconductance figures are discussed. An individual emitter resistor is the only circuit component which will compensate for inequalities in both current gain and transconductance. The currents split according to the transconductances. A step-by-step procedure to determine the emitter resistance when paralleling transistors is given. It is necessary to drive the lowest gain, lowest Gm unit to the average current by the same drive which will not cause the highest gain unit to exceed its maximum collector current.

7738 THERMISTORS IN TRANSISTOR CIRCUITS by L. H. Hardy and H. R. Emes (Carborundum); Semicon. Prod., Vol. 3, pp. 31-35, Aug. 1960

The use of thermistors for temperature compensation of transistor circuits is considered. Thermistors are available in a wide range of resistance values and temperature coefficients. Time constants similar to transistor time constants are available. Characteristics of available thermistors are discussed together with methods for determination of characteristics and a description of how they should be specified. Some typical applications for thermistors in compensating transistor circuits are also discussed. A method for obtaining the required thermistor characteristics for a specific transistor compensation application is outlined.

Methods of Cooling Semiconductor Devices - See 7697

AMPLIFIERS

7739 A TECHNIQUE FOR CASCADING TUNNEL-DIODE AMPLIFIERS by P. M. Chirlian (New York U.); Proc. IRE, Vol. 48, p. 1156 (L), June 1960

A tunnel-diode amplifier circuit that uses two tunnel diodes per stage, one in shunt and the other in series with the load, is described. The input resistance of the circuit can be made equal to the load resistance, so several stages can be cascaded to obtain a net gain equal to the product of the individual stage gains. The cascaded stages may be considered as a transmission line with gain; the frequency response of the amplifier circuit (or of the transmission line) can be adjusted by use of series and shunting impedances.

7740 OPTIMUM TWO-TERMINAL INTERSTAGE DESIGN FOR HIGH-FREQUENCY TRANSISTOR AMPLIFIER by W. H. Ku and H. J. Carlin (Brooklyn Polytech. Inst.); U.S. Gov. Res. Rep., Vol. 33, p. 505 (A), May 13, 1960 PB 144 821

The design of optimum two-terminal interstage is treated. In transistor feedback amplifier design, the most satisfactory interstage networks are two-terminal structures. For high-frequency transistors in cascade, the equivalent network can be considered to consist of a shunt resistance-capacitance load in parallel with the two-terminal interstage structure. The problem is to design a coupling network to obtain maximum gain-bandwidth product consistent with physical realizability conditions of a two-terminal structure for the prescribed shunt R-C load. The theoretical limitations on the performance of the optimum two-terminal interstage are examined and three basic methods of design are given. It is concluded that the optimum gain-bandwidth of a two-terminal interstage is reduced by the presence of the shunt resistive element. Optimum gain-bandwidth characteristics are deduced and used to determine the shunt equalizer network.

7741 REVIEW OF NONLINEAR DISTORTIONS IN TRANSISTOR STAGES, INCLUDING CROSS MODULATION [in German] by H. Lotsch (Telefunken); Arch. Elektr. Übertragung, Vol. 14, pp. 204-216, May 1960

A nonlinear transfer characteristic is approached by the first terms of a Taylor expansion and the distorted output voltage is calculated for a suitably chosen input voltage. This general derivation is specialized for the skewed transistor exponential function $I_B = f(U_{EB})$ and the equations for several distorted output voltages are stated. It is shown that (in the same way as in tubes) the important distortions are very closely interrelated, but, unlike the tubes, these distortions disappear at a special working point. The influence of the base resistance and the internal resistance of the generator is discussed with respect to the appearance of this zero and the frequency dependence of the distortions. To reduce cross modulation in a transistorized RF amplifier two possibilities are described to compensate for these distortions for a fixed or variable working point by means of predistortion or push-pull modulation. The different influence of a resistance in the base lead or of a resistance in the emitter lead that is by-passed capacitively for RF signals only is pointed out.

7742 THE COMMON COLLECTOR-COMMON EMITTER PAIR by M. S. Ghausi and D. O. Pederson (U. California); U.S. Gov. Res. Rep., Vol. 34, p. 152(A), Aug. 19, 1960 PB 146 093

The design and analysis of a common collector-common emitter pair selected from a cascade of identical pairs are presented. The primary interest is in low pass broadband amplifiers. Simple equivalent circuits for the pair are developed and a design procedure for achieving a flat-type magnitude transmission characteristic in the pass band is given. The gain bandwidth factor of a CC-CE pair is compared with the other broadband low pass amplifiers using the common emitter configuration with various broadbanding techniques. These other broadbanding techniques include: resistive broadbanding, series-peaking, local series feedback of a parallel RC network in the emitter lead, and shunt-peaking. It is shown that for large bandwidths the combinational pair of CC-CE is superior in gain-bandwidth factor except for the shunt-peaked amplifier.

Phase Splitter Video Amplifier - See 7785

7743 A SOLID-STATE VIDEO PROCESSOR WITH PULSE-FOR-PULSE AGC by R. E. Segal (Packard-Bell Electronics); 1960 IRE WESCON Conv. Rec., Part 2, pp. 35-42

The solid-state video processor with pulse-for-pulse AGC is a wideband video amplifier designed to receive an IF amplifier output ranging in amplitude from signals barely discernible in the noise to at least 30 db above that level. This video processor produces output pulses which have a limited two-volt output and a width equal to the 50 per cent width of the input. Input pulses have poor rise and fall times and therefore large inputs would be stretched considerably if a system of pulse-for-pulse AGC were not used. The video processor preserves the delay and width information over a large dynamic range by effectively slicing out the center portion of each pulse and processing this signal into a standard amplitude and shape. This action is performed on both the leading and trailing edges of each pulse using direct-coupled circuits. Enhancing of the rise and fall times, Zener diode limiting, and driving of long coaxial cables are discussed.

7744 TRANSISTORIZED DATA AMPLIFIER HAS HIGH GAIN-STABILITY by F. Offner (Offner Electronics); Electronics, Vol. 33, pp. 55-57, July 1, 1960

A transistorized data amplifier with gain and linearity constant to 0.01% from 15 to 35°C and to 0.02% from 0 to 55°C is described. The output chopper circuit prevents oscillation or overshoot and gives an output independent of dwell time with the output rising to its full value after a single chopper cycle. A single secondary winding and center-tapped capacitors give a chopper output equal to the total top-to-bottom height of the waveform, reducing ripple and eliminating initial switching transients. Amplifier stability with temperature change is obtained by operating point feedback. Gain is controlled by switching the number of turns used in a tertiary feedback winding. Output impedance is less than 1/100 ohm.

7745 NOISE SUPPRESSION FOR DIGITAL SIGNALS by F. W. Kear (Lytle); Electronics, Vol. 33, p. 80, July 15, 1960

Generation of an acceptable signal from a noisy pulse by junction transistor pulse-forming amplifiers is discussed. The sharp portion of the noisy pulse triggers the amplifiers into saturation and the less acceptable portion falls into the saturation region. The pulse circuit feeds an integrating circuit in the emitter of a unijunction transistor to provide a uniform output pulse train. Duration of the output pulse will be the time during which the integrated pulse voltage exceeds the preset firing voltage of the unijunction transistor. The standardized pulse train is used in digital readout equipment and in digital to analog conversion circuits.

7746 ELECTRICAL CIRCUIT EMPLOYING TRANSISTOR by L. C. Thomas (Bell Labs.); U.S. Pat. 2,964,651, Issued Dec. 13, 1960

A transistorized pulse regenerator circuit which is relatively insensitive to wide variations in applied potential and which may be controlled by pulses of small magnitude is described. The circuit comprises a point contact transistor with a current signal gain a greater than unity and a feedback path connected inductively between the collector and emitter of the transistor and in series between the collector and the primary of an output transformer. An essentially constant output voltage relative to a varying load is achieved through critically relating the feedback and output transformer characteristics. The circuit is relatively insensitive to ambient temperature changes and requires comparatively little power in the quiescent state.

7747 TRANSISTOR AMPLIFIER AND PULSE SHAPER by T. H. Bonn and J. P. Eckert, Jr. (Sperry Rand); U.S. Pat. 2,966,592 Issued Dec. 27, 1960

A non-regenerative amplifier which utilizes charge carrier storage (enhancement charge phenomenon) in transistors to provide pulse amplification and pulse shape regeneration in a single stage, with control of rise and fall times, is described. A shaping circuit, consisting of a diode rectifier in combination with a variable potential source, is connected to bypass the input or load, or both. The conduction time of the rectifier is controlled by a clock pulse. The shaping circuit is turned on at a predetermined time interval after cessation of the input signal to draw the enhancement charge and bypass the load, controlling the fall time. The shaper can be operated to bypass the input signal for a predetermined time interval to increase the output pulse rise time. A combination of modes of operation results in accurate control of rise and fall times and wave shape of the output pulse.

7748 TRANSISTORIZED BIPOLAR AMPLIFIER by H. M. Bissell and A. Zarouni (Bell Labs.); U.S. Pat. 2,964,656, Issued Dec. 13,1960

A bipolar amplifier which provides a pair of output pulses corresponding to the positive and negative excursions of high-frequency signals from a single-ended source is described. The amplified signal drives a transistor alternately to cutoff and saturation. A diode and transistor arrangement separates the pulses by polarity and directs them to independent channels interconnected by an impedance element. A pulse in either channel provides a discharge potential to the coupling capacitor in the other channel of such polarity as to increase the discharge rate during part of the discharge cycle. The diodes are oppositely poled and conduct alternate pulses. The positive excursion is applied to an n-p-n transistor and the negative part to a p-n-p transistor. These transistors are normally reverse-biased and are driven into saturation. The separated pulses are fed to regenerative pulse amplifying circuits with separate outputs.

7749 AN INTEGRATING AND DIFFERENTIATING AMPLIFIER FOR USE IN VIBRATION MEASUREMENTS by M. Kringlebotn (Tech. U., Norway); Electronic Engrg., Vol. 32, pp. 504-505, Aug. 1960

An amplifier designed for measuring vibrations is described. The signal source in the vibration measurements is assumed to be a velocity pick-up, and the amplifier output is delivered to a low-impedance load (e.g., a galvanometer with 25 Ω internal resistance). When used as an integrator the amplifier converts the input velocity signal to a signal which indicates the displacement and, when used as a differentiator, to a signal which indicates the acceleration of the pick-up. The amplifier may also be used for linear amplification of the velocity signal. The amplifier stages are stabilized with respect to temperature changes. The additional feedback also contributes to thermal stability. A single 12.6 V source is used.

7750 ANALYTICAL DESIGN OF TRANSISTOR PUSH-PULL AMPLIFIERS by R. H. Riggs (Avco); Electronics, Vol. 33, pp. 60-62, June 10, 1960

Exact equations which permit mathematical comparison of power amplifier performances without building the circuits are developed. Comparison of calculated and actual performance gave errors within the manufacturing tolerances in all cases. Exact equations are developed for the efficiency, power gain, maximum power output, power dissipated per transistor, and the impedance parameters required.

Transistor Switching Amplifier - See 7812

7751 LARGE-SIGNAL BEHAVIOR OF A DEGENERATE PARAMETRIC AMPLIFIER by Y. P. Vaddiparty (Ohio State U.); U.S. Gov. Res. Rep., Vol. 34, p. 429 (A), Oct. 14, 1960 PB 146 606

The results of a study of degenerate parametric amplifiers with strong saturating signals are reported. Certain peculiarities of behavior, including a shift in the frequency of maximum gain and sudden jumps in gain at certain frequencies in the pass band, have been observed. A semi-quantitative explanation is given in terms of the strong nonlinearity of the diode under saturating signals. The results may be useful in providing information on the signal-handling capacity of an amplifier, particularly for modulated signals.

7752 REACTANCE DIODES AND THEIR USE IN WIDEBAND WAVEGUIDE AMPLIFIERS [in German] by P. Bobisch and C. Sondhauss (Telefunken); Telefunken-Roehre, No. 38, pp. 115-124, Dec. 1960

In using semiconductor reactance diodes for parametric amplification in the kMc region by means of a periodically loaded waveguide, one must satisfy certain requirements with regard to the cartridge of these diodes. The problems of designing such an iterative traveling-wave parametric amplifier using waveguide techniques are discussed. In connection with a newly developed diode cartridge having disk-shaped electrodes, the construction of an iterative waveguide amplifier is described which at present contains only two diodes in cascade and is designed for the frequency range 2.7 to 2.9 kMc. Experimental results are also reported. Furthermore, the construction and performance of a frequency multiplier which operates up to 6 kMc are shown.

7753 A WIDE-BAND UHF TRAVELING-WAVE VARIABLE REACTANCE AMPLIFIER by R. C. Honey and E. M. T. Jones (Stanford Res. Inst.); IRE Trans., Vol. MTT-8, pp. 351-361, May 1960

The techniques developed for designing periodically loaded traveling-wave parametric amplifiers using variable-reactance diodes are described in detail. An amplifier was built and tested with two different sets of eight diffused junction silicon diodes. The performance of the amplifier with each set of diodes agrees substantially with the theoretical predictions, the measured noise figures being about 1.2 db higher than the theoretical values in each case. The gain of the second amplifier varied from a minimum of 6.7 db to more than 13 db over the band from 550 to 930 mc, with a measured noise figure of 2.3 db for wide-band noise inputs in the middle of the band, corresponding to about 4.9 db for single-frequency inputs.

Varactor Diodes for Strip Line Parametric Amplifiers - See 7698

7754 GAIN AND BANDWIDTH INCONSISTENCIES IN LOW FREQUENCY REACTANCE UP-CONVERTER PARAMETRIC AMPLIFIERS by A. K. Kamal and A. J. Holub (Purdue U.); 1960 IRE WESCON Conv. Rec., Part 2, pp. 80-85

The fact that the gain of a low frequency up-converter reactance parametric amplifier is seldom equal to the theoretical value given by the ratio of the upper side band frequency to the signal frequency is discussed. A first order explanation is presented by showing that a parameter a, which is an important factor in the gain equation, has to be equal to unity to give the theoretical gain. At low frequencies, however, this condition is very difficult to realize in practice. The bandwidth is shown to be less than that predicted by others when the factor a is not unity. The noise figure does not seem to be affected. An experimental amplifier is described and the above results are verified, showing complete agreement.

Parametric RF Amplifier - See 7777

2 kMc Parametric Amplifier - See 7845

7755 TRANSISTOR POWER AMPLIFIERS WITH NEGATIVE OUTPUT IMPEDANCE by W. Steiger (Hughes); IRE Trans., Vol. AU-8, pp. 195-201, Nov.-Dec. 1960

The results of a detailed analysis of two practical transistor amplifier configurations which produce negative output impedance are presented. A push-pull power amplifier, based on this analysis, uses the bias stabilizing elements of the output stage to obtain the necessary positive current feedback. The three-stage circuit delivers, without a transformer, 12 watts into 8 ohms or 8 watts into 16 ohms. The output impedance is adjustable from plus 1 ohm to either minus 7 or minus 14 ohms. The amplifier has been used successfully in an all-transistor stereophonic high-fidelity system.

7756 TRANSISTORS IN AUDIO- AND CARRIER-FREQUENCY AMPLIFIERS by K. Lamont (Assoc. Elect. Ind.); Electronic Tech., Vol. 37, pp. 292-299, Aug. 1960

The characteristics of common-emitter transistor amplifiers are discussed in relation to the specific requirements of communication systems. In audio and carrier telephone applications, it is necessary that the amplifiers shall have a constant gain, that

input and output impedance shall remain reasonably close to specified values and that the distortion products shall be very small, typically 80 db below the fundamental of any frequency in the pass-band. These performance characteristics are normally required to be met up to temperatures of $+55^{\circ}C$, preferably with germanium transistors. Practical methods of stabilizing both the bias point and the gain of a single stage are discussed, together with the gain and bandwidth achievable with the common-emitter connection. A two-stage feedback circuit is analyzed in detail, the behavior being illustrated by means of flow graphs. Finally, consideration is given to the problem involved in applying large amounts of feedback over several stages and of obtaining the desired input and output impedances. A practical design of a 25-db amplifier suitable for 5 telephone channels is given; the amplifier has 30 db of feedback applied over three stages. A further illustrative example is also given in the design of a typical channel amplifier.

OSCILLATORS

7757 MULTIVIBRATOR CIRCUITS WITH OUTPUT SIGNAL FEEDBACK FOR INCREASING TRIGGER SENSITIVITY by C. L. Wanlass (Thompson Ramo Wooldridge); U.S. Pat, 2,965,768, Dec. 20, 1960

A method of increasing trigger sensitivity in multivibrator circuits using output signal feedback is described. Both ac and dc feedback are considered. The ac feedback enhances the trigger sensitivity in that any increase in conduction through one transistor due to the application of an input pulse results in a corresponding increase in the back biasing voltage developed across the emitter feedback resistor of the other transistor. The dc feedback operates in a similar manner, tending to reduce the conduction of one transistor when there is high conduction through the other. It can therefore be used as a stabilization means. In the example cited, Zener diodes were used for static stability.

7758 HOW TO DESIGN TRANSISTOR BLOCKING OSCILLATORS by H. L. Morgan (ReDev Labs.); Electronic Equipm. Engrg., Vol. 8, pp. 73-76, Sept. 1960

Design considerations and equations for control of blocking oscillator pulse width by use of transformer saturation, transformer inductance, external gating, RC control, and delay lines are presented. With transformer saturation, variations in core material and change in saturation flux density with temperature affect pulse width. The transformer inductance can be stabilized by selection of core material or by air-gaps but effects of base resistance and beta variation prevent close control of pulse width. If an external gating signal is used to cutoff the transistor, power requirements are increased. Delay lines can be used to terminate pulses by connecting in the circuit so that the waveform reflected from the shorted end turns off the oscillator. Use of a series resistor and capacitor between the feedback winding and transistor base provides linear pulse width control independent of transformer and transistor characteristics.

High-Frequency Varactor Diodes for Phase-Locked Oscillators - See 7698

7759 A NOVEL SINGLE TRANSISTOR RC OSCILLATOR by E. T. Emms (Genl. Precision Systems); Electronic Engrg., Vol. 32, pp. 506-508, Aug. 1960

A novel single transistor RC oscillator which will oscillate with the majority of low frequency transistors even with the transistor current gain at the lower limit is described. The circuit employs a modification of the parallel-T network. The effect of finite transistor input impedance and output capacitance is discussed.

7760 OSCILLATOR PERFORMANCE OF TRANSISTORS IN THE HF TO UHF RANGE by W. M. Feist (Diamond Ord. Fuze Labs.); U.S. Gov. Res. Rep., Vol. 33, p. 499 (A), May 13, 1960 PB 145 270

An outline of the factors to be considered in the design and construction of high-frequency transistor oscillators having optimal output efficiency is given. The design and construction of test oscillators covering the range from about 10 to over 1000 mc is described.

SWITCHING CIRCUITS

7761 COMPARISON OF SATURATED AND NONSATURATED SWITCHING CIRCUIT TECHNIQUES by G. H. Goldstick (Natl Cash Register); IRE Trans., Vol. EC-9, pp. 161-175, June 1960

The concept that the junction transistor is a charge-controlled current source is reviewed. Saturated operation and nonsaturated operation are defined on the basis of minority and majority carrier distributions in the base region. Several common emitter switching circuits are analyzed. The switching efficiency, a figure of merit based on the charge storage properties of the transistor, is introduced. Saturated and nonsaturated operation are compared on the basis of switching efficiency, transient waveforms, stability of the voltage levels, power dissipation, noise rejection and suppression ability, and circuit complexity. Currently used antisaturation techniques are discussed.

7762 MULTIDIODE SWITCHES by J. Galejs (Sylvania); IRE Trans., Vol. MTT-8, pp. 566-569 (L), Sept. 1960

The feasibility of using multidiode shunt or series type switches for controlling microwave signal transmission is examined. After establishing equivalent circuits representative of the diodes in the "on" and "off" states of the switch, a specific realizable single diode switch is assumed for the calculations. Characteristics of a multipole switch which consists of a number of diodes in individual transmission line branches are derived for the two switch types. Several measurements made on an 8-diode series switch are given.

7763 SWITCHING AND MEMORY CRITERIA IN TRANSISTOR FLIP-FLOPS by D. K. Lynn and D. O. Pederson (U. California) 1960 IRE Int. Conv. Rec., Part 2, pp. 3-10

A simple criterion for determining which storage elements of a transistor flip-flop can provide memory in a flip-flop used with a mono-polarity pulse train input at one port is proposed. A typical transistor (or vacuum tube) flip-flop has many energy storage elements. However, only certain of these can provide the necessary memory if the flip-flop is to be used with a mono-polarity pulse train input at one port. For example, the excess

minority carrier storage in the base region of a transistor or the charge on shunt capacitances to ground do not provide memory. A knowledge of the minimum amount of memory is also very important in the design of flip-flops for optimum speed (repetition rate). This latter problem is closely related to the switching criterion of the circuit. As examples, typical circuits such as the collector-coupled (or the so-called Eccles-Jordan circuit) are used. Experimental results concerning minimum memory and maximum repetition frequency are presented.

7764 INDICATING DEVICE FOR ELECTRONIC COUNTERING CIRCUITS by R. Favre (Fabriques Movado, Switzerland); U.S. Pat. 2,966,614, Issued Dec. 27, 1960

A circuit which makes possible the use of high voltage low current gas discharge tubes as indicator lights for 10w voltage bistable transistor flop-flops is described. The control windings of two magnetic amplifiers form the load resistances of the flop-flop transistors and control the application of the output of a pulse generator through the windings of the magnetic amplifiers to the gas discharge indicating tubes. A decade counter indicating device employing the magnetic amplifier principle is also described.

7765 INPUT CIRCUITS AND MATRICES EMPLOYING ZENER DIODES AS VOLTAGE BREAKDOWN GATING ELEMENTS by C. L. Wanlass (Thompson Ramo Wooldridge); U. S. Pat. 2,965,767, Issued Dec. 20, 1960

The utilization of a Zener diode in a dc pulse gating system to provide proper biasing and pulsing operating levels is described. The use of a Zener diode in gating circuits is shown to overcome the limitations of conventional pulse coincidence and dc gating systems and to operate a current sensitive flip-flop without the necessity of a coupling capacitor. The Zener diode is used in both "and" and "or" gating circuits as a voltage breakdown element between two signals and also to provide an effective current source for driving a storage element. Logical matrices using Zener diode "and" and "or" circuits are also described.

7766 FREQUENCY SELECTIVE TRANSISTOR SWITCH by R. Murray, Jr. (Westinghouse); Electronic Equipm. Engrg., Vol. 8, pp. 49-50, Oct. 1960

A frequency selective transistor switch which is triggered by a preselected narrow frequency band is described. A parallel resonant circuit is tuned to a selected frequency. The inductance consists of two inductors in series with an inductance ratio of 5:1. A germanium diode detector circuit, connected across the smaller inductor, develops a dc output voltage with a magnitude proportional to the input frequency. This provides the input to a regenerative-type switching circuit which controls an output transistor, held in cutoff by a forward-biased diode in its emitter circuit. When the input signal is above a predetermined value, the output of the regenerative circuit changes from one voltage extreme to the other, providing enough drive to switch the output transistor from cutoff to saturation.

7767 A CLASS OF OPTIMAL NOISELESS LOAD-SHARING MATRIX SWITCHES by R. T. Chien (IBM); IBM J. Res. and Dev., Vol. 4, pp. 414-417 (L), Oct. 1960

Minimization of the number of input wires and input drivers in noiseless load-sharing matrix switches is discussed. A mathematical interpretation of the function of a load sharing switch in terms of a winding matrix and its identification with a special class of orthogonal matrices is presented, and the results obtained by Paley on the construction of orthogonal matrices are then used in the logical design.

7768 DYNAMIC BISTABLE OR CONTROL CIRCUIT by E. O. Keizer (RCA); U.S. Pat. 2,964,637, Issued Dec. 13, 1960

A simplified bistable circuit which uses the rectification characteristic and the voltage sensitive junction capacitance characteristic of semiconductor diodes is described. The diode junction capacitance is controlled by the rectifying action of the diode. An inductor and a capacitor are connected in series with the diode and a variable voltage ac source. The diode is poled such that the capacitor is charged negatively by the diode rectifying action and provides reverse bias for the diode. The two stable states are determined by the equilibrium between bias voltage and peak ac voltage across the rectifying diode. The minimum transition time from one stable state to another is 3-10 cycles of the exciting frequency. A light sensitive control circuit is provided by using a light sensitive semiconductor diode.

7769 DYNAMIC BISTABLE OR CONTROL CIRCUIT by H. D. Helms (RCA); U.S. Pat. 2,964,646, Issued Dec. 13, 1960

A simple, high-speed circuit having a bistable characteristic and a sensitive input-output characteristic is described. The circuit utilizes the variable capacitance characteristic of a semiconductor junction in the form of either back-to-back junction diodes or a single transistor, in series with an inductor and energized by a high frequency ac source. The circuit can find application in memories, ring counters, shift registers, or in control and modulating or detection circuits.

Diode-Transistor Switching Circuits - See 7797

7770 TRANSITOR SWITCHING CIRCUITS by H. S. Yourke (IBM); U.S. Pat. 2,964,652, Issued Dec. 13, 1960

Several examples of transistor switching circuitry employing an improved variation of grounded base operation are described. The improvement is accomplished by providing a transistor switching circuit having a common point to which is attached a constant current source. Multiple current paths are provided between the common point and a reference potential, each of which has an asymetric impedance and at least one of which is a transistor. A difference in potential may be applied between the points in the paths to control the path through which the constant current flows. The circuit refinement provides faster switching speeds, minimizes the number of power supplies needed, and makes each stage independent with respect to loading.

7771 MAGNETIC CORE FLIP-FLOP by R. C. Lamy (IBM); U.S. Pat. 2,966,664, Issued Dec. 27, 1960

A bistable flip-flop circuit employing saturable magnetic cores having high remanence and low coercive force as memory elements is described. Non-destructive sampling of the state of the device is accomplished through the use of sampling windings which encircle only a portion of the flux path of the core. Output readings of the flip-flop differ from those of conventional flip-flops in that they are in the form of pulses rather than dc levels of output. The core material employed is 4-79 Mo Permaloy or similar material.

Energy Switching with Four-Layer Diodes - See 7822

OTHER SOLID STATE DEVICE CIRCUITS

7772 SOLID-STATE PULSE MODULATOR by W. H. Lob (Northeastern U.); Electronics, Vol. 33, pp. 72-74, July 22, 1960

A pulse modulator using silicon gated diodes as switches, with a switch recovery time of less than 50 μsec, which has a peak power output of 360 w is described. Input to output delay is 1.3 μsec with jitter of 0.01 μsec. A second silicon gated diode switch replaces the conventional charging choke. This recharging switch holds off the supply voltage while the pulse forming network discharges through the discharge switch and the output transformer. A time-delay circuit triggers the recharge switch at the end of the bottoming period (2 μsec) and the pulse forming network recharges. The modulator is ready to be triggered again as soon as the recharge switch has recovered. A series relay protects against runaway and an RC circuit prevents operation before the circuit reaches the initial quiescent state. The modulator will accept an input pulse width of 1-10 μsec with a minimum pulse spacing of 35 μsec and a maximum pulse rate of 5000 pps.

7773 CONTROLLED RECTIFIER FREQUENCY MULTIPLIER USES INVERTER PRINCIPLES by C. W. Flairty and J. D. Harnden, Jr. (GE); Electronic Equipm. Engrg., Vol. 8, pp. 107-111, Aug. 1960

A preliminary study of a frequency changer using silicon controlled rectifiers which has an output frequency independent of the supply frequency is presented. Commutation is obtained primarily from capacitors rather than from line voltage. Three-phase, 60-cycle input is converted to single-phase power at a frequency controlled by the gate signal of the SCR's. The SCR's are connected in full-wave fashion with a commutating capacitor and air core inductance across the winding. An adjustable frequency oscillator supplies a saturable reactor which furnishes a firing signal to each SCR gate on alternate half cycles of the control signal frequency. By alternately triggering the two SCR's in each inverter section, current flow switches between them and an alternating output voltage of the same frequency as the gate signal is produced. The upper frequency limit is primarily determined by the SCR turn-off time.

7774 PULSE GENERATOR FOR SYNCHRONIZING EVENTS by R. E. Daniels and C. Swoboda (Argonne Natl. Lab.); Electronics, Vol. 33, p. 63, June 10, 1960

A junction transistor pulse generator which provides either a positive or negative output pulse of 1 μsec duration, ±0.4 μsec, into a 90 ohm load with a maximum repetition rate of 40 kc is described. Rise and fall times of the isolated output pulse are 0.2 μsec with less than 10 per cent sag with a 90 ohm load and less than 5 per cent overshoot on open circuit. The generator can be triggered by positive or negative pulses greater than 5 v with rise times greater than 2 v/μsec.

Ultrafast Rise Time Pulse Generator - See 7795

7775 SEQUENCE DETECTION USING ALL-MAGNETIC CIRCUITS by H. D. Crane (Stanford Res. Inst.); IRE Trans., Vol. EC-9, pp. 155-160, June 1960

A technique for detecting specific sequences of pulses occurring on a net of input lines is described. This technique lends itself to realization in all-magnetic networks by the use of multi-aperture magnetic devices (MAD's). The resulting circuits are remarkably simple and reliable. Processing rates in excess of 100,000 characters per second may be achieved. Examples of systems using arrays of such detectors are given. One example involves a system for detecting handwritten characters which makes use of a special pen having the property of generating specific sequences of pulses as symbols are written. The second example relates to the problem of monitoring text for the detection of specific words (letter sequences) and phrases (series of sequences).

Transistorized Ripple Filters - See 7811

APPLICATIONS OF SOLID STATE DEVICES

GENERAL

Radar Transponder for Missile Tracking - See 7791

Magnetic Recording Technique for Satelites - See 7792

7776 IGNITION SYSTEM by E. W. Meyer, J. G. Naborowski and R. J. Latorre (Electric Auto-Lite); U.S. Pat. 2,966,615, Issued Dec. 27, 1960

An internal combustion engine ignition system designed to eliminate ignition failures due to the formation of objectionable films on conventional breaker points is described. This is accomplished by utilizing a transistor for the function of establishing and breaking the primary current of the ignition coil. The transistor switching pulse is provided with conventional breaker points, but the currents involved are substantially lower than those required in non-transistorized ignition systems. An ignition coil with low primary inductance is used to prevent transistor damage resulting from coil kick-back.

RADIO

7777 PARAMETRIC RADIO FREQUENCY AMPLIFIER by A. Szerlip (Packard-Bell Electronics); 1960 IRE WESCON Conv. Rec., Part 2, pp. 62-79

The results of a theoretical analysis and an experimental study concerning the use of parametric amplifiers in communication receivers are presented including an analysis of circuit stability for the general case. This analysis shows that a parametric amplifier operating in the difference mode can become unstable that the same amplifier operating in the sum mode is unconditionally stable; and that the amplifier operating in both the sum and difference modes is capable of stable operation. The necessity for parametric amplifiers to fulfill additional requirements in multi-signal communication environments, as opposed to those required in single signal radar and satellite applica-

tions, is recognized; and a study to fulfill these requirements is given. This study describes construction of a low frequency amplifier (2 Mc) for intermodulation investigation, measuring techniques, and test results. The report concludes with a brief discussion of studies in progress on experimental high frequency (225-400 Mc) parametric amplifiers.

7778 PORTABLE RADIO USES DRIFT-FIELD TRANSISTORS by R. A. Santilli and H. Thanos (RCA); Electronics, Vol. 33, pp. 48-50, July 8, 1960

A transistorized AM/FM portable radio using drift-field transistors in the tuner and IF strip is described. The drift-field transistor has a small effective base width, low feedback capacitance, high collector-breakdown voltage and is capable of oscillation and amplification in the FM band. An inductor in the emitter-base circuit of the oscillator corrects for the transconductance phase shift. At 10.7 mc, the IF strip has a neutralized gain per stage of 23 db; at 455 kc, a neutralized gain per stage of 40 db is obtained. Point-contact germanium diodes are used for AM and FM detection. The circuit design is presented in detail.

7779 TRANSISTORIZED AUTOMOBILE RECEIVERS EMPLOYING DRIFT TRANSISTORS by R. A. Santilli and C. F. Wheatley (RCA); Semicon. Prod., Vol. 3, pp. 29-35, June 1960

Six all-transistor automobile radios designed to use a five-stage lineup including rf amplifier, converter, if amplifier, first-audio, and power-output stages are described. The six receivers differ in having three-coil or four-coil tuners and Class A or Class B output. All six variations have a sensitivity of approximately two microvolts antenna signal for one watt of audio power. Sensitivity for a 20-db signal-to-noise ratio is five to ten microvolts (depending upon circuit). The Class A output circuit delivers about four watts of undistorted power and the Class B output circuit about eight watts of undistorted power. The receivers "overload" at about one volt on the antenna.

7780 SIGNAL-SEEKING AUTO RADIO USES SEMICONDUCTOR TUNING by J. G. Hammerslag (Hughes Products); Electronics, Vol. 33, pp. 60-62, July 22, 1960

The use of semiconductor variable capacitors as tuning elements in radio receivers to effect savings in size, weight and cost is described. Maximum to minimum capacitance ratios of 35:1 have been obtained. At present, the Q of available silicon capacitors is relatively low. A signal-seeking receiver can be made by using an RC circuit to vary the tuning capacitance and thereby to sweep the broadcast band.

7781 VOLTAGE SENSITIVE DIODE TUNING SYSTEMS by R. S. Tilton and L. V. Bessen (USASRDL); U.S. Gov. Res. Rep., Vol. 34, p. 149 (A), Aug. 19, 1960 PB 146 933

An investigation of voltage-sensitive variable-capacitance semiconductor diodes for use in tuning systems is discussed. Variations of C and Q with voltage and temperature in the 10-18 mc frequency range are reported. Circuits for obtaining straightline-frequency tuning, tracking of ganged diodes, and temperature compensation are described.

7782 A TRANSISTORIZED AM-FM RECEIVER USING MADT TRANSISTORS by J. Heinchon and T. C. Lawson (Philco); IRE Trans., Vol. BTR-6, pp. 42-46, Nov. 1960

The selection of transistors whose characteristics optimize the performance of a completely transistorized AM-FM receiver is discussed. The selection of transistors is difficult since many of the transistors are used for both AM and FM operation frequency ranges. One of the RF transistors selected, the L5442, is a developmental transistor and has a typical gain and noise figure of 17 and 3-3.5 db, respectively. The circuit and the transistors employed in it are described.

TELEVISION

7783 POWER SOURCES FOR LOW HEATER POWER TUBES IN TRANSISTORIZED RECEIVERS by B. M. Soltoff and C. B. Tyson (Philco); IRE Trans., Vol. BTR-6, pp. 38-41, Nov. 1960

The problem of finding a location for the power source for the low-power heater of the CRT designed for a completely transistorized battery operated television receiver is discussed. The power source must be placed so that it supplies the needed voltage within specified limits without drawing excess power from the battery or affecting normal operation. Four locations were investigated — the vertical output stage, the horizontal output stage, the power supply section, and the horizontal output transformer core — and the results for these locations are presented. The horizontal output core appears to be the most versatile choice; however, the choice may vary with receivers.

7784 TRANSISTORIZED TV AND FM TUNERS by K. Wittig (Std. Coil Prod.); Semicon. Prod., Vol. 3, pp. 19-25, July 1960

Some of the design considerations for VHF front ends, using madt and mesa transistors as rf amplifiers, mixers and oscillators, are described. Both common emitter and common base configurations are compared as to their characteristics and suitability. Practical applications are explained by means of Standard Coil TV and fm tuner schematics. Input and interstage matching are discussed together with agc methods and their effect on bandpass characteristics.

7785 PHASE SPLITTER VIDEO AMPLIFIER FOR TRANSISTOR TV by Z. Wiencek (Warwick Mfg.); IRE Trans., Vol. BTR-6, pp. 18-24, Nov. 1960

A phase splitter video amplifier for a transistorized TV receiver is described. A common-emitter p-n-p transistor and a common-base n-p-n transistor in phase-inverting configuration drive the grid and cathode of the picture tube. Equivalent circuit, voltage gain, input impedance, thermal stability and band width limitations are analyzed for this configuration. It is shown that the phase splitter has the advantages over presently used types of better power economy, lower voltage and power transistor ratings, higher input impedance, high voltage gain and no phase shift problems. An input signal of one volt (p-p) yields the equivalent of 50 volts (p-p) for each electrode of the picture tube.

Power Supply for a Television Camera - See 7821

7786 VIDEO TRANSMISSION OVER TELEPHONE CABLE PAIRS BY PULSE CODE MODULATION by R. L. Carbrey (Bell Labs.);

Proc. IRE, Vol. 48, pp. 1546-1561, Sept. 1960

An experimental seven digit pulse code modulation (PCM) system for the transmission of monochrome and color television signals over seven pairs of 22-gauge exchange area telephone cable is described. A beam coding tube converts the signal to seven parallel digits of a binary Gray code at a 10 Mc rate. All circuits except the coding tube deflection amplifier are transistorized. The coded digits are sent over the cable in parallel form with alternate groups converted to complements of the coded signal, thus substantially removing the low frequency component. This makes it possible to use simple repeaters without special compensation for duty factor variation. A repeater group is used after every 3000 foot section of cable. One ten megabit repeater, consisting of an amplifier and blocking oscillator, is required for each digit. All seven digit repeaters are retimed with a common timing wave. At the decoding terminal, transmitted complements are restored to Gray code before translation to natural binary. A binary weighted resistance network decoder converts the signals to a quantized reproduction of the video signal. Good quality composite color and monochrome pictures are obtained with six digits. Seven digits are believed to be necessary for broadcast quality with some margins. Waveform photographs illustrate the various functions, and photographs of decoded pictures are shown.

TELEPHONY AND TELEGRAPHY

Amplifiers for Audio and Carrier Telephone Applications - See 7756

7787 DIAL TONE GATING CIRCUIT by H. R. Hofmann (Bell Labs.); U.S. Pat. 2,966,556, Issued Dec. 27, 1960

A simplified telephone dial tone gating circuit which provides amplification of a signal along one direction of a talking path and attenuation of the signal in the opposite direction and which accomplishes this objective without termination of the talking path at the gating circuit is described. The circuit comprises two n-p-n transistors connected in shunt with their collectors connected to the talking path. The normally nonconducting transistors when connected to a signal source act to amplify the tone signal in the subscriber direction and ground the signal in the direction of the relatively closer operator.

7788 NEGATIVE IMPEDANCE REPEATER by G. F. Cerofolini (Automatic Electric Lab.); U.S. Pat. 2,963,558, Issued Dec. 6, 1960

A telephone repeater providing two negative impedance converters with the use of a single pair of amplifying devices and other circuit components in common is described. The circuit has connections for push-pull coupling the pair of amplifying devices between two sets of terminals of one converter and for parallel coupling the pair of amplifying devices between the two sets of terminals of the other converter. A prototype of the invention uses Linvill type transistorized push-pull amplifiers with emitter input, collector output, and common base.

7789 DELAY AND AMPLITUDE CORRECTIVE SYSTEM by W. D. Cannon (Western Union); U.S. Pat. 2,966,633, Issued Dec. 27, 1960

A system designed to correct delay and frequency distortion in transmission lines is described. The circuit comprises a plurality of active networks connected in cascade and provides independent adjustments for delay and frequency correction. Transistors are employed as current amplifiers to drive transistorized impedance transforming elements. The use of transistors provides compactness and reliability and permits the use of a communication channel for the provision of the system's small power requirements.

RADAR

7790 ACTIVE HIGH FREQUENCY SPECTROMETER FOR IONOSPHERIC ECHO SOUNDING IV. NUMERICAL REGISTRATION OF PULSE DELAYS [in German] by E. Harnischmacher and H. Porsche (Deutsche Bundespost); Arch. Elekt. Uebertragung, Vol. 14, pp. 503-507, Nov. 1960

An automatic transistorized apparatus for the numerical determination of echo heights is described. The pulse time delay is measured in a binary code, the result is converted into a decimal number and finally is printed out and perforated by a Telex paper tape recorder.

7791 SOLID-STATE MODULATOR FEEDS SUBMINIATURE TRANSPONDER by L. Diven (Motorola); Electronics, Vol. 33, pp. 48-51, July 1, 1960

A silicon transistor radar transponder, tunable from 5400-5900 Mc with PRF's from 340-1707 pps, which has a range tracking error of less than two yards at 200 miles and a change in delay of transponder reply of ±6 μsec for input signals from 0 to -40 dbm is described. Peak output power is 400 watts. A 10 Mc video amplifier bandwidth and an AGC circuit reduce delay variations by providing the modulator with a constant amplitude pulse with unchanging rise time. The modulator trigger uses four Shockley four-layer diodes in series, triggered by an avalanche triode. DC bias on the video detector crystal optimizes sensitivity and compensates for temperature change. Increased signal level increases the crystal bias, providing up to 45 db of video attenuation. The transponder is useful in missile test firings and for tracking short-range missiles.

RECORDING AND REPRODUCTION

All-Transistor Stereophonic High-Fidelity System - See 7755

7792 A WIDEBAND MAGNETIC RECORDING SYSTEM by M. E. Anderson, J. A. Granath and D. C. Reukauf (Armour Res. Found.); 1960 IRE WESCON Conv. Rec., Part 5, pp. 40-45

A video magnetic recording and reproducing technique suitable for airborne and mobile use, and particularly suitable for satellite applications is described. The principal features of the system are: non-mechanical scanning for long head and tape life without maintenance, high frequency recording capability with low tape speed, low power drain through use of all solid-state circuitry, with only one drive motor (for tape transport),

high area density of information stored on tape by use of multi-channel multiplexing, and potential for very compact size and low weight.

7793 THE SENSITIVITY OF REPRODUCING HEADS IN HIGH-FREQUENCY MAGNETIC RECORDING SYSTEMS by W. T. Frost (Ampex Data Prod.); 1960 IRE WESCON Conv. Rec., Part 5, pp. 46-49

The sensitivity of a reproducing head in high-frequency magnetic recording systems is defined in terms of the frequency losses in the head core. The variation in sensitivity with frequency in a high-frequency reproducing head is calculated and a method of measuring the sensitivity is presented with experimental results.

COMPUTERS

Pulse Sequence Detection for Character Recognition - See 7775

7794 UTILIZING AN ELECTRONIC COMPUTER TO OPTIMIZE A TRANSISTOR NOR CIRCUIT by E. L. Cox and L. L. Hall (Diamond Ord. Fuze Labs.); U.S. Gov. Res. Rep., Vol. 33, p. 499 (A), May 13, 1960

The accuracy with which a transistor NOR circuit can be designed for minimum power dissipation has been increased by including an additional parameter not considered in a previous analysis. The method of design involves determining the values of the input resistors, R_i, the maximum collector current, I_C, the collector resistor, R_C, and the collector supply voltage V_{CC}, from the basic NOR circuit parameters (β/S, I_{CBO}, M, N, V_{BE}). The determination of R_i consists of obtaining two analytical expressions, one larger and one smaller than the optimum R_i. The optimum R_i is then obtained by numerical interpolation on an electronic computer and is subsequently used to compute the other quantities. The flow diagram of the computer program is included, as are graphical results indicating the trends of minimum power dissipation with changes in the basic NOR circuit parameters.

7795 MILLIMICROSECOND PULSE INSTRUMENTATION FOR MICROWAVES by J. T. Tippett (Dept. of Def.); IRE Trans., Vol. I-9, pp. 32-34, June 1960

Instrumentation for the application of microwave energy to computer circuits requires that performance of microwave pulse circuits with transition times of less than 0.5 μsec be easily examined. A circuit utilizing a fast microwave diode switch as an ultrafast rise time pulse generator, a dual output detector, and a traveling-wave oscilloscope for use with pulse amplitude modulated microwave computer components are discussed. Using this same equipment with system modifications, test equipment can be built for phase pulse modulated microwave circuits. The microwave diode switch consists of a special germanium diode mounted in waveguide. Both the diode and waveguide mount were designed for minimum transition time between the operating states of the circuit involved. The detector was designed for use with a 1N23-type diode and has dual coaxial cable outputs. A traveling-wave oscilloscope was used for display. This system, with the use of a traveling-wave amplifier, was used for displaying pulse power levels of 0.1 milliwatt with easy visual observations on the oscilloscope. No limitations were seen which would prevent this system from being used with lower pulse power levels if a higher gain, low-noise traveling-wave amplifier is used.

7796 TUNNEL DIODE LOGIC CIRCUITS by W. F. Chow (GE); Electronics, Vol. 33, pp. 103-107, June 24, 1960

The operation of logic circuits using tunnel diodes in both the analog-threshold and majority logic conditions is presented. The logic circuit operates as an AND gate of n inputs if the gate threshold current level is equally contributed by n input circuits and as an OR gate if any one of the inputs furnishes the threshold current. The logic decision is based on the analog summation of input signals and the threshold level of the gate (analog-threshold logic). Majority logic circuits are formed by series connecting two diodes across a center-tapped secondary with the diodes forming one arm of a bridge. Non-unilateral behavior is overcome by using a rectifying diode to block backward transmission or by using a three-phase power supply. The tunnel diode characteristic is represented as a piecewise linear function and the equations for analog-threshold and majority logic are developed.

Parametric Switching Circuits - See 7769

Zener Diode Logic Circuits - See 7765

7797 DIODE-TRANSISTOR SWITCHING CIRCUITS by W. B. Cagle and W. H. Chen (Bell Labs.); U.S. Pat. 2,964,653, Issued Dec. 13, 1960

An improved digital information handling circuit employing diodes and transistors is described. The improvement consists essentially of the alternation of diode gates and transistor amplification stages in such a manner that gain is distributed and impedances are low, with the result that cross talk and noise pickup are reduced. In addition, the interconnection of successive stages through a single diode gate allows a driving transistor to draw reverse base current from its controlled transistor to speed up its de-energization. The circuit described may be used to construct AND, OR, negation, and other logic circuits.

7798 TRANSISTOR-DIODE LOGIC by R. A. Carlsen (Michigan U.); U.S. Gov. Res. Rep., Vol. 34, p. 154 (A), Aug. 19, 1960 PB 146 942

The design features of direct-coupled transistor-diode logic are discussed. The effect of diode reverse transients on circuit performance, the dependence of the number of gate drives on transistor and diode properties, and isolation obtained between input and output gate terminals for the circuit presented are considered. The unique feature of the circuit is the use of the low collector-to-emitter transistor as a replacement for a diode clamp.

7799 DIODELESS CORE LOGIC CIRCUITS by S. B. Yochelson (Goodyear Aircraft); 1960 IRE WESCON Conv. Rec., Part 4, pp. 82-95

A logic mechanization system suitable for digital computers and data processors is described. This system is based on the use of conventional square-loop ferrite magnetic cores for all operations. It differs from common core-diode or core-transistor logic systems in that no semiconductors or other active coupling

elements are needed and differs from other diodeless core logic systems in that there are no inherent limits on speed, logic capabilities, or branching (fan out) capabilities other than the characteristics of the cores themselves. The system uses the threshold characteristics of the magnetic cores as the nonlinearity needed to achieve directivity of information flow. In addition to the cores needed as information storage elements, added cores are used in place of the diodes or similar nonlinear devices found in conventional core logic systems. Control of directivity is achieved by biasing certain cores up to their thresholds, resulting in the inhibiting of some cores from switching and the aiding of the switching of others. Arrangements are made so that the voltages induced into each coupling loop by a switching core are always opposed by another switching core. Hence, there is no need to reset some cores slowly.

Magnetic Core Flip-Flop - See 7771

7800 PARAMETRON COMPUTER CIRCUITS by K. Nagamori (Nippon Elect.); Electronics, Vol. 33, pp. 73-78, June 3, 1960

The use of ferrite cores to perform logic functions by utilizing parametric oscillation is described. The secondary windings on two cores are resonated to one-half the primary excitation frequency. Parametric oscillation results from the change in inductance resulting from the changing permeability of the cores. Oscillation stabilizes either in phase (0 condition) or 180° out of phase (π condition) with the excitation current, depending upon the phase of oscillation present prior to excitation, and remains unchanged unless excitation ceases. The parametron can be used as a two-valued logic element with 0 and π conditions corresponding to ZERO and ONE. Control of oscillation phase is performed by information given prior to excitation. Parametrons can be combined to perform usual logic functions.

7801 A BINARY COUNTER USING TRANSISTORS WITH A RESOLUTION TIME SMALLER THAN A MICROSECOND [in Italian] by D. Brini and L. Tabellini; Alta Frequenza, Vol. 29, pp. 393-400, July-Aug. 1960

A binary counter using ordinary production transistors, built according to criteria of extreme simplicity, is described. A resolution of 0.2 μs has been obtained although in this case the system is rather critical in regard to components. A resolution of about 0.7 μs can be obtained with absolute operating stability and with an extreme independence from output variations.

100 Mc Transistor Counter - See 7839

Binistor Ring Counters - See 7709

7802 25-MC CLOCK-RATE COMPUTER CIRCUITS FOR OPERATION FROM -20°C TO + 100°C by C. R. Cook, Jr. (Texas Instr.); 1960 IRE WESCON Conv. Rec., Part 4, pp. 105-115

Pulse generators, full adders, and shift registers designed and built for operation at clock-rates up to 25 Mc and over a temperature range from -20°C to + 100°C are described. Current-mode, inhibit and complementary circuit techniques have been used to obtain maximum speed with two types of presently available silicon transistors. The complete system is reasonably simple. Conventional high-frequency circuit packaging techniques were used. The full adder circuit results in sums and carry serial information propagating speeds at 100°C that previously were only possible using parallel organization. It will give a SUM or CARRY with less than 20-mμsec delay (average delay is less than 10 mμsec) when used in a serial application. With parallel organization, the carry propagation time is less than 15 mμsec per stage, at 100°C. The full adder consists of ten transistors, one diode, 11 resistors and 3 inductors.

7803 TRANSISTOR-CAPACITOR SHIFT REGISTER by R. W. Hofheimer (Lincoln Lab.); Semicon. Prod., Vol. 3, pp. 31-32 July 1960

A shift register in which capacitors are used as the information storage elements is described. The chief advantages are circuit simplicity and high bit rate capability.

7804 PULSED RF STORAGE IN LONG DELAY, BROADBAND CLOSED LOOP SYSTEMS by O. A. Huettner (ITT Labs.); 1960 IRE WESCON Conv. Rec., Part 2, pp. 13-23

The design and adjustment of broadband, closed loop, pulsed R storage systems employing fused silica delay lines are discussed. The operating bandwidth of this storage device is in the order c 40 megacycles; the storage time is in the order of several milliseconds. A quantitative analysis of the storage time, in term of delay attenuation, media delay, regeneration-enhanced loo noise, and broadband amplifier noise figure and saturation characteristics is developed. Specific design requirements of the broadband amplifiers, equalization networks and automatic gain control circuitry are also discussed. Some peculiarities associated with operation of broadband fused silica delay lines in this application are detailed, and practical design solutions to these peculiarities are indicated.

7805 A TUNNEL DIODE TENTH MICROSECOND MEMORY b M. M. Kaufman (RCA); 1960 IRE Int. Conv. Rec., Part 2, pp. 114-123

An experimental 64-bit computer memory which utilizes a basi cell consisting of a resistor loaded tunnel diode with transforme coupled output is described. The basic cell operates at baseband and has destructive readout. The output transformer, a printed circuit with ferrite core, gives a large enough output signal to permit a tenth microsecond read-plus-write time. Considerations and techniques for tight packaging are discussed and an overall volume of 0.2 x 0.2 x 0.3 inches for the memory cell is seen as feasible for a 32 x 32 element memory which is to be constructed.

7806 THREE-HOLE CORES FOR COINCIDENT-FLUX MEMOR by H. F. Priebe, Jr. (Bell Labs.); Electronics, Vol. 33, pp. 94 97, July 29, 1960

A high-speed 1,120 bit coincident-flux memory, using three-hole cores, with a memory-scan time of 125 μsec is described. The memory has 40 rows of 28 bits each with destructive read-out used. The output signals from each row are strobed by a clock pulse in the readout detectors. Updating takes place in the readout register. Read and write pulse durations are 1 μsec with 1 μsec available between the two pulses for updating. The read pulse leaves all cells in a horizontal row in the ZERO flux state. A horizontal write pulse writes a ZERO in the core and a combined vertical and horizontal pulse writes a ONE. Horizontal access is accomplished with a matrix and two translators. Core output voltage and switching time vary with temperature and pulse current variations. The worst combination results in a SNR of 2.77:1. Operation is reliable from 30-140°F with ±20% supply voltage variation permissible.

7807 PULSE SENSING SYSTEM by C. W. Williams (IBM); U. S. Pat. 2,966,595, Issued Dec. 27, 1960

A circuit which senses the occurrence of electrical pulses of the type that are derived from magnetic core storage devices is described. Operation of the circuit depends upon the unique step-like magnetization characteristic of certain core materials, such as perminvar, to effect a kind of gating action. Two stages of transistor amplification are utilized in conjunction with the perminvar cores, the driving transistors being arranged in a common base push-pull fashion in order to negate the effects of common mode voltages arising from spurious noise. The senses of the core windings can be arranged to accommodate pulses of optional polarity.

7808 ELECTRICAL READOUT FROM THIN FERROMAGNETIC FILMS by S. Feinstein and H. J. Weber (Servomechanisms); Electronics, Vol. 33, pp. 100-102, July 29, 1960

Astatic interrogation and readout of thin ferromagnetic film with an improved signal-noise ratio is discussed. The film is a nickel-iron compound vaporized in a vacuum and deposited through a mask on a heated glass substrate in the presence of a local magnetic field. The film is 1000-2000 A thick and has a square hysteresis loop along the easy axis of magnetization. Astatic balance is achieved by placing a square hysteresis loop material between the drive line and one side of the pickup loop and pulsing the drive line with single polarity pulses, saturating the material with a resultant constant permeability. Reversing the driving pulse polarity switches the material from one remanence to the other with a large change in permeability. This alters the flux distribution and upsets the pickup loop balance resulting in an output pulse. The pickup loop is terminated to minimize ringing.

7809 A NEW CORE SWITCH FOR MAGNETIC MATRIX STORES AND OTHER PURPOSES by I. P. V. Carter (IBM); IRE Trans. Vol. EC-9, pp. 176-191, June 1960

The conventional uses of magnetic switch cores to drive matrix stores in both current-driven and voltage driven modes are analyzed. A new method of using switch cores is proposed and analyzed which offers, at the cost of replacing in every selection line the usual switch-core and terminating resistor by two smaller cores, intrinsic pulse shaping and amplitude regulation, and much reduced power dissipation, particularly in the driving stages. Constructional details of an application of the new method to drive a store 100x80x10 are given, and waveforms for this store are shown. All address decoding and driving are performed by 34 transistors. A model of a multiple coincidence store 101x101 with a cycle time of 1 μsec has also been constructed and details are given.

Optimal Load-Sharing Matrix Switches - See 7767

Storage Light Intensifier Display Panel- See 7718

7810 DISPLAY DEVICE SEGMENTS AND CIRCUITS THEREFOR by L. D. Barter and P. R. Gilson (Beckman Instr.); U.S. Pat. 2,963,692, Issued Dec. 6, 1960

A display device circuit which detects an inoperative condition in a display lamp and thus prevents the transmittal of incorrect information to an observer is described. An indication of inoperative condition of the lamp is provided whether or not the lamp is energized through the connection of a diode, a source of forward bias, and an ammeter or some other type of current detector in parallel with the lamp in such a fashion that when the lamp is inoperative or non-conductive, current flows in the diode and current detector circuit. The presence or absence of current flow in the current detector is used as an indication of the operativeness of the lamp.

POWER

7811 A NOTE ON TRANSISTORIZED RIPPLE FILTERS by B. W. Moore and J. P. O'Neil; AWA Tech. Rev., Vol. 11, No. 3, pp. 169-177, 1960

Some basic problems in the design of transistor smoothing circuits for dc power supplies are discussed and a circuit which provides for optimum efficiency over a wide range of load currents without the necessity for critical adjustment is described.

7812 A TRANSISTOR SWITCHING CIRCUIT FOR POWER REGULATION APPLICATIONS by M. J. Wright (J. Lucas Group Res. Ctr.); Electronic Engrg., Vol. 32, pp. 484-487, Aug. 1960

A dc transistor amplifier circuit for power control applications is described. Positive feedback is used to make the amplifier oscillate continuously, the output stage being switched between bottomed and cut-off conditions. The input signal modulates the mark-to-space ratio and so varies the mean current fed to an inductive amplifier load. The primary application considered for the circuit is voltage control of shunt fed dynamos or alternators, but its use in mains or battery-driven regulated power supplies is briefly mentioned. The principal advantages of a switching amplifier are (1) high efficiency and (2) low power dissipation in the series control transistor.

7813 CURRENT TRANSISTOR STABILIZERS FOR ELECTROMAGNETS OF MEDIUM POWER (1 TO 10 KW) [in French] by M. Sauzade (Lab. d'Electronique de la Faculté des Sciences); J. Phys. Radium, Vol. 21, Suppl. to No. 11, pp. 161A-170A, Nov. 1960

After an outline of the general principle of high power stabilized supply for electromagnets, different expressions for computing the essential characteristics are given. An approximate computation of the feedback loop gain allows one to find the condition of stability. Various methods are used to measure the degree of magnetic field stability.

7814 TRANSISTORIZED POWER SUPPLIES FOR A MASS SPECTROMETER by R. D. Russell and F. Kollar (U. Brit. Columbia); Can. J. Phys., Vol. 38, pp. 616-623, May 1960

A transistorized magnet current power supply and a filament emission control designed for use in a mass spectrometer are described. The mass spectrometer is a 12-in radius 90° instrument used at mass 250 with a 5000-volt accelerating voltage. The magnet, which supplies a field of more than 5000 gauss over an area of 800 cm^2 and across a gap of 1.9 cm, and which weighs three quarters of a ton, is supplied from a regulated supply dissipating about 50 watts. The filament emission control takes about 30 watts from the mains.

7815 TRANSISTORIZED FREQUENCY STABILIZATION FOR REFLEX KLYSTRONS USED IN MAGNETIC RESONANCE by P. Jung (European Res. Assoc.); J. Sci. Inst., Vol. 37,

pp. 372-374, Oct. 1960

A fully transistorized frequency stabilizer for reflex klystrons which is suitable for magnetic-resonance experiments and other microwave applications that require frequency stability is described. In a typical case (klystron, type 2K25, cavity Q = 3000) the effect of ripple and drift of the power supply is reduced by a factor of 1000.

7816 PASSIVE BRIDGE TYPE VOLTAGE OR CURRENT STABILIZERS [in French] by A. Caravel (Lab. d'Electrotechnique de la Faculté des Sciences de Grenoble); J. Phys. Radium, Vol. 21, Suppl. to No. 11, pp. 187A-190A, Nov. 1960

The use of a stabilizing Zener diode leaves a slight variation of the output voltage when the input voltage varies. To suppress this residual effect the diode is introduced into a Wheatstone bridge as one of the arms and the bridge is dynamically balanced. A careful choice of the elements gives a small output resistance. The anode current of a pentode can be regulated by the same means.

7817 AN INVESTIGATION OF LONG-TERM STABILITY OF ZENER VOLTAGE REFERENCES by R. P. Baker (Sandia) and J. Nagy, Jr. (Daystrom); IRE Trans., Vol. I-9, pp. 226-231, Sept. 1960

A wide range of environmental conditions could preclude the use of conventional standard cells as references for precise electrical measurements. As a solution to this problem silicon junction ("Zener") diodes have been investigated for use as a voltage reference in a militarized test set capable of operating many months in adverse environments without restandardization. It was found that diodes which have sufficient stability to replace unsaturated standard cells can be selected with respect to temperature coefficient, noise, and long-term stability. The average standard deviation observed for 11 selected diodes tested for four months is 3.1 PPM.

7818 DC TO AC CONVERTER by V. E. Carstedt and R. H. Wood; U.S. Pat. 2,964,717, Issued Dec. 13, 1960

A novel transistor oscillator circuit which provides a stable output frequency and excellent rectangular wave shape characteristics despite wide variations in the input DC voltage and the output load impedance is described. The bases of two transistors are coupled through resistors to a transformer winding on either side of the emitters. The ends of the transformer winding are connected to the primary of a linear feedback transformer. The ends of the secondary of this feedback transformer are connected to the two bases of the two transistors. Upon application of DC voltage to the input, the two transistors alternately become conductive and non-conductive, enabling an output voltage to be obtained from the transformer winding which is stable at a frequency determined by the inductance and resistance of the feedback transformer secondary.

7819 STATIC INVERTER DELIVERS REGULATED 3-PHASE POWER by M. Lilienstein (Amer. Electronics); Electronics, Vol. 33, pp. 55-59, July 8, 1960

Use of silicon-controlled rectifiers in conjunction with magnetic amplifiers to provide regulated three-phase power with less than 2 per cent harmonic content and 70-75 per cent efficiency is described. A Hartley oscillator feeds a six-element ring counter to provide timed switching pulses for three silicon-controlled rectifier switches. Each switch feeds a single-phase power transformer which provides a square wave output to a magnetic amplifier. The magnetic amplifier delays the leading edge and filters attenuate the harmonics. The power transformer has a tertiary winding with two rectifiers across it which returns reactive power to the battery for a lead or lag PF load. A spill-over transformer across the magnetic amplifier reduces losses from high voltage spikes. A three-legged output autotransformer provides exactly 120° phase shift. The output varies from 114-115½ volts up to 1½ times overload.

7820 CIRCUIT ARRANGEMENTS FOR OPERATING LOW PRESSURE ELECTRIC DISCHARGE LAMPS by I. F. Davies and J. C. Vickery (GE Ltd.); U.S. Pat. 2,964,676, Issued Dec. 13, 1960

A circuit designed to operate low pressure electric discharge lamps, comprising an oscillator circuit which is arranged to be energized by a direct current source and which supplies oscillatory power to the lamp, is described. The active element of the oscillator is a matched pair of p-n-p germanium junction transistors connected in push-pull. Regenerative feedback is provided by a transformer with a secondary feedback winding.

7821 POWER SUPPLY CIRCUIT by G. H. Fathauer (Thompson Ramo Woolridge); U.S. Pat. 2,963,619, Issued Dec. 6, 1960

A power supply constructed from a minimum number of components and providing an adjustable regulated output is described. The circuit provides a high voltage output from a low voltage DC source through rectification of the voltage across a LC parallel circuit which is intermittently connected to the DC source. Voltage regulation is effected through utilization of the variable impedance characteristic found in a Zener diode during reverse current flow. The circuit is particularly useful for developing the high voltage required for operation of a television camera tube. In this instance, the circuit is powered by the energy released from the horizontal deflection coils during retrace.

7822 FUZING APPLICATION OF THE FOUR-LAYER DIODE by D. J. Russell (Naval Ord. Test Sta.); U.S. Gov. Res. Rep., Vol. 33, p. 506(A), May 13, 1960 PB 144 986

Application of the four-layer diode to fuzing systems is discussed. The device can perform both the operations of timing and energy switching. Energies of up to one million ergs can be switched using units with higher breakover voltages. A limited testing program has indicated that the usefulness of the four-layer diode as a timer would probably be restricted by its temperature sensitivity. Testing programs also indicate that the diode can withstand at least 10 g vibration near its resonant frequency and a steady acceleration of at least 9,000 g.

CONTROL

7823 DESIGN OF STATIC RELAYS FOR SIGNALING AND CONTROL by R. Langfelder (Walter Kidde); Electronics, Vol. 33, pp. 64-68, July 22, 1960

The design of static relays using semiconductor elements is described. The characteristics of photoconductors, diodes, transistors and silicon-controlled rectifiers are compared and circuit designs utilizing each are presented. Snap action can

be provided by using regenerative elements or by using nonregenerative elements connected in regenerative circuits. Design of signal relay circuits is discussed. Relay operation with signals as low as 50 mv has been achieved and signal attenuation at the load of several hundred to one has been obtained. At present, static relays are in general larger than equivalent mechanical relays.

INSTRUMENTATION

7824 MEASUREMENT OF THE INTENSITY IN ELECTRON DIFFRACTION BY A CdS SINGLE CRYSTAL by S. Takagi and F. Fujimoto (U. Tokyo); J. Phys. Soc. Japan, Vol. 15, pp. 1607-1614, Sept. 1960

A method of measuring the intensity of electrons in electron diffraction patterns by the electron-bombardment-induced-current (EBIC) in a CdS single crystal is described. The CdS detector is moved in the diffraction camera by a screw which is driven by a synchronous motor. EBIC is measured directly by an automatic recording millivoltmeter. EBIC properties of good crystals selected from those prepared by Frerichs' method are given. It is shown that the intensity can be measured within 2-3 per cent error, if suitable precautions are made. An example of the measurement on TlCl is also given.

7825 A SAMPLING PULSE OSCILLOSCOPE UNIT TRANSISTORIZED, 'SPOUT' by P. Emile, Jr. and G.R. Yetter (Diamond Ord. Fuze Labs.); U.S. Gov. Res. Rep., Vol. 33, p. 499 (A), May 13, 1960 PB 144 706

A Sampling Pulse Oscilloscope Unit Transistorized, "SPOUT", capable of resolving repetitive pulses with risetimes in the order of 1 mμs is described. SPOUT was designed as a plug-in-unit for a standard oscilloscope. A narrow pulse (approximately 1 mμs wide) is generated by an avalanche transistor switch and used to sample repetitive, unamplified input pulses. From the samples, a composite picture of the input pulse is formed on a cathode-ray tube (CRT). The main advantage of SPOUT and sampling oscilloscopes in general is the possibility of viewing narrow (mμs) pulses with a low frequency CRT by trading sampling time for bandwidth. The disadvantages of the sampling method are that the pulse must be repetitive, the maximum and minimum input pulse rates are limited, and only a small dynamic range of input pulses can be observed.

7826 CONSTRUCTION OF A MAGNETIC FIELD METER FOR THE HARMONICS METHOD [in German] by K. Brankoff (Karl Marx U.); Nachrichtentech., Vol. 10, pp. 247-256, June 1960

An instrument for measuring small magnetic field strengths (approximately 10^{-5} to 10^{-1} oe) is described. The nonlinearity of the magnetization curve of a ferromagnetic material is utilized. The field being tested generates, in a transformer, the odd multiples of the basic frequency. The field being tested is automatically compensated by a counter field and the odd multiples of the basic frequency disappear. The field of compensation is indicated by an instrument.

7827 TRANSISTORIZED AUTODYNE DETECTOR FOR ESR AND NSR by F. Bruin and P. C. Van Soest (American U.); Rev. Sci. Instr., Vol. 31, p. 909, Aug. 1960

A transistorized autodyne detector of magnetic resonance absorption is described. The circuit is the transistor equivalent of the vacuum tube oscillator developed by Hopkins. An oscilloscope trace of electron paramagnetic resonance in DPPH at 30 Mc obtained with the detector is presented. The trace is inferior but comparable to that obtained with a vacuum tube detector. Improvements in high frequency and noise characteristics of transistors will make the detector very useful for scanning magnetic fields.

7828 A SUBTLE ERROR IN RF POWER MEASUREMENTS by S. J. Raff and G. U. Sorger (Weinschel Engrg); IRE Trans., Vol. I-9, pp. 284-291, Sept. 1960

In the measurement of RF power by dc or AF substitution, using balanced-bridge methods, there is generally a systematic error because of the very small variation of the bolometer resistance over the AF cycle. For a barretter in a typical bridge circuit using a 10-kc audio frequency, this error is shown to be of the order of 5 per cent. For thermistors, the error is generally smaller, but because of the complex thermal behavior of the thermistor, the error is not accurately calculable. The nature and origin of this error is discussed and data are presented from which its magnitude and direction can be calculated as a function of the bridge circuit parameter, the AF and the bolometer time constant, whenever the latter is unique.

Thermistor Bolometer - See 7721

7829 DUAL PHOSPHOR DETECTORS by R. Monaghan and B. F. Wilson (Well Surveys); IRE Trans., Vol. NS-7, pp. 32-35, Dec. 1960.

Radiation detectors in which two scintillation phosphors with different decay times are mounted on a single photomultiplier tube are described. The separation of the scintillations from each phosphor in a pulse length discrimination circuit permits the use of pairs of phosphors which are individually most efficient for the detection of particular types of radiation. The dual phosphor detector is compact and is suitable for use in survey meters and well logging instruments to record different types of radiation simultaneously. A transistor pulse separator for use with the detectors is also described.

Piezoelectric Force Gage - See 7729

7830 PORTABLE WATER VELOCITY METER by J. M. Edington and L. Molyneux (U. Durham); J. Sci. Instr., Vol. 37, pp. 455-457, Dec. 1960

Wilkie has described an instrument for measuring the velocity of water, in which the rate of rotation of a small polystyrene rotor is measured by electronic means, using valves as the active circuit elements. The present paper describes a circuit in which the valves are replaced by transistors and which is designed so that compensation for changes in the conductivity of the water occurs automatically. As the instrument is small and light and powered by a self-contained battery, it is particularly suitable for field work.

Measurement of Vibration - See 7749

7831 DETECTION OF MINIMUM IONIZING PARTICLES IN

SILICON P-N JUNCTIONS by H. M. Mann and W. W. Managan (Argonne Natl. Lab.); Rev. Sci. Instr., Vol. 31, pp. 908-909, Aug. 1960

The resolution of internal conversion electrons at eight energies from 62.5 kev to 1.046 Mev in diffused silicon p-n junction detectors by the use of an optimum reverse bias for each energy is discussed. For example, 1.046 Mev electrons can be resolved with a minimum bias of 200 volts. A larger bias increases the line width. The observed line widths suggest that the detectors can be used for minimum ionizing particles.

7832 TRANSISTORIZED TACHOMETER by W. H. Follett (U. Michigan); Electronic Equipm. Engrg., Vol. 8, pp. 62-63, Aug. 1960

A tachometer which can be quickly connected and disconnected from an engine and which permits direct reading of engine rpm from a meter is described. A probe made from RG 58 A/U coaxial cable, with one inch of shielding removed to permit coupling, is hooked over an ignition wire. A pulse is capacitatively coupled to a mono-stable multivibrator to provide an output pulse whose frequency is equal to the engine sparking frequency. A buffer between the multivibrator and a milliammeter prevents meter current flow between pulses. The average value of the current is proportional to engine rpm. A calibration signal is provided by clipping and differentiating the line voltage and applying it to the multivibrator. A regulated supply voltage limits output pulse amplitude variations.

NEW PRODUCTS

7833 STRONTIUM TITANATE SINGLE CRYSTALS (National Lead Co., 111 Broadway, New York 6, N.Y.)

Strontium titanate single crystals are announced. The material has a high index of refraction through the visible and the infrared regions of the spectrum, a high dielectric constant, and a high resistivity. The crystal can be used in lenses, prisms, and windows for infrared optics and has potential applications in the field of microwaves and as a dielectric. Either pure or doped boules ranging in size from 100 to 500 carats are available.

7834 RESISTIVITY TEST SET (Semimetals, Inc., 133-20 91st Ave., Richmond Hill 18, N.Y.)

A test set in which semiautomatic resistivity measurements can be performed on semiconductor slices is announced. The measurements can be carried out with an accuracy within 2 per cent. The apparatus employs a 4-point probe head in which each probe needle is guided by two ruby jewels. The needle points are spaced either for silicon or germanium depending on application and the variation in point spacing is limited to ±0.01 mm.

7835 SILICON VARACTOR DIODES (Sylvania Electric Products Inc., 100 Sylvan Rd., Woburn, Mass.)

Silicon epitaxial varactor diodes which exhibit cut-off frequencies as high as 150 kMc at 75 v breakdown voltage and cut-off frequencies as high as 100 kMc and capacitance values as low as 0.15 pF at 6 v are announced. The devices can be used in harmonic generators because of their exceptional power handling capabilities. In addition they can be used as modulators and high Q voltage variable capacitors at lower frequencies.

7836 GALLIUM ARSENIDE VARIABLE REACTANCE DIODES (Tyco Semiconductor Corp., Bear Hill, Waltham 54, Mass.)

A series of low capacitance gallium arsenide point contact variable reactance diodes for low-noise parametric amplifier use and other microwave applications such as harmonic generators and switches is announced. The diodes are packaged in a reversible double ended ceramic/metal microwave cartridge which can be converted to the single ended configuration by means of an adapter base. They can operate at liquid nitrogen temperature and have a maximum power dissipation of 150 mw at 10 kMc and 25° C ambient temperature.

7837 TRINISTOR CONTROLLED RECTIFIER (Westinghouse Electric Corp., Semiconductor Dept., Youngwood, Pa.)

The trinistor controlled rectifier, a three terminal silicon device which can be used to control large amounts of power, is announced. The characteristics of the device are similar to those of a thyratron, in that the device blocks voltage in the forward direction below a critical breakover voltage. If the critical voltage is exceeded or a proper gate signal is applied the device switches rapidly to the conducting state. The device is available with peak reverse voltage to 480 v, breakover voltage to 400 v, 50 a forward current, and 600 nsec switching.

7838 UNI-TUNNEL DIODES (Hoffman Electronics Corp., 1001 Arden Drive, El Monte, Calif.)

A series of silicon uni-tunnel or "backward" diodes is announced. The devices exhibit a high conductance at very low voltages as a result of tunneling in the forward direction and a conventional tunnel diode current characteristic on the order of microamps in the reverse direction. The minimum forward current at 0.25 v ranges from 0.5 ma to 10.0 ma and the maximum forward current is 5 times this minimum value. The devices can be operated and stored over the temperature range -85°C to +200°C.

7839 MADT SWITCHING TRANSISTOR (Philco Corp., Lansdale Div., Lansdale, Pa.)

The 2N769 micro alloy diffused base transistor which can switch at rates up to 300 Mc is announced. The device features an 800 Mc gain bandwidth product, low hole storage factor, and low emitter and collector diode capacities. It is designed for use in saturated switching circuits and is manufactured by a fully automated and mechanized transistor production facility. The device has been utilized in a 100 Mc counter.

7840 PHOTRAN PNPN SILICON PHOTOSWITCH (Solid State Products, Inc., 1 Pingree St., Salem, Mass.)

Photran, a light-activated p-n-p-n silicon switch is announced. The device has an impedance of over 10 megohms in the "off" state and an impedance of under 10 ohms in the "on" state. Its output is determined primarily by the load and is independent of light input at all intensities above the triggering level. The miniature detector can deliver up to 300 ma load current at up to 200 v with an efficiency exceeding 98 per cent. This high output allows the direct actuation of a load without intermediate relays, amplifiers, magnetic amplifiers, or similar elements. The device has applications in counting, sorting, power control, limit switching, programming, and optical logic control.

NEW PRODUCTS (Cont'd)

7841 FERRITE MODULATOR (FXR, Inc., 25-26 50 Street, Woodside 77, New York)

The model X158A absorption type ferrite modulator which operates over the frequency range 8.2-12.4kMc is announced. The modulator is ideal for use in precision microwave measurements since it produces true amplitude modulation with negligible frequency modulation. It can also be used in communication systems, as a square-wave chopper, a microwave switch, and as a variable attenuator. A minimum of 25 db of dynamic attenuation is provided for coil currents of 100ma. Over most of the frequency range attenuations as high as 60 db are achieved with the same field. Many commercial audio oscillators can be used to drive the solenoid for a modulated response in the neighborhood of 1 kc.

7842 TUNNELTRON (Arthur D. Little, Inc., Acorn Park, Cambridge 40, Mass.)

The "tunneltron", a negative resistance circuit element formed by placing an insulating film less than one-millionth of an inch thick between strips of two superconducting metals, is announced. The device has been made with a film of aluminum, an insulating film of aluminum oxide, and a film of lead. It has also been fabricated with a film of lead, a film of insulating material such as barium stearate, and a film of either tin or indium. The tunneltron has potential applications in ultra-sensitive amplifiers and computers.

7843 TRANSISTOR FREQUENCY RESPONSE METER (Molecular Electronics, Inc., 85 Weyman Ave., New Rochelle, N.Y.)

A battery powered, transistorized instrument for measuring the frequency response of p-n-p or n-p-n silicon or germanium transistors in the frequency range 50 - 750Mc is announced. The emitter current of the transistor under test can be varied from 0 to 10ma in 1 ma steps and the collector voltage of the transistor under test can be varied from 0 to 15v in 1.5v steps. Provision is also made for the external biasing of the test transistor beyond these limits. Measurements can be made with an accuracy of ±5 per cent. The instrument can be used in both laboratory and production testing.

7844 MICROCIRCUIT ASSEMBLER (Kulicke and Soffa Mfg. Co., Inc., Philadelphia, Pa.)

Two instruments for positioning and bonding ultra-fine wire and microcomponents during the fabrication of microcircuits are announced. One instrument can be used with substrates up to one inch square and the other can be used with substrates up to 1.25 inches square. The latter instrument can be supplied with eight tools needed during the assembly process. The instruments provide high precision in positioning, ease and speed of operation, and positive control of such factors as heat and pressure.

7845 2000 MC PARAMETRIC AMPLIFIER (Micromega Corp., 4134 Del Rey Ave., Venice, Calif.)

A 2000 Mc parametric amplifier which has a bandwidth of 15 Mc, a gain of 17 db, a noise figure of 3 db, and a tuning range of 100 Mc is announced.

CONFERENCE PROGRAMS ABSTRACTED

in SOLID STATE ABSTRACTS, Vol. 1, No. 6

Sixth Conference on Magnetism and Magnetic Materials, Nov. 14-17, 1960, New York, N.Y. (Sixth Conf. Magnetism and Magnetic Materials)

1960 Thanksgiving Meeting of the American Physical Society, Chicago, Ill., Nov. 25-26, 1960 (Bull. Am. Phys. Soc., Ser. II, Vol. 5, Nov. 25, 1960)

1960 IRE WESCON Convention, Los Angeles, Calif., Aug. 23-26, 1960 (1960 IRE WESCON Conv. Rec.)

International Atomic Energy Agency Conference on the Use of Radioisotopes in the Physical Sciences and Industry, Copenhagen, Sept. 6-17, 1960 (J. Appl. Rad. Isotopes, Vol. 9, Dec. 1960)

International Union of Crystallography; 5th General Assembly, International Congress and Symposia, Cambridge, England, Aug. 15-24, 1960 (Acta Cryst., Vol. 13, Dec. 1960)

1960 Fall Meeting of the Electrochemical Society, Houston, Tex., Oct. 9-13, 1960 (J. Electrochem. Soc., Vol. 107, Dec. 1960)

SUBJECT INDEX

A

Absorption Bands in Indium Antimonide, Lattice 7673
Acceptor Levels in Germanium, Copper 7587
Adders, Transistor 7802
Adsorption of Krypton on Irradiated Alumina 7582
Alkali Halide:
  Crystals, Formation of Cuprous Halide Films on 7580
  Solid Solutions 7554
Alloying of Semiconductor Devices, Jig for 7711
Alumina, Adsorption of Krypton on Irradiated 7582
Alumina:
  Ceramics,
    Lattice Defects in 7553
    Thermoluminescence in 7553
Aluminum Phosphide,
  Electroluminescence of 7589
  Photovoltaic Effect and Photoconductivity of 7589
  Preparation of 7589
Ammonium:
  Cupric Tutton Salt, Spin-Spin Relaxation in 7659, 7660
  Halides, Proton Motions in 7585
Amplifiers,
  Parametric 7845
  Parametric:
    Gain and Bandwidth Inconsistencies in Low Frequency 7754
    Large-Signal Behavior of Degenerate 7751
    Radio Frequency 7777
    Traveling-Wave 7752, 7753
    Varactor Diodes for Strip Line 7698
  Solid State: Video Processor with Pulse-for-Pulse AGC 7743
  Transistor:
    Audio- and Carrier-Frequency Telephone 7756
    Bipolar 7748
    Common Collector-Common Emitter Pair Broadband 7742
    Cross Modulation in 7741
    Data 7744
    Distortion in 7741
    Integrating and Differentiating 7749
    Linear 7744
    Negative Output Impedance 7755
    Optimum Two-Terminal Interstage Design for High-Frequency 7740
    Power 7750, 7755
    Pulse:
      -Forming 7745
      Regenerator 7746, 7747
    Push-Pull 7750
  Tunnel Diode: Cascaded 7739
  Video: Phase Splitter 7785
Anisotropic:
  Conduction in Nonstoichiometric Rutile 7618
  Ferromagnetic Resonance Linewidth in Ferrites 7650
  Magnetization 7644
Anisotropy of:
  Surface Breakdown of Germanium in Strong Fields 7632
  the Intrinsic Domain Magnetization of a Ferromagnet 7645
Annealing:
  of Electron Radiation Damage in Graphite 7583
  on the Physical Properties of Alkali Halide Solid Solutions, Effect of 7554
Antiferromagnets, Properties of 7634
Antimony-Doped Germanium, Spin Resonance Spectrum in 7663
Arsenic in Germanium, Diffusion Coefficient of 7568
Assembler for Microcircuits 7844
Auger Electron Ejection from Germanium and Silicon by Noble Gas Ions 7631
Automobile Radio Receivers,
  Transistor 7779
  Varactor Diode 7780
Avalanching Germanium Junctions, Emission of Light from 7675, 7676, 7719

B

Backward:
  Diodes 7838
  Diodes, Tunnel Currents in 7633
Barium Strontium Titanate, Electrically Variable Delay Lines Using 7727
Barium Titanate,
  Cubic-Hexagonal Transition in 7548
  Hysteresis Loops of Polarized Polycrystalline 7601
  Polymorphism of 7548
  Transitional DC Conduction Processes in 7596
  UHF Spectra of Single Crystal 7593
Barium Titanate-Barium Stannate Solid Solutions, High Temperature Phase Transition in 7599
Barium Tungstanate, Thermal Electron Emission from 7630
Beryl, Paramagnetic Resonance and Optical Spectrum of Iron in 7667
Binding:
  of Hydrogen in Molecules and Crystals, Chemical 7585
  Properties of LiH 7681
Binistor Ring Counters 7709
Bismuth Telluride,
  Thermal Diffusivity of 7688
  Thermoelectric Properties of 7687
Bismuth Telluride-Bismuth Selenide Solid Solution Alloys, Lattice Constants of 7551
Bleaching of Color Centers in KCl 7555
Blocking Oscillators, Design of Transistor 7758
Bolometers, Thermistor 7721, 7722
Boron in:
  Silicon, Determination of 7563
  Steel, Detection of 7563
Breakdown:
  Avalanches in Ge, Optical Radiation from 7675, 7676, 7719
  in Dielectrics, Theory of 7594
Brittleness of Sodium Chloride Crystals, Environmental Effects on the 7695
Burnout of Crystal Diodes 7699

C

Cadmium:
  in Germanium,
    Diffusion of 7569
    Solubility of 7569
Cadmium Sulfide, Observation of Exciton Motion in 7604
Cadmium Sulfide:
  Photoconductor Storage Light Intensifier Display Panel 7718
  Single Crystals, Measurement of Intensity in Electron Diffraction by 7824
Cadmium Telluride Junctions, Quantum Efficiency of 7717
Calcium Fluoride, Maser Action from U^{3+} Ions in 7669
Calcium-Iron-Oxygen Compounds, Ferrimagnetic 7651
Calcium Tungstate, Spin Echo Experiments in Cerium and Erbium Doped 7668
Cameras, Power Supply for Television 7821
Carrier:
  -Carrier Scattering on Mobility in Semiconductors, Theory of the Effects of 7612
  Lifetime in Transistors, Control of 7707
  Mobilities in Ge-Si Alloys 7619
Carriers:
  in Germanium, Drift Mobility of 7609
  - See also Electrons, Holes
Cascading Tunnel Diode Amplifiers 7739
Ceramics, Thermoluminescence in Alumina 7553
Cerium Doped Calcium Tungstate, Spin Echo Experiments in 7668
Character Recognition, Magnetic Pulse Sequence Detector for 7775
Chromium^{3+} in Ruby, Relaxation Times of 7655
Circulators with Masers, Use of 7724
Cleavage Planes of the III-V Compounds and Ge 7559
Cobalt, Polarization of Conduction Electrons in 7643
Cobalt^{2+}, Spin Hamiltonian of 7654
Cobalt Chloride, Magnetic Phase Transitions of 7653
Color Center Concentration by Microwave Faraday Rotation, Measurement of 7666
Color Centers, Bleaching of 7555
Communication Receivers, Parametric Radio Frequency Amplifier for 7777
Computer:
  Circuits,
    Instrumentation for the Application of Microwave Energy to 7795
    Parametron 7800
  Circuits - See also Counters, Logic Circuits, Storage
  to Optimize Transistor Logic Circuits, Use of a 7794
Conduction:
  in:
    N-Type Germanium, Effect of Shear on Impurity 7614
    Nonstoichiometric Rutile, Anisotropic 7618
    Organic Solids 7621
  Processes in Ceramic Barium Titanate, Transitional DC 7596
Conductivity, Monte-Carlo Calculation for a Size Effect in Electrical 7611
Conductivity:
  of Ge-Si Alloys 7619
  of Low-Impedance Materials, Measurement of the Complex 7592
  on the Electric Strength of KCl and NaCl, Effect of Ionic 7594
Controlled:
  Rectifier Frequency Multiplier 7773
  Rectifiers, Trinistor 7837
Converters, Power: DC to AC 7819
Converters Under Constant Heat Flux, Performance of Thermoelectric 7722
Cooling Semiconductor Devices, Methods of 7697
Copper, Effect of Oxygen on the Magnetoresistance of 7628
Copper Halides, Optical Properties of 7671
Copper in Germanium, Acceptor Levels of 7587
Counters,
  Binistor Ring 7709
  100 Mc Transistor 7839
  Transistor Binary 7801
Critical Fields of Thin Superconducting Films 7626
Cross Relaxation Effect of Chromium and Iron in Potassium Cobalticyanide 7667
Crystal, Surface States of a One-Dimensional 7587
Crystallography of FeNiN 7575
Crystals, Effect of Screw Dislocations on the Yield Strength of 7694
Cuprous Halide:
  Films, Diffusion in 7580
  Films on Alkali Halide Crystals, Formation of 7580
Cuprous Oxide, Diffusion of Zinc in 7567
Current Stabilizers for Electromagnets, Transistor 7813

D

Decoration of Dislocations Inside Large Crystals 7557
Defects:
  in LiF and KCl 7556

in ZnS 7561
Produced by γ Irradiation, Hole-Capture Cross Section of 7605
with Dislocations in Silicon, Interaction of Point 7573
Deformation:
of Germanium 7690
Potentials in Germanium 7586
Delay:
Line Storage, Fused Silica 7804
Lines, Electrically Variable 7727
Detectivity of Detectors Limited by Radiation Noise 7714
Detector for Paramagnetic Resonance, Transistor Autodyne 7827
Detectors, Information Capacity of Radiation 7715
Diamagnetism, Theory of 7670
Dielectric:
Constant of Barium Titanate at High Frequencies 7593
Properties of Lead Titanate Zirconate Ceramics 7603
Dielectrics,
Ferroelectric Ceramics as Nonlinear 7602
Theory of Breakdown in 7594
Differentiating Amplifier, Transistor 7749
Diffusion:
Coefficient of:
Arsenic in Germanium 7568
Lithium in Silicon 7571
Oxygen in Germanium 7570
Oxygen in Silicon 7570
Tin in Selenium 7547
Zinc in Gallium Arsenide 7572
Coefficients of Ionized Impurities in Semiconductors 7566
in Cuprous Halide Films 7580
of Cadmium in Germanium 7569
of Iron in Germanium 7569
of Silver in Germanium 7569
of Tantalum in Germanium 7569
of Tellurium in Germanium 7569
of Zinc in:
Cuprous Oxide 7567
Gallium Arsenide 7566
Diode:
Frequency Multiplier, Controlled Rectifier 7773
-Magnetic Amplifier Power Converters 7819
Nonreciprocal Phase Shifter 7735
Pulse Modulator 7772
Switching Circuits, Four-Layer 7823
-Transistor Switching Circuits 7797, 7798
Diodes,
Backward 7838
Crystal: Deterioration of 7699
Junction:
Assembly Process for 7705
Cartridge with Disk-Shaped Electrodes for 7752
Direct Viewing of Imperfections in 7704
Gallium Arsenide Varactor 7836
Gallium Phosphide 7703
High-Frequency Varactor 7698
High Power Silicon 7702
Noise Performance of Tunnel 7700, 7701
Silicon Varactor 7835
Spreading Resistance in 7696
Thermal Spreading Resistance in 7696
Trinistor Controlled Rectifier 7837
Tunnel Currents in Indium Antimonide 7633
Varactor Package for Microwave Frequencies 7698
Methods of Cooling 7697
Tunnel 7838
Dislocations:
in Silicon,
Helical 7558
Interaction of Point Defects with 7573
in Silver Chloride, Observation of 7557
of Like and Unlike Signs, Forces Between 7560
on Plastic Flow in Crystals, Effect of 7694
on the Yield Strength of Crystals, Effect of Screw 7694
Display:
Device Circuits 7810
Panel, Storage Light Intensifier 7718, 7719
Distortion in Transistor Stages 7741
Distribution Coefficient of Tin in Selenium 7547
Domain:
Magnetization of a Ferromagnet, Anisotropy of the Intrinsic 7645
Structure in Yttrium Iron Garnet 7646
Donor State Wave Functions, Strain-Induced Changes of 7614
Drift Mobility of Carriers in Germanium 7609
Duplexing Systems with Masers, Use of 7724

E

Effective Mass, Theory of Electron 7606
Elastic Constants of Yttrium Iron Garnet 7691
Electrical:
Conductivity, Monte-Carlo Calculation for a Size Effect in 7611
Conductivity:
in the Si-Co System 7620
of Ge-Si Alloys 7619
Electroluminescence of Aluminum Phosphide 7589
Electroluminescent Phosphors, Preparation of (Zn,Hg)S and (Zn,Cd,Hg)S 7677
Electron:
Detection in Silicon Junctions 7831
Diffraction, Measurement of Intensity in 7824
Effective Mass in Solids, Theory of 7606
Ejection from Germanium and Silicon by Noble Gas Ions, Auger 7631
Emission from Barium Tungstanate, Thermal 7630
Irradiated Lead Sulfide Films, Photoelectromotive Forces in 7678
Mobility:
and Scattering Processes in Silver Bromide 7610
in Doped Silicon 7608
Multiplication in Cadmium Telluride Photocells 7717
Paramagnetic Resonance of Color Centers in Potassium Chloride 7665
-Phonon Scattering 7611
Tunneling Between Two Superconductors 7627
Electronic Properties of Metals and Alloys, Theory of the 7591
Electrons:
in Ferromagnetic Metals, Polarization of Conduction 7643
- See also Carriers
Emission from Barium Tungstanate, Thermal Electron 7630
Energy:
Band Structure of Aluminum Phosphide 7589
Gap of Solid Solutions of In_2Te_3 with II-VI Tellurides 7546
Transport in Disordered Lattices 7590
Epitaxial Varactor Diodes, Silicon 7835
Erbium Doped Calcium Tungstate, Spin Echo Experiments in 7668
Esaki Diodes - See Tunnel Diodes
Exchange Interaction in Conductive Organic Solids 7621
Exciton Motion in Cadmium Sulfide, Observation of 7604

F

Faraday Rotation, Measurement of F-Center Concentration and Relaxation Time by Microwave 7666
F-Center:
Concentration by Microwave Faraday Rotation, Measurement of 7666
Electrons, Spin Relaxation of 7664
FeNiN, Preparation and Crystallography of 7575
FeOOH, Morphology of α and γ 7550
Fe_2O_3, Morphology of γ 7550
Fermi:
Contact Interaction of the Magnetic Field at the Nucleus in Ferromagnets 7638
Surfaces of the Hexagonal Close-Packed Metals, Effect of Spin-Orbit Splitting on the 7591
Ferrimagnetic:
Calcium-Iron-Oxygen Compounds 7651
Resonance:
Field of Terbium Doped Yttrium Iron Garnet 7647
in Three-Sublattice Systems 7648
Ferrite:
Core Parametron Computer Circuits 7800
Modulator 7841
Phase Shifter for the UHF Region 7723
Ferrites,
Anisotropic Ferromagnetic Resonance Linewidth in 7650
Magnetic After-Effect in Magnesium Manganese 7642
Ferrites at High Signal Levels, Measurement of Microwave 7641
Ferroelectric:
Ceramics, Determination of the Nonlinear Characteristics of 7602
Delay Lines, Electrically Variable 7727
$PbNb_2O_6$, Phase Transitions in 7600
Ferroelectrics, Applications of 7726
Ferromagnetic:
Films, Electrical Readout from Thin 7808
Metals, Polarization of Conduction Electrons in 7643
Resonance:
Line Shape in Insulators, Theory of 7649
Linewidth in Ferrites, Anisotropic 7650
Superconductors, Properties of Some 7625
Ferromagnets,
Anisotropy of the Intrinsic Domain Magnetization of 7645
Fermi Contact Interaction of the Magnetic Field at the Nucleus in 7638
Magnetocrystalline Anisotropy in 7644
Ferromagnets with General Spin, Properties of Heisenberg 7634
Films,
Electrical Readout from Thin Ferromagnetic 7808
Preparation and Properties of Thin Silicon 7578
Filters, Transistor Ripple 7811
Flaws in Heavily Doped Semiconductors, Solubility of 7545
Floating-Zone Refining of GaAs, Apparatus for the 7576
Four-Layer Diode Switching Circuits 7823
Fracture in Elemental and Compound Semiconductors, Brittle 7559
Frequency:
Multiplier, Controlled Rectifier 7773
Response Meter, Transistor 7843
Stabilization for Reflex Klystrons, Transistor 7815
Furnace for the Preparation of Intermetallic Semiconductor Compounds, High Pressure 7577
Fuzing Systems, Use of Four-Layer Diodes in 7822

G

Gallium Arsenide,
Apparatus for the Floating-Zone Refining of 7576
Diffusion of Zinc in 7566, 7572
Gallium Arsenide Varactor Diodes 7836
Gallium Phosphide, Preparation and Properties of 7703
Gating Elements, Zener Diodes as Voltage Breakdown 7765
Germanium,
Acceptor Levels of Copper in 7587
Cleavage Planes of 7559
Deformation of 7690

Deformation Potentials in 7586
Dependence of Lifetime on Gamma-ray Irradiation of 7605
Diffusion Coefficient of:
Arsenic in 7568
Oxygen in 7570
Diffusion of:
Cadmium in 7569
Iron in 7569
Silver in 7569
Tantalum in 7569
Tellurium in 7569
Drift Mobility of Carriers in 7609
Effect of Shear on Impurity Conduction in N-Type 7614
Impurity Conduction and Magnetoresistivity in N-Type 7613
Oxidation of 7581
Radiation from Breakdown Avalanches in 7675, 7676
Solubility of Ag, Fe, Cd, Te, and Ta Radioisotopes in 7569
Spin Resonance Spectrum in Antimony-Doped 7663
Thermal Conductivity of 7683
Germanium:
by Noble Gas Ions, Auger Electron Ejection from 7631
in Strong Fields, Anisotropy of Surface Breakdown of 7632
Junctions, Direct Viewing of Imperfections in 7704
Germanium-Silicon Alloys,
Electrical Conductivity and Hall Effect of 7619
Mobilities in 7619
Preparation of 7619
Glasses, Optical Properties of Semiconducting 7674
Graphite, Annealing of Electron Radiation Damage in 7583
Growth:
of Aluminum Phosphide Crystals 7589
of Gallium Arsenide Crystals, Apparatus for the 7576
Poisoning of Lithium Fluoride from Aqueous Solutions 7579
Guanidine Aluminum Sulfate Hexahydrate, Reversal of the Spontaneous Polarization in 7598

H

Hall:
Effect in:
Ge-Si Alloys 7619
Sodium Chloride, Ionic 7597
Mobility, Measurement of High Temperature 7597
Harmonic Generators, Silicon Varactor Diode 7835
Heat Treatment on the Electrical Properties of P-Type Silicon, Effect of 7617
Heisenberg Magnets with General Spin, Properties of 7634
Hexammine Nickel Halides, Low-Temperature Magnetic Behavior of 7652
Hole:
-Capture Cross Section of Defects Produced by γ Irradiation 7605
Mobility in:
Doped Silicon 7608
Selenium 7607
Holes - See also Carriers
Hysteresis Loops of Polarized Polycrystalline Barium Titanate 7601

I

Ignition System for Internal Combustion Engines, Transistor 7776
Imperfections in Germanium Junctions, Direct Viewing of 7704
Impurities in:
NaCl, Phonon Scattering by Chemical 7684
Semiconductors,
Diffusion Coefficients of Ionized 7566
Solubility of Charged 7545
Impurity Conduction in N-Type:
Germanium 7613
Germanium, Effect of Shear on 7614
Information Capacity of Radiation Detectors 7715
Infrared Spectra of Crystals 7672
Indium Antimonide,
Effect of Landau Levels Upon Tunnel Currents in 7633
Lattice Absorption Bands in 7673
Voight Effect in 7679
Indium Arsenide,
Thermal Conductivity of 7685
Voight Effect in 7679
Indium Telluride with II-VI Tellurides, Energy Gap of Solid Solutions of 7546
Indium Telluride-Cadmium Telluride System, Solid Solution in the 7546
Indium Telluride-Mercuric Telluride System, Solid Solution in the 7546
Indium Telluride-Zinc Telluride System, Solid Solution in the 7546
Insulators, Theory of Ferromagnetic Resonance Line Shape in 7649
Integrating Amplifier, Transistor 7749
Intermetallic Semiconductor Compounds, Use of a High Pressure Furnace in the Preparation of 7577
Interstitials in Alkali Halides, Formation of 7556
Inverters, Diode-Magnetic Amplifier 7819
Ion:
Drift in Silicon, Effect of Li-B Ion Pairing on Li^+ 7574
Pairing in Silicon, Effect of Li-B 7574
Ionic:
Conductivity on the Electric Strength of KCl and NaCl, Effect of 7594
Hall Effect in Sodium Chloride 7597
Ionizing Particle Detectors, Silicon Junction 7831
Iron, Polarization of Conduction Electrons in 7643
Iron in:
Beryl, Paramagnetic Resonance and Optical Spectrum of 7667
Germanium,
Diffusion of 7569
Solubility of 7569
Iron - See also Fe
Ising Model, Monte Carlo Computations on the 7639

J

Junction Layer Microcircuits, Laminar 7736
Junctions,
Detection of Minimum Ionizing Particles in 7831
Emission of Light from Avalanching Germanium 7675, 7676, 7719
Quantum Efficiency of Cadmium Telluride 7717

L

Landau Levels Upon Tunnel Currents in Indium Antimonide, Effect of 7633
Lattice:
Constants of Bi_2Te_3-Bi_2Se_3 Solid Solution Alloys 7551
Defects in Alumina Ceramics 7553
Lattices, Energy Transport in Disordered 7590
Lead Niobate, Phase Transitions in Ferroelectric 7600
Lead Sulfide Films, Photoelectromotive Forces in Electron Irradiated 7678
Lead Titanate Zirconate Ceramics, Dielectric Properties of 7603
Lifetime in Transistors, Control of Carrier 7707
Light:
-Activated P-N-P-N Switches 7840
in Paramagnetic Crystals, Microwave Modulation of 7720
Intensifier Display Panel, Storage 7718
Pulses, Transistors as Generators of High-Speed 7719
Linewidth Variations in the Magnetic Spectrum of Divalent Nickel in Sapphire 7657
Lithium-Boron Ion Pairing in Silicon 7574
Lithium Fluoride,
Formation of Interstitials in 7556
Plastic Properties of 7693
Lithium Fluoride:
Crystals, Effect of Surface Condition on the Mechanical Properties of 7689
from Aqueous Solutions, Growth Poisoning of 7579
Single Crystals, Recovery Properties of 7692
Lithium Hydride,
Binding Properties of 7681
Preparation and Properties of Single Crystals of 7681
Lithium in Silicon, Diffusion Constant of 7571
Logic Circuits,
Diode-Transistor 7797, 7798
Magnetic Core 7799
Tunnel Diode 7796
Use of a Computer to Optimize Transistor 7794
Zener Diode 7765

M

Magnesium-Group IV Compounds, High Pressure Furnace for the Preparation of 7577
Magnesium, Magnetoresistance of 7591
Magnesium Manganese Ferrites, Magnetic After-Effect in 7642
Magnesium Oxide Single Crystals, Plastic Properties of 7693
Magnetic:
After-Effect in Magnesium Manganese Ferrites 7642
Behavior of Some Cubic Crystals, Low-Temperature 7652
Core:
Logic Circuits 7799
Storage 7806
Switch for Magnetic Matrix Stores 7809
Trigger Circuits 7771
-Transistor Pulse Sensing System 7807
Field Meter 7826
Phase Transitions of Cobalt Chloride 7653
Pulse Sequence Detector 7775
Recording Systems,
Sensitivity of Reproducing Heads in 7793
Wideband 7792
Resonance, Transistor Frequency Stabilization for Reflex Klystrons Used in 7815
Spin Configurations in the Cubic Spinel, Classical Theory of 7636
Superconductors, Properties of Some 7625
Susceptibility of Conductive Organic Solids 7621
Systems with Dilution, Behavior of 7635
Torque Measurements on Doped Yttrium Iron Garnet 7640
Magnetism: Monte Carlo Computations on the Ising Model 7639
Magnetization, Anisotropic 7644
Magnetization of a Ferromagnet, Anisotropy of the Intrinsic Domain 7645
Magnetometer, Ferromagnetic 7826
Magnetoresistance of:
Copper, Effect of Oxygen on the 7628
Magnesium, Theory of the 7591
Magnetoresistivity in N-Type Ge, Low-Temperatures 7613
Maser:
Action from U^{3+} Ions in CaF_2 7669
Operation at High Temperatures 7725
Masers, Use of Circulators with 7724
Matrix Switches, Optimal Load-Sharing 7767
Mechanical Recovery Properties of Lithium Fluoride Single Crystals 7692

Measurement of:
Color Center Concentration by Microwave Faraday Rotation 7666
Microwave:
Ferrites at High Signal Levels 7641
Resistivity by Eddy Current Loss in Small Spheres 7616
Paramagnetic Relaxation Time 7655
RF Power, Errir in the 7828
the Complex Conductivity of Low-Impedance Materials 7592
Thermal Diffusivity of Semiconductors by Angstrom's Method 7688
Transistor:
Admittance Parameters 7731
Frequency Response 7732, 7843
Volume Resistivity at Microwave Frequencies 7615
Mechanical Properties:
of Lithium Fluoride Crystals, Effect of Surface Condition on the 7689
- See Elastic Constants, Plastic Properties
Meissner Effect in the Quasi-Chemical Equilibrium Theory of Superconductivity 7624
Memory - See Storage
Metals, Effect of Spin-Orbit Splitting on the Fermi Surfaces of the Hexagonal Close-Packed 7591
Meter, Transistor Water Velocity 7830
Microcircuits,
Assembler for 7844
Laminar Junction Layer 7736
Microwave:
Computer Circuits, Instrumentation for 7795
Ferrites at High Signal Levels, Measurement of 7641
Generation and Amplification, Atomic and Molecular Resonances for 7725
Modulation of Light in Paramagnetic Crystals 7720
Resistivity by Eddy Current Loss in Small Spheres, Measurement of 7616
Missile Tracking, Transponder for 7791
Mobilities in:
Doped Silicon, Hole and Electron 7608
Ge-Si Alloys 7619
Mobility:
and Scattering Processes in Silver Bromide, Electron 7610
in Selenium, Hole 7607
in Semiconductors, Theory of the Effects of Carrier-Carrier Scattering on 7612
Modulation of Light in Paramagnetic Crystals, Microwave 7720
Modulator, Ferrite 7841
Moisture Gettering with Porous Vycor 7713
Monte Carlo:
Calculation for a Size Effect in Electrical Conductivity 7611
Computations on the Ising Model 7639
Morphology of Synthetic Submicroscopic Crystals of FeOOH and Fe_2O_3 7550
Multivibrators, Increasing the Trigger Sensitivity of 7757

N

Negative Resistance as an Equivalent Circuit Element 7733
Network Theory: Synthesis of Driving Point Impedances 7734
Nickel, Polarization of Conduction Electrons in 7643
$Nickel^{2+}$, Paramagnetic Resonance Lines of 7656
$Nickel^{2+}$ in Sapphire, Linewidth Variations in the Magnetic Spectrum of 7657
Noise:
Performance of Tunnel Diodes 7700, 7701
Spectrum of Semiconductors, Generation-Recombination 7629
Suppression for Digital Signals 7745

O

Optical:
Activity in Tellurium 7680
Properties of:
Copper Halides 7671
Vitreous Semiconductors 7674
Radiation from Breakdown Avalanches in Germanium 7675, 7676
Organic Solids, Electronic Conduction and Exchange Interaction in a Class of Conductive 7621
Oscillators,
Increasing the Trigger Sensitivity of Multivibrator 7757
Parametric: Phase Locked 7698
Piezoelectric: Excitation of 7730
Transistor:
Blocking 7758
DC to AC Converter 7818
HF to UHF 7760
RC 7759
Oscilloscope, Transistor Sampling Pulse 7825
Oxidation of Germanium 7581
Oxygen:
in Germanium, Diffusion Coefficient of 7570
in Silicon, Diffusion Coefficient of 7570
on the Magnetoresistance of Copper, Effect of 7628

P

Paramagnetic:
Crystals, Microwave Modulation of Light in 7720
Relaxation:
Effect of Chromium and Iron in Potassium Cobalticyanide 7661
Time Measurements 7655
Resonance:
Absorption of $Nickel^{2+}$ in Sapphire 7657
and Optical Spectrum of Iron in Beryl 7667
Line Shape 7656
of $Cobalt^{2+}$ 7654
of Color Centers in Potassium Chloride 7665
Spin:
Relaxation of F-Center Electrons 7664
Resonance by Microwave Faraday Rotation, Measurement of 7666
-Spin Relaxation, Theory of 7658, 7659, 7660
Spins and the Crystal Lattice, Power Transfer Between 7662
Stimulated Infrared Emission from Trivalent Uranium 7669
Paramagnetism - See also Masers
Parametric:
Amplifiers 7845
Amplifiers,
Gain and Bandwidth Inconsistencies in Low Frequency 7754
Large-Signal Behavior of Degenerate 7751
Traveling-Wave 7752, 7753
Use of Semiconductor Reactance Diodes in 7752
Varactor Diodes for Strip Line 7698
Device as a Nonreciprocal Element 7735
Radio Frequency Amplifier 7777
Switching Circuits 7769
Trigger Circuits 7768, 7769
Parametron Computer Circuits 7800
Passivation of Micro-Components, Surface 7706
Permittivity, Measurement of 7592
Persistent-Current Superconducting Devices, Study of 7728
Phase:
Shifter for the UHF Region, Ferrite 7723
Shifter, Parametric Device as a Nonreciprocal 7735
Transition in $BaTiO_3$-$BaSnO_3$ Solid Solutions 7599
Transitions in Ferroelectric $PbNb_2O_6$ 7600
Phonon Scattering by Chemical Impurities in NaCl 7684
Phosphor Radiation Detectors, Dual 7829
Phosphors, Preparation of (Zn,Hg)S and (Zn,Cd,Hg)S Electroluminescent 7677
Photoconductivity of Aluminum Phosphide 7589
Photoelectric Sensitivity of Selenium Cells Subjected to a Magnetic Field 7716
Photoelectromotive Forces in Electron Irradiated Lead Sulfide Films 7678
Photovoltages in Silicon Films, Larger-than-Bandgap 7578
Photovoltaic Effects in Aluminum Phosphide 7589
Piezoelectric:
Barium Titanate, DC Resistance of Polycrystalline 7596
Excitation of Quartz Oscillators 7730
Force Gage 7729, 7730
Plastic:
Flow in Crystals 7694
Properties of Lithium Fluoride and Magnesium Oxide Single Crystals 7693
Polarization:
Effect in Electrical Conductivity of Al_2O_3 7595
in Guanidine Aluminum Sulfate Hexahydrate, Reversal of the Spontaneous 7598
of Conduction Electrons in Ferromagnetic Metals 7643
Polymorphism of:
Barium Titanate 7548
the Thallium Halides 7549
Potassium Chloride,
Bleaching of Irradiated 7555
Defects in 7556
Effect of Ionic Conductivity on the Electric Strength of 7594
Electron Paramagnetic Resonance of Color Centers in 7665
Potassium Chloride-Potassium Bromide Solid Solution, Effect of Annealing on 7554
Potassium Cobalticyanide, Cross Relaxation Effect of Chromium and Iron in 7661
Power:
Converters, DC to AC 7818
Inverters, Diode-Magnetic Amplifier 7819
Measurements, Error in RF 7828
Regulation, Transistor Switching Circuit for 7812
Supplies for Mass Spectrometers, Transistor 7814
Supplies, Zener Diode Regulated 7821
Supply for a Low Pressure Electric Discharge Lamp, Transistor 7820
Precipitation Phenomena in Silicon 7573
Pulse:
Circuits, Microwave 7795
Code Modulation System for Video Transmission 7786
-Forming Amplifiers, Transistor 7745
Gating System, Zener Diode 7765
Generator for Synchronizing Events, Transistor 7774
Generators,
Transistor 7802
Transistors as High-Speed Light 7719
Ultrafast Rise Time 7795
Modulator, Diode 7772
Regenerators, Transistor 7746, 7747
Sensing System, Transistor-Magnetic Core 7807
Sequence Detector, Magnetic 7775
Pure Silicon, Application of Radiochemistry to the Preparation of 7562
Purification Factor Characterization of Zone Refining 7564

Q

Quantum Efficiency of Cadmium Telluride Junctions 7717
Quartz Oscillators, Piezoelectric Excitation of 7730
Quartz, Thermal Conductivity of Fused 7682

R

Radar:
  Ionospheric Echo Sounding, High Frequency Spectrometer for 7790
  Transponder, Transistor 7791
Radiation, Hole-Capture Cross Section of Defects Produced by γ 7605
Radiation:
  Damage in Graphite, Annealing of 7583
  Detectors,
    Dual Phosphor 7829
    Information Capacity of 7715
  • Detectors Limited by Radiation Noise, Detectivity of 7714
  from Breakdown Avalanches in Germanium 7675, 7676
  on the Properties of Surfaces, Effect of 7582
Radical-Anion Salts, Thermoelectric Power of Some 7621
Radio:
  Circuits, Transistor 7779
  Receiver, Transistor AM-FM 7782
  Tuning Circuits, Varactor Diode 7780, 7781
  Using Drift Transistors, Portable 7778
Reactance Diodes in Wideband Waveguide Amplifiers, Use of 7752
Recording Systems,
  Sensitivity of Reproducing Heads in Magnetic 7793
  Wideband Magnetic 7792
Recovery Properties of Lithium Fluoride Single Crystals 7692
Rectification in Aluminum Phosphide, Point Contact 7589
Regulators,
  Passive Bridge Type Voltage and Current 7816
  Transistor Current 7813
  Zener Diode Voltage 7821
Relaxation, Theory of Spin-Spin 7658, 7659, 7660
Relaxation:
  Time by Microwave Faraday Rotation, Measurement of 7666
  Times, Measurement of Paramagnetic 7655
Relays for Signaling and Control, Diode and Transistor 7823
Reproducing Heads in Magnetic Recording Systems, Sensitivity of 7793
Resistivity:
  at Microwave Frequencies, Measurement of Volume 7615
  of Silicon, Effect of Heat Treatment on the 7617
  Test Set 7834
Resonance:
  Line Shape in Insulators, Theory of Ferromagnetic 7649
  - See also Ferrimagnetic Resonance, Ferromagnetic Resonance, Paramagnetic Resonance
Ruby,
  Microwave Modulation of Light in 7720
  Relaxation Times of Chromium^{3+} in 7655
Ruby:
  Maser Operation at High Temperatures 7725
  Masers, Use of Duplexing Systems with 7724
Rutile, Anisotropic Conduction in Nonstoichiometric 7618

S

Sapphire,
  Linewidth Variations in the Magnetic Spectrum of Nickel^{2+} in 7657
  Polarization Effect in the Electrical Conductivity of 7595
Satellies, Wideband Magnetic Recording System for 7792
Scattering:
  by Chemical Impurities in NaCl, Phonon 7684
  on Mobility in Semiconductors, Theory of the Effects of Carrier-Carrier 7612
  Processes in Silver Bromide 7610
Selenium,
  Diffusion Coefficient of Tin in 7547
  Distribution Coefficient of Tin in 7547
  Hole Mobility in 7607
Selenium and Tellurium, Solid Solutions of 7552
Selenium Cells Subjected to a Magnetic Field, Photoelectric Sensitivity of 7716
Semiconducting:
  Phases in Systems with Transition Metals, Formation of 7584
  Properties in the Si-Co System 7620
Semiconductor:
  Compounds, Furnace for the Preparation of Intermetallic 7577
  Devices, Methods of Cooling 7697
Semiconductors,
  Diffusion Coefficients of Ionized Impurities in 7566
  Solubility of Charged Impurities in 7545
  Solubility of Flaws in Heavily-Doped 7545
  Voight Effect in 7679
Shear on Impurity Conduction in N-Type Germanium, Effect of 7614
Shift Registers,
  Transistor 7802
  Transistor-Capacitor 7803
Silicon,
  Application of Radiochemical Techniques in the Preparation of High-Purity 7562
  Determination of Boron in 7563
  Diffusion:
    Coefficient of Oxygen in 7570
    Constant of Lithium in 7571
  Effect of Heat Treatment on the Electrical Properties of P-Type 7617
  Helical Dislocations in 7558
  Hole and Electron Mobilities in Doped 7608
  Lithium-Boron Ion Pairing in 7574
  Precipitation Phenomena in 7573
Silicon:
  by Noble Gas Ions, Auger Electron Ejection from 7631
  Containing Oxygen and Carbon, Strain Aging in 7573
  Films,
    Larger-than-Bandgap Photovoltages in 7578
    Preparation and Properties of 7578
Silicon-Cobalt:
  Compounds, Thermoelectric Power of 7620
  System, Semiconducting Properties of Compounds in the 7620
Silver Bromide, Electron Mobility and Scattering Processes in 7610
Silver Chloride, Observation of Dislocations in 7557
Silver in Germanium,
  Diffusion of 7569
  Solubility of 7569
Sodium Chloride,
  Effect of Ionic Conductivity on the Electric Strength of 7594
  Ionic Hall Effect in 7597
  Phonon Scattering by Chemical Impurities in 7684
Sodium Chloride-Sodium Bromide Solid Solution, Effect of Annealing on 7554
Solid Solutions, Effect of Annealing on the Physical Properties of Alkali Halide 7554
Solid Solutions:
  in the Bi_2Te_3-Bi_2Se_3 System 7551
  of In_2Te_3 with II-VI Tellurides, Energy Gap of 7546
  of Te and Se 7552
  of (Zn,Hg)S 7677
Solubility of:
  Ag, Fe, Cd, Te and Ta Radioisotopes in Ge 7569
  Charged Impurities in Semiconductors 7545
  Flaws in Heavily-Doped Semiconductors 7545
Spectrometer for Ionospheric Echo Sounding, High Frequency 7790
Spin:
  Configurations in the Cubic Spinel, Classical Theory of 7636
  Echo Experiments in Cerium and Erbium Doped Calcium Tungstate 7668
  Hamiltonian:
    Constants in YIG, Calculation of Uniaxial 7637
    of Co^{2+} 7654
  -Orbit Splitting on the Fermi Surfaces of the Hexagonal Close-Packed Metals, Effect of 7591
  Relaxation of F-Center Electrons 7664
  Resonance Spectrum in Antimony-Doped Germanium 7663
  -Spin Relaxation, Theory of 7658, 7659, 7660
Spreading Resistance in Cylindrical Devices 7696
Stereophonic High-Fidelity System, Transistor Amplifier for a 7755
Storage,
  Fused Silica Delay Line 7804
  Magnetic Core 7806
  Magnetic Core Switch for Magnetic Matrix 7809
  Tunnel Diode 7805
Storage Light Intensifier Display Panel 7718, 7719
Strain Aging in Silicon Crystals Containing Oxygen and Carbon 7573
Strontium Titanate Single Crystals, Commercial Availability of 7833
Superconducting:
  Device Utilizing Tunneling 7842
  Devices, Study of Persistent-Current 7728
  Films, Critical Fields of Thin 7626
  Transition in Purified Tantalum 7623
Superconductivity,
  Analog Solution for the Static London Equations of 7622
  Meissner Effect in the Quasi-Chemical Equilibrium Theory of 7624
Superconductors,
  Electron Tunneling Between 7627
  Properties of Some Ferromagnetic 7625
Surface:
  Breakdown of Germanium in Strong Fields, Anisotropy of 7632
  Condition on the Mechanical Properties of Lithium Fluoride Crystals, Effect of 7689
  Heterogeneity in Irradiated Solids 7582
  Passivation of Micro-Components 7706
  States of a One-Dimensional Crystal 7588
Susceptibility of Some Radical-Anion Salts 7621
Switches,
  Frequency Selective Transistor 7766
  Multidiode 7762
  Optimum Noiseless Load-Sharing Matrix 7767
Switching:
  and Memory Criteria in Transistor Flip-Flops 7763
  Circuits,
    Diode-Transistor 7797, 7798
    Four-Layer Diode 7823
    Parametric 7769
    Transistor 7761, 7770
  Circuits for Power Regulation, Transistor 7812
  in Guanidine Aluminum Sulfate Hexahydrate 7598
  Transistors 7707, 7708, 7709, 7839, 7840

T

Tachometer, Transistor 7832
Tantalum in Germanium,
  Diffusion of 7569
  Solubility of 7569
Tantalum, Superconducting Transition in Purified 7623
Telephone:
  Amplifiers, Audio- and Carrier-Frequency Transistor 7756
  Cable Pairs by Pulse Code Modulation, Video Transmission over 7786
  Dial Tone Gating Circuit, Transistor 7787
  Negative Impedance Repeaters, Transistor 7788
Television:
  Cameras, Power Supply for 7821
  Receivers, Power Sources for Low Heater Power Tubes in Transistor 7783
  Tuners, Transistor 7784
  Video Amplifiers, Transistor 7785
Tellurium:
  and Selenium, Solid Solutions of 7552
  by Zone Melting, Purification of 7565
  in Germanium,
    Diffusion of 7569
    Solubility of 7569
Tellurium, Optical Activity in 7680
Tellurium-Selenium System, Lattice Constants of Solid Solutions in the 7552
Terbium Doped Yttrium Iron Garnet, Ferrimagnetic Resonance Field of 7647
Thallium Halides,
  Polymorphism of 7549
  Preparation of Thin Layers of the 7549
Thermal:
  Conductivity, Theory of Lattice 7686
  Conductivity of:
    Fused Quartz 7682
    Germanium 7683
    Indium Arsenide 7685
    Sodium Chloride 7684
  Diffusivity of Semiconductors by Angstrom's Method, Measurement of 7688
  Spreading Resistance in Mesa Diodes 7696
Thermistor Bolometer 7722
Thermistors, Flake 7721
Thermistors for Temperature Compensation of Transistor Circuits, Use of 7738
Thermoelectric:
  Converters Under Constant Heat Flux, Performance of 7722
  Power of:
    Si-Co Compounds 7620
    Some Radical-Anion Salts 7621
  Properties of Bismuth Telluride and Related Materials 7687
Thermoluminescence in Alumina Ceramics 7553
Thin Layers of the Thallium Halides, Preparation of 7549
Tin in Selenium,
  Diffusion Coefficient of 7547
  Distribution Coefficient of 7547
Torque Measurements on Doped Yttrium Iron Garnet 7640
Tourmaline Piezoelectric Force Gage 7729
Transistor:
  Admittance Parameters, Measurement of 7731
  Autodyne Detector for Paramagnetic Resonance 7827
  Binary Counter 7801
  -Capacitor Shift Register 7803
  Circuits, Use of Thermistors for Temperature Compensation of 7738
  Counter, 100 Mc 7839
  Current Stabilizers for Electromagnets 7813
  Delay and Amplitude Corrective System for Transmission Lines 7789
  -Diode Switching Circuits 7797, 7798
  Frequency:
    Response, Measurement of 7732
    Response Meter 7843
    Stabilization for Reflex Klystrons 7815
  High Frequency Spectrometer for Ionospheric Echo Sounding 7790
  Ignition System for Internal Combustion Engines 7776
  Logic Circuits, Use of a Computer to Optimize 7794
  -Magnetic Core Pulse Sensing System 7807
  Operation Beyond Cutoff Frequency 7710
  Power Supplies for Mass Spectrometers 7814
  Pulse:
    Generators - See Pulse Generators
    Regenerators 7746, 7747
  Radio Circuits - See Radio Circuits, Transistor
  Ripple Filters 7811
  Sampling Pulse Oscilloscope 7825
  Switching Circuit for Power Regulation 7812
  Tachometer 7832
  Television Circuits - See Television Circuits, Transistor
  Trigger Circuits - See Trigger Circuits
  Water Velocity Meter 7830
Transistors,
  Control of Carrier Lifetime in 7707
  Junction:
    Binistor 7709
    Collector Spreading Resistance 7696
    Diffused Base Microalloy 7839
    High-Power High-Frequency 7712
    P-N-P-N 7708, 7840
    Switching 7707, 7708, 7709, 7839, 7840
  Methods of Cooling 7697
  Parallel Operation of Power 7737
  Use of Porous Vycor for Moisture Gettering in 7713
Transistors as Generators of High-Speed Light Pulses, Use of 7719
Transition:
  in Barium Titanate, Cubic-Hexagonal 7548
  Metals, Crystal-Chemical Characteristics of Semiconducting Compounds of 7584
Transmission Lines, Correction of Delay and Frequency Distortion in 7789
Trigger Circuits,
  Binistor 7709
  Indicator Lights for Transistor 7764
  Magnetic Core 7771
  Parametric 7768, 7769
  Switching and Memory Criteria in Transistor 7763
Trinistor Controlled Rectifiers 7837
Tunnel:
  Currents in Indium Antimonide, Effect of Landau Levels on 7633
  Diode:
    Amplifiers, Cascading 7739
    Logic Circuits 7796
    Storage 7805
  Diodes 7838
  Diodes, Noise Performance of 7700, 7701
Tunneling:
  Between Two Superconductors 7627
  in Superconductors, Device Utilizing 7842
Tunneltron 7842

U

Uranium, Stimulated Infrared Emission from Trivalent 7669

V

Valence Band in Germanium Under Shear, Change of the 7586
Varactor:
  Diode:
    Nonreciprocal Phase Shifter 7735
    Package for Microwave Frequencies 7698
    Radio Receivers 7780, 7781
  Diodes,
    Gallium Arsenide 7836
    Silicon 7835
  Diodes for Phase-Locked Oscillators 7698
Video:
  Processor with Pulse-for-Pulse AGC 7743
  Transmission over Telephone Cable Pairs by Pulse Code Modulation 7786
Voight Effect in Semiconductors 7679
Vycor, Moisture Gettering with Porous 7713

W

Wave Functions, Strain-Induced Changes of Donor State 7614

Y

Yield Strength of Crystals, Effect of Screw Dislocations on the 7694
Yttrium Iron Garnet,
  Calculation of Uniaxial Spin Hamiltonian Constants in 7637
  Domain Structure in 7646
  Elastic Constants of 7691
  Ferrimagnetic Resonance Field of Terbium Doped 7647
  Torque Measurements on Doped 7640

Z

Zener:
  Diode:
    Logic Circuits 7765
    Voltage:
      and Current Regulators 7816
      References, Long-Term Stability of 7817
  Diodes as Voltage Breakdown Gating Elements 7765
Zinc in:
  Cuprous Oxide, Diffusion of 7567
  Gallium Arsenide, Diffusion of 7566, 7572
(Zn,Hg)S, Solid Solutions of 7677
Zinc Sulfide Crystals, Defects in 7561
Zone:
  Melt Purification of Tellurium, Evaluation of 7565
  Refining of GaAs, Apparatus for the Floating- 7576
  Refining, Purification Factor Characterization of 7564

AUTHOR INDEX

Abrahams, M. S. 7559
Allegretti, J. E. 7736
Allen, J. W. 7566
Allerton, G. L. 7615
Anderson, M. E. 7792
Arnott, R. J. 7575
Artamonov, O. M. 7678
Atlas, L. M. 7553

Baasch, T. L. 7721
Baba, H. 7562
Baker, R. P. 7817
Barnes, W. J. 7563
Barter, L. D. 7810
Batifol, E. 7568
Bechman, R. 7730
Bell, R. L. 7690
Bessen, L. V. 7781
Bierstedt, P. E. 7621
Bissell, H. M. 7748
Blatt, J. M. 7624
Blet, G. 7716
Bloembergen, N. 7720
Blumberg, W. E. 7664, 7666
Bobisch, P. 7752
Boelger, B. 7662
Bogdanov, S. V. 7599
Bonfield, W. 7690
Bonn, T. H. 7747
Boyle, A. J. F. 7643
Bozorth, R. M. 7625
Brankoff, K. 7826
Braun, P. G. 7651
Brini, D. 7801
Bron, W. E. 7555
Brown, F. C. 7610
Bruin, F. 7827
Budnick, J. I. 7623
Buehler, G. V. 7723
Bullough, R. 7573
Bunbury, D. St. P. 7643
Burnham, D. C. 7610
Busch, G. 7619
Buschert, R. C. 7707
Butler, Jr., T. W. 7726

Cagle, W. B. 7797
Callen, E. R. 7644
Callen, H. B. 7644, 7650
Cannon, W. D. 7789
Caravel, A. 7816
Carbrey, R. L. 7786
Carlin, H. J. 7740
Carlsen, R. A. 7798
Carstedt, V. E. 7818
Carter, I.P.V. 7809
Carter, J. L. 7724
Caspers, W. J. 7658, 7659, 7660
Castro, P. S. 7722
Castro, R. L. 7618
Cerofolini, G. F. 7788
Champlin, K. S. 7629
Charap, S. H. 7645
Chen, W. H. 7797
Chien, R. T. 7767
Childs, C. B. 7557
Chirlian, P. M. 7739
Chizhikov, D. M. 7547
Chow, W. F. 7796
Chynoweth, A. G. 7633, 7676
Cluley, H. J. 7687
Cohen, J. 7595
Cohen, M. H. 7591, 7606
Cook, Jr., C. R. 7802
Cooper, R. 7594
Cooper, R. W. 7640
Cowles, L. E. J. 7688
Cox, E. L. 7794
Crane, H. D. 7775
Csavinszky, P. 7613
Cunnell, F. A. 7572, 7576

Daniels, R. E. 7774
Dash, W. C. 7558
Davidson, Jr., W. F. 7718
Davies, I. F. 7820
Davis, D. D. 7625
Davis, R. E. 7703
Devor, D. 7725
Devyamkova, E. D. 7682
Devyatkova, E. D. 7683
DeWolf, N. 7709
Diamond, H. 7593
Diven, L. 7791
Dolecek, R. L. 7628
Doviak, R. J. 7699
Drewes, G. W. J. 7652
Dubrovskii, G. B. 7717
Dudkin, L. D. 7584
Duraffourg, G. 7568
Dvir, M. 7667

Eckert, Jr., J. P. 7747
Edel'shtein, V. M. 7547
Edington, J. M. 7830
Edwards, C. 7643
Einspruch, N. G. 7691
Ekstrom, L. 7559
Elliott, R. J. 7634
Emes, H. R. 7738
Emile, Jr., P. 7825
Emms, E. T. 7759

Falicov, L. M. 7591
Fathauer, G. H. 7821
Fatuzzo, E. 7598
Favre, R. 7764
Feinstein, S. 7808
Feist, W. M. 7760
Firestone, R. F. 7553
Flairty, C. W. 7773
Follett, W. H. 7832
Fray, S. J. 7673
Freeman, A. J. 7638
Fritsche, H. 7614
Frost, W. T. 7793
Fujimoto, F. 7824

Galejs, J. 7762
Gerson, R. 7603
Ghausi, M. S. 7742
Giaever, I. 7627
Gilman, J. J. 7694
Gilson, P. R. 7810
Giordmaine, J. A. 7655
Giraudier, L. 7577
Glaister, R. M. 7548
Goggin, P. R. 7583
Gold, L. 7564
Gold, R. D. 7698
Goldstick, G. H. 7761
Gooch, C. H. 7572
Granath, J. A. 7792
Green, A. 7688
Greenaway, D. L. 7587
Grimmeiss, H. G. 7589
Gritton, G. V. 7681
Gummel, H. K. 7676
Gurevich, V. M. 7596
Guttman, L. 7639

Haas, C. 7570
Hagstrum, D. 7631
Hall, J. J. 7586
Hall, L. L. 7794
Hall, T. C. 7706
Ham, F. S. 7606, 7654
Hammerslag, J. G. 7780
Hanna, D. A. 7601
Happ, W. W. 7722
Hardy, L. H. 7738
Harnden, Jr., J. D. 7773
Harnischmacher, E. 7790
Hartman, T. E. 7691
Havens, Jr., W. W. 7585
Heinchon, J. 7782
Heller, W. R. 7555
Helms, H. D. 7769
Henkels, H. W. 7702
Higgin, R. M. 7594
Hofheimer, R. W. 7803
Hofmann, H. R. 7787
Hoh, S. R. 7727
Hollander, Jr., L. E. 7618
Holub, A. J. 7754
Honey, R. C. 7753
Hook, H. O. 7718
Hoskins, R. 7725
Howard, R. E. 7556
Huettner, O. A. 7804

Ichimiya, T. 7562
Ignatkov, V. D. 7569
Ittner, III, W. B. 7626
Ivankina, J. S. 7554

Johnson, C. M. 7723
Johnson, F. A. 7673
Johnson, V. 7564
Johnston, T. L. 7695
Jones, E. M. T. 7753
Jones, R. C. 7714, 7715
Jones, R. H. 7673
Jung, P. 7815

Kalish, I. H. 7711
Kallmann, H. 7578
Kamal, A. K. 7735, 7754
Kaplan, T. A. 7636
Katz, E. 7597
Katzman, M. 7724
Kaufman, M. M. 7805
Kay, H. F. 7548
Kear, F. W. 7745
Keizer, E. O. 7768
Kendall, H. W. 7719
Kennedy, D. P. 7696
Kepler, R. G. 7621
Keyes, R. W. 7663
Khan, I. H. 7549
Khomenko, L. A. 7569
Kikuchi, T. T. 7657
Kirvalidze, I. D. 7617
Kischio, W. 7589
Klein, M. V. 7684
Klemens, P. G. 7686
Knox, R. S. 7610
Koenig, S. H. 7586
Koerts, W. 7652
Kohane, T. 7616
Kollar, F. 7814
Kolomiets, B. T. 7674
Konopleva, R. F. 7605
Kosenko, V. E. 7569
Kraemer, L. M. 7580
Kringlebotn, M. 7749
Kritikos, H. 7699
Krupicka, S. 7642
Ku, W. H. 7740
Kwestroo, W. 7651

Lamont, K. 7756
Lamy, R. C. 7771
Langfelder, R. 7823
LaRosa, R. 7701
Latorre, R. J. 7776
Lawson, T. C. 7782
Leef, G. R. 7727
Li, C. H. 7695
Ligenza, J. R. 7581
Lilienstein, M. 7819
Lob, W. H. 7772
Logan, R. A. 7633
Lombardini, P. P. 7699
Loos, J. 7649
Lotsch, H. 7741
Low, W. 7667
Lucas, M. S. P. 7728
Ludwig, G. W. 7654
Luethi, B. 7611
Luke, W. G. 7729
Lynn, D. K. 7763

Mader, C. L. 7681
Maiman, T. 7725
Managan, W. W. 7831
Mann, H. M. 7831
Markham, J. J. 7665
Marks, G. S. 7601
Marshall, S. A. 7657
McAleer, W. J. 7578
McLean, T. P. 7612
McMillan, M. 7656
Melik-Gaikazyan, I. Ya. 7554
Mel'nikov, A. I. 7630
Merrifield, R. E. 7621
Meyer, E. W. 7776
Meyers, N. H. 7622
Miller, S. L. 7707
Mims, W. B. 7668
Minkowski, J. M. 7661
Minnaja, N. 7670
Miselyuk, E. G. 7569
Mogen, D. C. 7737
Moizhes, B. Ya. 7682
Moll, J. L. 7545
Molyneux, L. 7830
Monaghan, R. 7829
Moore, B. W. 7811
Moore, D. L. 7702
Morgan, H. L. 7758
Morozov, A. I. 7632
Morosov, A. V. 7630
Morrison, S. K. 7697
Mueller, C. W. 7698
Muldawer, L. 7551
Murray, Jr., R. 7766

Naborowski, J. G. 7776
Nagamori, K. 7800
Nagy, Jr., J. 7817
Nassau, K. 7668
Navon, D. 7708
Newman, R. C. 7573
Nielsen, E. G. 7700
Nikitin, E. N. 7620
Nikitine, S. 7671
Noble, G. A. 7665
Nomura, R. C. 7680
Nozaki, T. 7562

Offner, F. 7744
Ollom, J. F. 7641
O'Neil, J. P. 7811
Opechowski, W. 7656
Orloff, W. 7732
Owen, H. A. 7728

Paige, E. G. S. 7609, 7612
Palik, E. D. 7679
Palma, M. U. 7652
Palma-Vittorelli, M. B. 7652
Parker, C. A. 7563
Pavlov, B. V. 7674
Pearson, J. J. 7637
Pearson, R. F. 7640
Pederson, D. O. 7742, 7763
Pell, E. M. 7571, 7574
Pemrov, A. V. 7682
Pershan, P. S. 7720
Peterson, J. D. 7705
Phariseau, P. 7588
Philips, Jr., W. L. 7692, 7693
Pittelli, E. 7650
Pollak, P. I. 7578
Porsche, H. 7790
Portis, A. M. 7666
Poulis, N. J. 7653
Powell, R. C. 7592
Pretzel, F. E. 7681
Price, P. J. 7663
Priebe, Jr., H. F. 7806
Proffitt, P. M. C. 7687

Rabenau, A. 7589
Raff, S. J. 7828
Rand, M. J. 7713
Rasmussen, A. L. 7592
Ray, B. 7546
Razbash, R. Ya. 7599
Read, P. L. 7597
Redmond, K. 7731
Reich, B. 7732
Reinberg, A. R. 7657
Reingold, I. 7724
Reiss, R. 7671
Reukauf, D. C. 7792
Reynolds, W. N. 7583
Rez, I. S. 7596
Riggs, R. H. 7750
Roth, W. L. 7561
Rubin, R. J. 7590
Rupert, G. N. 7681
Rush, J. J. 7585
Rushing, C. C. 7681
Russell, D. J. 7822
Russell, R. D. 7814
Ryvkin, S. M. 7605

Sandberg, I. W. 7734
Sandulova, A. V. 7567
Santilli, R. A. 7778, 7779
Sauzade, M. 7813
Sears, G. W. 7579
Segal, R. E. 7743
Seifert, J. R. 7615
Sheard, F. W. 7685
Shockley, W. 7545
Shoenbert, D. J. 7736
Shul'man, A. R. 7630
Shvartsenau, N. F. 7565
Silverstein, S. 7711
Sims, G. D. 7733
Slifer, L. W. 7729
Slifkin, L. 7557
Smart, J. S. 7635
Smirnov, I. A. 7682, 7683
Smith, A. W. 7646
Smith, W. A. 7594
Smoluchowski, R. 7556
Smorodina, T. P. 7552
Sobolevskaya, R. B. 7630
Soltoff, B. M. 7783
Sondhauss, C. 7752
Sorger, G. U. 7828
Sorokin, P. P. 7669
Spear, W. E. 7607
Steiger, W. 7755
Stephenson, I. M. 7733
Stevenson, M. J. 7669
Stewart, W. C. 7728
Stokes, R. J. 7695
Storms, E. K. 7681
Strakhov, L. P. 7678
Struzhinskii, V. A. 7712
Subbarao, E. C. 7600
Swoboda, C. 7774
Szerlip, A. 7777
Szigeti, B. 7672

Tabellini, L. 7801
Takagi, S. 7824
Taylor, T. I. 7585
Teaney, D. T. 7666
Teitler, S. 7679
Thanos, H. 7778
Thomas, D. G. 7604
Thomas, L. C. 7746
Tilton, R. S. 7781
Tippett, J. T. 7795
Tomono, M. 7704
Tyson, C. B. 7783

Vaddiparty, Y. P. 7751
Vail, C. R. 7728
van der Lugt, W. 7653
van Ligten, R. H. 7708
van Oosterhout, G. W. 7550
Van Soest, P. C. 7827
Vickery, J. C. 7820
Vincent, J. 7716
Vodicka, V. W. 7710
Vogt, O. 7619
von Aulock, W. H. 7641

Wachtel, A. 7677
Wakefield, J. 7573
Walker, L. R. 7647
Wangsness, R. K. 7648
Wanlass, C. L. 7757, 7765
Watkins, G. D. 7654
Watson, R. E. 7638
Weber, H. J. 7808
Weertman, J. 7560
Welsh, J. P. 7697
Westwood, A. R. C. 7689
Wheatley, C. F. 7779
Wickham, R. 7576
Wiegand, D. A. 7556
Wiencek, Z. 7785
Wiese, J. R. 7551
Wilcox, L. R. 7720
Wilhelmsen, C. R. 7701
Williams, A. J. 7625
Williams, C. W. 7807
Williams, G. W. 7646
Willis, J. B. 7573
Wilson, B. F. 7829
Wittig, K. 7784
Wold, A. 7575
Wolfe, P. N. 7602
Wolff, P. A. 7633, 7675
Wolfstirn, K. B. 7608
Wood, R. H. 7818
Woodbury, H. H. 7654
Woolley, J. C. 7546
Wright, M. J. 7812
Wyder, P. 7611

Yaroshetskii, I. D. 7605
Yetter, G. R. 7825
Yochelson, S. B. 7799
Young, D. A. 7582
Yourke, H. S. 7770
Yueh-ch'ing, C. 7567

Zarouni, A. 7748
Zavadovskaya, E. K. 7554
Zelinka, R. J. 7737
Zhukov, V. F. 7617
Zuleeg, R. 7710

FOR SURFACE STUDIES

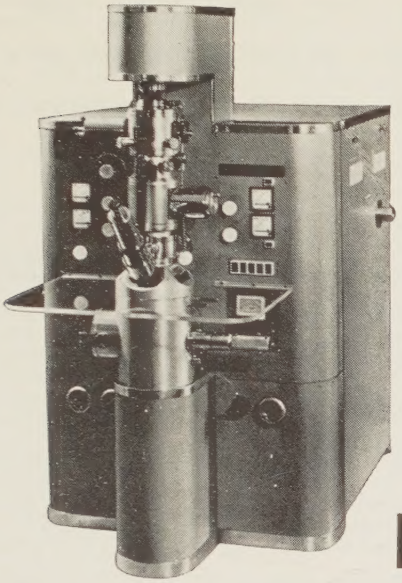

KE1

Trüb, Täuber Secondary Electron Emission Microscope

for direct viewing of metallic and semiconducting specimens by means of secondary electrons released from ion bombardment of the surface — featuring . . .

- Images free of distortion and deformation
- Enlargement up to 1500 X electronoptically
- Resolution 500–600Å
- Object temperature 150°–800° C
- Observable surface of the object 25 mm square
- Differentiation of the material

The Instrument Includes . . .

Electrostatic immersion objective
Ion beam system
Revolving contrast diaphragms
2 electromagnetic projectors
Observation chamber with fluorescent image screen
Recording chamber with plate cassette
High-intensity optical microscope
All-metal housing with vacuum equipment including diffusion pump
High-voltage equipment for 45 kV
Measuring instruments and control equipment

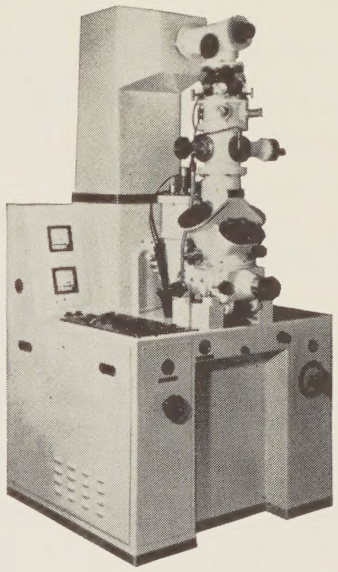

KD3

Trüb, Täuber Electron Diffractograph

for determining the crystalline structure of surfaces, thin layers, and extremely small quantities of material, including dynamic processes — featuring . . .

- Cold-cathode electron gun with practically unlimited life
- Simple design — dependable operation, extreme flexibility
- Balanced optical system
- High resolving power
- Large variety of specimen holders for various methods of investigation
- Devices for heating and cooling the test specimens (from liquid nitrogen to 1000°C)
- Devices for discharging, etching, surface evaporating
- Various cameras for photographic recording on plates and films
- Unique kinematic recorder

Specifications

Acceleration Voltage —	
continuously adjustable:	10 to 50 kV
ripple (fractional):	$\approx 10^{-4}$
stability:	$\pm 0.1\%$
Final vacuum:	approx. 2×10^{-5} mm Hg
Magnification with electronic lens:	75X
Minimum line width:	0.001 mm
Minimum diameter of beam for focussing on specimen, without additional diaphragms:	4μ

Distributed by:

NEW ENGLAND SCIENTIFIC INSTRUMENTS CO.

238 MAIN STREET • CAMBRIDGE 42, MASSACHUSETTS • Kirkland 7-1997

Electron Microscopes • Nuclear Induction Spectrographs • High Voltage Oscillographs • Precision Laboratory Instruments • Nuclear Track Microscopes

ORDER FORM

Please enter my subscription to the following publications: . . . . . .

SOLID STATE ABSTRACTS (JOURNAL)

☐ VOL. II (1961 ABSTRACTS) $25.00 ☐ VOL. I (1960 ABSTRACTS) $25.00

SOLID STATE ABSTRACTS ON CARDS

	1961	1960	1959	1957 1958	FIVE YEARS ORDERED TOGETHER
ALL CATEGORIES (Complete)	☐ $250.00	☐ $250.00	☐ $250.00	☐ $350.00	☐ $1000.00
SEMICONDUCTOR ABSTRACTS (Selected from all categories)	☐ $175.00	☐ $175.00	☐ $175.00	☐ $300.00	☐ $800.00
MAGNETIC, DIELECTRIC, etc. ABSTRACTS (Selected from all categories)	☐ $100.00	☐ $100.00	☐ $100.00	☐ $175.00	☐ $ 450.00

A subscription to Solid State Abstracts (journal) is included with any of the above without additional charge.

CATEGORY M (Metallurgy)	☐ $ 50.00	☐ $ 50.00	☐ $ 50.00	☐ $ 75.00	☐ $ 200.00
CATEGORY P (Physics)	☐ $ 75.00	☐ $ 75.00	☐ $ 75.00	☐ $125.00	☐ $ 325.00
CATEGORY D (Devices)	☐ $ 75.00	☐ $ 75.00	☐ $ 75.00	☐ $100.00	☐ $ 300.00
CATEGORY B (Circuits) A (Applications)	☐ $ 75.00	☐ $ 75.00	☐ $ 75.00	☐ $125.00	☐ $ 325.00

A subscription to Solid State Abstracts (journal) is included with any order for two or more of the above categories without additional charge.

COMPUTER ABSTRACTS ON CARDS

☐ VOL. II (1961 ABSTRACTS) $100.00 ☐ VOL. I (1960 & 1959 ABSTRACTS) $100.00

☐ CHECK HERE IF A HOLE IN THE BOTTOM OF EACH CARD IS DESIRED FOR LIBRARY FILING.

NAME _____

TITLE _____

COMPANY _____

ADDRESS _____

SPECIAL SHIPPING INSTRUCTIONS _____

_____

PAYMENT ENCLOSED ☐ PLEASE BILL US ☐

CAMBRIDGE COMMUNICATIONS CORPORATION

238 MAIN STREET, CAMBRIDGE 42, MASSACHUSETTS

These prices are effective on all orders received prior to June 1, 1961.

SOLID STATE ABSTRACTS ON CARDS

The flood of information deluging research personnel in the solid state field is so vast that it would appear impossible to have all the papers published during the past several years at one man's fingertips: yet this is precisely what SOLID STATE ABSTRACTS ON CARDS enables you to do.

The abstracts prepared for the journal are also printed on 3" x 5" index cards. Each card contains one or more classification numbers which make it easy to file the cards in a logical sequence and thereby to build a cumulative reference file on literally thousands of solid state topics. Printed index tabs are also supplied with each order to facilitate the filing and use of the system. The journal SOLID STATE ABSTRACTS serves as an author index and a detailed subject index to the abstracts. Thus one can locate information by any one of the three primary methods — logical relationships, alphabetically by topic, and alphabetically by author.

M6.3.4.1.1; P2.0.3.4 Ge

6672 TRANSITORY ELECTRICAL PROPERTIES OF N-TYPE GERMANIUM AFTER A NEUTRON PULSE by H. J. Stein (Sandia); J. Appl. Phys., Vol. 31, pp. 1309-1313, Aug. 1960

An investigation of the stability of neutron bombardment damage in Sb-doped Ge is discussed. Continuous measurements of the electrical conductivity and Hall mobility following a neutron pulse were made in the temperature range from 77° to 308°K with a time resolution of 1 sec. At temperatures near 195°K an initial decrease in conductivity and mobility was followed by an additional decrease which exhibited nearly second-order kinetics. At 273°K and above an initial decrease in conductivity and mobility was followed by a recovery consistent with an activation energy of 0.68 ev. The void region model of Gossick and Crawford is employed to explain the initial decrease in mobility and a major portion of the initial decrease in conductivity

Note that this card is also cross referenced and can be located in the metallurgy section.

Sample SOLID STATE ABSTRACTS ON CARDS

P2.1.0.5.9 $BaTiO_3$

6674 MEASUREMENTS OF THE DIELECTRIC CONSTANT OF $BaTiO_3$ SINGLE CRYSTALS IN THE PARAELECTRIC REGION AT X BAND by A. Lurio and E. Stern (IBM Watson Lab.); J. Appl. Phys., Vol. 31, pp. 1805-1809, Oct. 1960

Measurement of the dielectric constant and loss tangent of single crystals of $BaTiO_3$ as a function of temperature in the frequency range of 8.2 to 12.4 kMc is discussed. The technique consists of looking for transmission resonances through the crystal whenever its thickness became $\lambda/2$ (where λ is the wavelength in the material). From the Curie-Weiss behavior of the dielectric constant in the paraelectric region, the A constant was determined to be $3.77 \times 10^{-5} °C^{-1}$.

Sample page from our 6000 Topic Classification System

P2 ELECTRICAL PROPERTIES (see also P4.4, P5.3, a, b)

- P2.0 General
  - P2.0.1 Theory of the Electrical Properties of Solids
    - P2.0.1.0 General
  - P2.0.2 Measurement of the Electrical Properties of Solids (see also under specific properties)
  - P2.0.3 Effect of:
    - P2.0.3.1 Temperature (see also P5)
    - P2.0.3.2 Pressure
    - P2.0.3.3 Deformation
    - P2.0.3.4 Radiation (see also P4)
    - P2.0.3.5 Dislocations (see also M3.2.1.2.5.2)
    - P2.0.3.6 Impurities
    - P2.0.3.7 Melting
    - P2.0.3.8 High Fields
    - P2.0.3.9 Crystalline Order
      - P2.0.3.9.1 Long Range
      - P2.0.3.9.2 Short Range
    - P2.0.3.10 Heat Treatment
  - P2.0.4 Electrical Properties of Special Structures
    - P2.0.4.1 Single Crystals
    - P2.0.4.2 Thin Films
      - P2.0.4.2.1 Theory
    - P2.0.4.3 Grain Boundaries
- P2.1 Dielectric Properties
  - P2.1.0 General
    - P2.1.0.3 Effect of:
      - P2.1.0.3.6 Electromagnetic Radiation
    - P2.1.0.5 Dielectric Constant (Permittivity)
      - P2.1.0.5.3 Effect of (Variation with):
        - P2.1.0.5.3.1 Temperature
        - P2.1.0.5.3.2 Pressure
        - P2.1.0.5.3.3 Frequency
      - P2.1.0.5.9 Dielectric Constant of Specific Materials
    - P2.1.0.6 Charge on (or in) Dielectrics
      - P2.1.0.6.3 Effect of:
        - P2.1.0.6.3.4 Electric Field
        - P2.1.0.6.3.5 Geometry
        - P2.1.0.6.3.6 Radiation
          - P2.1.0.6.3.6.1 X-Rays
          - P2.1.0.6.3.6.2 Beta-Rays
    - P2.1.0.7 Current Flow in Dielectrics (see also P2.2.6)
      - P2.1.0.7.4 Carriers
    - P2.1.0.8 Dielectric Loss

This unique service provides more than 5000 references each year at a cost which is less than one week's salary for a senior scientist. If your interests do not cover the entire solid state field, you may purchase only the cards in one or more of the individual categories shown on the previous page or you may select all the cards related to either semiconductor or magnetic, dielectric, and metallic materials and devices.

Cambridge Communications Corporation also publishes COMPUTER ABSTRACTS ON CARDS which provides the same kind of complete information retrieval service for the field of electronic computers that SOLID STATE ABSTRACTS ON CARDS provides for the Solid State field.

For prices and order information . . . please see the opposite page.

may cost your company many times the price of

SOLID STATE ABSTRACTS ON CARDS
or
COMPUTER ABSTRACTS ON CARDS

These cards enable anyone — scientist, engineer, librarian — to maintain a cumulative reference file of up-to-date information in the solid state or computer fields. Classification numbers on each card make it easy to file this information in a logical sequence and hundreds of guide cards make it possible to locate required references immediately.

Take full advantage of the billions of dollars of research results that are reported each year. These annotated and classified bibliographies of current research in the solid state and computer fields are inexpensive insurance that your scientific efforts are not duplicating the work of others.

For further information please see inside back cover.

CAMBRIDGE COMMUNICATIONS CORPORATION
238 Main Street • Cambridge 42, Massachusetts